A STUDY OF CHOPPER-FED D.C. SERIES MOTOR

BY

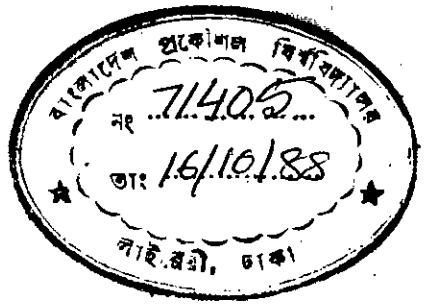

MD. MAHMUDUR RAHMAN

A THESIS

SUBMITTED TO THE DEPARTMENT OF ELECTRICAL AND ELECTRONIC ENGINEERING IN PARTIAL FULFILLMENT OF THE REQUIREMENTS FOR THE DEGREE

OF

MASTER OF SCIENCE IN ENGINEERING

DEPARTMENT OF ELECTRICAL AND ELECTRONIC ENGINEERING

BANGLADESH UNIVERSITY OF ENGINEERING AND TECHNOLOGY, DHAKA

OCTOBER, 1988.

To my

Twin Brother

Md. Mostafizur Rahman

Accepted as satisfactory in partial fulfillment of the requirements for the degree of Master of Science in Engineering (Electrical and Electronic).

BOARD OF EXAMINER

1. _____ 3/10/88 — Chairman (Supervisor)
(Dr. Enamul Basher)
Associate Professor,
Department of Electrical and Electronic
Engineering, BUET, Dhaka.

2. _____ — Member
(Dr. Md. Mujibur Rahman)
Professor and Head,
Department of Electrical and Electronic
Engineering, BUET, Dhaka.

3. _____ 3/10/88 — Member
(Dr. Syed Fazl-i Rahman)
Professor and Dean,
Faculty of Electrical and Electronic
Engineering, BUET, Dhaka.

4. _____ — Member
(Dr. Shahidul Islam Khan)
Assistant Professor,
Department of Electrical and Electronic
Engineering, BUET, Dhaka.

5. _____ 3/10/88 — Member (External)
(Dr. A. M. Zahoorul Huq)
391 Baitul Aman Housing Estate
Road No. 6, Shymoli,
Dhaka-7.

CERTIFICATE

Certified that this work was done by me and it has not been submitted elsewhere for the award of any degree or diploma.

Countersigned

(Dr. Enamul Basher)
Supervisor

Signature of the student

(Md. Mahmudur Rahman)

ACKNOWLEDGMENT

It is a matter of great pleasure on the part of the author to acknowledge his heartiest gratitude and profound respect to his supervisor, Dr. Enamul Basher, Associate Professor of the Department of Electrical and Electronic Engineering, BUET for his valuable guidance, constant encouragement and whole hearted supervision throughout the progress of the work, without which this thesis would never have materialised.

The author also expresses his sincere gratitude to Dr. Md. Mujibur Rahman, Professor and Head, Department of Electrical and Electronic Engineering, BUET for his encouragement and all out support to complete the work successfully.

The author also wishes to acknowledge his gratitude to Dr. S. F. Rahman, Professor and Dean, Faculty of Electrical and Electronic Engineering, BUET for his valuable suggestions and encouragement.

Thanks are also due to Dr. S. I. Khan, Assistant Professor, Department of Electrical and Electronic Engineering, BUET for his all along encouragement and useful suggestions.

The author is also indebted to the Director and personnel of the Computer Centre, BUET for their cooperation.

The author would also like to thank all staff of the Department of Electrical and Electronic Engineering, BUET for their friendly help and assistance.

Finally the author wishes to remember all the members of his family, who have been all along a constant source of inspiration through out the progress of this work and who will remain ever as such.

ABSTRACT

The main problem in the analysis of the chopper-fed dc series motor arises due to the nonlinear relation between the armature induced voltage and the armature current. Because of this, the differential equations which describe the operation of the motor in different modes of a chopper cycle are nonlinear. Exact solution of these equations can only be obtained numerically by the use of considerable computation time.

This thesis describes certain approximations which permit the derivation of simple but accurate analytical methods for the analysis of dc series motor fed from a chopper. Choppers can be operated either with Time Ratio Control (TRC) or Current Limit Control (CLC). The present work is concerned with the modelling and analysis of dc series motor controlled by a chopper with TRC. Two different mathematical models have been formulated. The first one is based on some empirical formula, derived from some experimental results of the motor. In the second model the motor performance is simulated by some non-linear differential equations, which have been solved numerically. Standard fourth order Runge-Kutta numerical method is used. Effect of magnetic saturation is efficiently incorporated in this model through representing the magnetising curve mathematically by the arc-tan curve. Both the models are applied to predict the steady state performances of dc series motor controlled by chopper, taking into account, the saturation of the magnetic circuit, effect of eddy currents in the field cores and the armature reaction. The results are analysed and compared with the practical measurements. The experimental performance agrees very well with the predicted performance.

LIST OF SYMBOLS AND ABBREVIATIONS

a = Number of pair of parallel paths.

a_1, b_1, d_1 = Constants to represent the magnetising characteristics through arc-tan curve.

E = Armature induced voltage.

E_o = Open circuit voltage.

F_a = Armature reaction mmf.

F_d = Total mmf in the direct axis.

F_{ed} = Eddy current mmf in the direct axis.

i_a = Instantaneous value of armature current.

i_p = Peak value of current ripple.

I_{a1}, I_{a2} = Minimum and maximum levels of steady state current.

i_{ed} = Eddy current.

i_d = Total exciting current referred to the base coil.

K = Back emf coefficient of machine in volts/amp/rad-sec^{-1}.

K' = Back emf coefficient of machine in volts/rad-sec^{-1}.

= $K.I_{av}$

k_1 , k_2 = Frolich's constants.

$L(I_{av})$ = DC inductance of combined armature and field as a function of average armature current.

L_{eq} = Equivalent armature circuit inductance with eddy current.

L_a , L_s = Inductance of armature coil and series field coil respectively.

L_{a1}, L_{s1} = Leakage inductance of the armature coil and series field coil respectively.

L_{ed} = Inductance of the eddy current path.

n = A constant dependent on the design of the magnetic circuit

N_a = Number of turns of the armature coil.

N_a' = Equivalent number of turns of armature coil.

N_s , N_e = Number of turns per pole pair of the series field coil and some arbitrarily chosen base coil.

p = Number of pole pairs.

R = Total armature circuit resistance.

R_{eq} = Total equivalent armature circuit resistance with eddy currents.

R_s = Resistance of the series field coil.

R_a = Resistance of the armature coil.

R_{ed} = Resistance of the eddy current path.

T = Period of the chopper.

T_a = Armature circuit time constant.

V = DC supply voltage.

V_a = Instantaneous output voltage of the chopper.

Z = Number of armature conductors.

σ, λ = Constants dependent on the machine.

δ = Mark period ratio of the chopper.

δ_c = Commutation interval per period of the chopper.

ω = Motor speed in rad/sec.

ω_o = Rated motor speed in rad/sec.

α = (i_p / I_{a2})

Δv_b = Brush voltage drop.

ϕ = Flux.

ϕ_{ma} = Air-gap flux.

ψ_{aq}, ψ_s = Flux linkages of the armature and series field coils respectively.

α_i = (Pole arc/pole pitch).

Ω = ohm.

CLC = Current Limit Control.

DELVB = Brush Voltage Drop.

DELT = Increment of Time.

mmf = Magnetomotive force.

OCC = Open circuit characteristics.

p.u. = Per unit.

pd = Potential difference.

PARC = Pole Arc.

PPITCH = Pole Pitch.

rad = Radian.

sgn = sign.

TRC = Time Ratio Control.

CONTENTS

CHAPTER 1

INTRODUCTION

1.1 GENERAL

The electrical machine is one link in the chain of a drive system. As a link, the electrical machine is influenced by the rest of the chain, and in turn influences the behavior of the whole system. For analysis of electric-machine systems, an accurate model of dc machine is desired, since dc machines are widely used in various electric drives.

In most of the industries, controlling system is the prime concern of the industrialists. Because depending on the processes carried out, the speed of the driving mechanism, its torque, current, voltage etc. may be required to be controlled to conform the load duty cycle. Control is necessary also for stabilizing the drive system by quick response to any changes. The outstanding characteristic of dc motors is their versatility. By means of various combinations of shunt, series and separately excited field windings they can be designed to have a wide variety of built-in speed-torque characteristics for both dynamic and steady state operation. Because of the ease with which they can be controlled, systems of dc motors are often used in applications requiring a wide range of speed variation or precise control of motor output. Due to these inherent advantages, dc motors are in wide application, both in high power industrial and electric traction drives as well as in low power drives needed for different servo systems.

In almost all industrial applications, such as in paper, cement, sugar and textile mills as well as in different metallurgical fields, the control of speed and position of the drives are very much required. The classical method of speed control were those using motor-generator set (Ward-Leonard method). But apart from slower response, inaccuracy, high cost and system loss, the classical method of control possesses all the disadvantages of rotating

machines. However the method of control shifted from rotary to static with the advent of amplidyne and metadyne but still the problem of fast response and efficient operation remain unsolved together with the problem caused by the bulkiness of the equipment [1,2].

In modern dc drives, thyristorized power converter has replaced the classical motor-generator control set, since it provides faster response at a lower cost [2,3,4]. The most salient features of the thyristor are the high accuracy, compactness, fast response and easy routine maintenance for trouble free operation. For these reasons, now a days, most of the conventional control systems have been effectively replaced by thyristor controlled one, such as converters, inverters and cycloconverters.

Thyristor choppers are now very widely used for controlling dc separately and series excited motors. The output voltage of choppers is usually controlled either by using Time Ratio Control (TRC) or by using Current Limit Control (CLC) [5]. In TRC, the ON to OFF time ratio is adjusted. The chopper may then be operated, either at a fixed frequency and variable ON to OFF time ratio, or, at a fixed ON (or OFF) time and variable frequency. In CLC, the load current is restricted between specified maximum and minimum values by using suitable firing techniques. Although both the schemes have relative advantages and limitations [6], choppers with variable ON time and fixed frequency are preferable because these are simple and provide flexibility in control and quick response. But dc motors supplied from chopper run at adverse condition resulting from periodic on-off of the dc voltage. The motor performance characteristics deviate from the usual dc motor characteristics. For effective control of dc motor with chopper in the control chain exact performance curves are required. Apart from that designing of chopper-fed dc motor requires theoretical derivation of these curves using design parameters. So the present work sets as its objective the analysis of dc motor performance when it is supplied from the output of a chopper.

1.2 LITERATURE SURVEY

Within the last years the economical availability of large thyristors has led to the highly efficient use of power pulse controlled dc motors [7-11]. The control circuitry consists of entirely static components and with the exception of the thyristor losses, the minor control module losses and some additional loss within the motor, no other additional losses are encountered. By proper control of the current pulses, both torque and speed can be regulated during motoring and braking operation, including the regenerative mode.

Thyristors are now widely used for different control systems due to their quick response, flexibility in control, higher efficiency and compactness. Many articles and literature have been published by different authors covering the application and control circuitry of the device. F.W. GUTZWILLER [12] has tried his best to present the device as an important component of the control and power system. In 1966 D.W.BORST, E.J.DIEBOLD and F.W.PARRISH [13] have carried out some work on the analytical performance, phase control and firing scheme of the device. The control and power engineers are mostly interested to achieve the quicker response of the control device, but the classical work in this context is quite inadequate. The recent introduction of microprocessor in the field of industrial control system has played a very important role. The conventional firing scheme of the thyristor has been replaced by microprocessor based firing schemes [14,15,16]. In various industrial and traction applications the thyristorized control device is used in different aspects, specially in speed, torque and current control of motors. Analytical solution of the thyristorized drives have been made by many and most substantial works have been carried out in the past few decades [5,17-23].

The representation of electrical machine used for thyristorized drives including all the facts and phenomena is not completely done till to date. Most of the authors represented the machine excluding nonlinearity to simplify

the analysis. For the linear model laplace transform and fourier series analysis are used by some authors [17,20] to determine the output characteristics of chopper-fed dc motor. A systematic development of the analysis, design and testing of a thyristor (SCR) controlled separately excited dc motor drive system was carried out by P.C.SEN and M.L.MACDONALD [20]. The motor armature voltage was supplied from a three phase fully controlled six-pulse thyristor bridge. Closed loop control was analyzed using transfer function techniques and the necessity of an inner current loop was also demonstrated. A combination of fourier analysis of load voltage waveform and laplace transformation was applied for determining the performance of a separately excited dc motor fed from a chopper controlled supply, under all modes of operation by S.N. SINGH and D.R.KOHLI [17]. In their analysis the effect of commutation interval of the chopper circuit was taken into consideration. The analysis was used to predict both the steady state and transient response.

TAKEUCHI [24] has analyzed a dc series motor fed by a pulse width modulated chopper with square wave output voltage neglecting the nonlinearity of magnetic circuit. The analysis of a dc separately excited motor fed by a chopper with square wave output voltage and time ratio control has been described by K.NITTA ET AL [25]. The steady state performance of a separately excited dc motor has been analyzed by PARIMELALAGAN and RAJGOPALAN [26] based on the assumptions of negligible commutation interval, negligible ripple in the armature current and constant current during commutation. FRANKLIN [18] has analyzed a dc series motor fed by current limit controlled chopper. In this work the magnetisation characteristics of the motor between the two current limits is approximated by a straight line. This method is, however, unsuitable for the analysis of pulse-width modulated chopper controlled drive as the two extreme limits of current fluctuations are not known before hand. The papers by DUBEY ET AL [5,27-29] describes methods of analyzing dc motor controlled by either current limit control or pulse width control. The analysis has been

carried out by approximating the chopper output voltage as a square wave either by assuming the commutation interval to be negligible [5,27] or by modifying the effective value of duty interval approximately taking into account the effect of commutation interval [29]. It is further assumed that fluctuation in speed during a chopping cycle is negligible. In the paper by DUBEY and DAMPLE [28] speed is assumed as constant during the chopping period and also for a given ON time an initial value of load current is required to be assumed at the begining of duty interval. In another paper [30] the authors S.N.SINGH and D.R.KOHLI have presented a method of analyzing chopper-fed separately excited dc motors under continuous conduction mode of operation. Fourier analysis and laplace transformation were used to develop the mathematical expressions for current and speed which were, however, dependent on each other.

A generalized method of analysis of chopper fed dc separately excited motor has been presented by H.SATPATHI, G.K.DUBEY and L.P.SINGH [31] taking into account the effect of source inductance, chopper commutation interval, discontinuous conduction and the effect of armature reaction of the motor. S.N.BHADRA, N.K.DE and A.K.CHATTOPADHYAY [32] in the year of 1981 has published a paper which presents a comprehensive analysis that predicts the performance of a thyristor-chopper controlled dc series motor during regenerative braking operation. The analysis takes into account all the possible modes of operation during this type of braking, the nonlinearity of the magnetisation characteristics including the variation of field inductance and the effect of the commutating capacitor in the chopper circuit on the braking performance.

In 1972 W.FRANKLIN [18] as mentioned earlier has studied the theoretical relationship between current, flux and pulse duration, of a series motor supplied with power pulses taking into account the nonlinearity of the magnetic field by suitable approximation. The magnetisation curve was represented by a technique based on the principle of equivalent magnetic energy. The stored

magnetic energy, as derived from the approximation is made equal to the value obtained from the actual curve. But as it complicates the system equations its digital computer simulation becomes very difficult. In 1981 by the author G.K. DUBEY and W.SHEPHERD [21], a paper was published which deals with the transient analysis of a chopper controlled dc series motor with TRC or CLC controlled including magnetic saturation. The magnetisation curve was represented by them in a piece-wise linear form as follows:

i) In the unsaturated portion of the magnetisation curve it is approximated by a straight line passing through the point corresponding to the value of current under consideration and the origin.

ii) For other portion (the saturated portion) of the magnetisation curve it is approximated by a straight line passing through the point of consideration and having a slope equal to the slope of the magnetisation curve at that point.

The same piece-wise linear technique was used by M.H.RASHID [22] to analyze the dynamic performances of an armature voltage-controlled chopper circuit with a low-pass input filter taking the account of nonlinearities such as the magnetic saturation and the product of variable terms. S.N.BHADRA, M.K.DE. and A.K.CHATTOPADHYAY [32] has used minimum error criterion to represent magnetic saturation by odd order polynomial. The same technique is followed by A.YABLON and J.APPELBAUM [33] who have considered both linear and nonlinear models and analyzed with the aid of the SUPER SCEPTRE computer program. F.P.DEMELLO and L.N.HENNETT [34] in their paper, published in 1986 have used arc-tan curves for representing the magnetisation characteristics. But this arc-tan curve can not represent the magnetisation characteristics properly since it has got indeterminate behavior at high value of intensity.

In 1983 R.S.RAMSHAW and G.XIE [23] have presented a simulation model of dc machine, making some assumptions such as, losses due to hysteresis and eddy current are lumped and distribution of air-gap flux is assumed sinusoidal.

Direct and quadrature axis representation is used for expressing the flux by a higher order polynomial. This model accounts for magnetic saturation. The intrinsic nonlinearity of the set of differential equation was also taken into consideration. From this highly parameterised, nonlinear mathematical model a general multiport model and its dual for electric circuit simulation were also presented. In the same year H.SATHPATHI, G.K.DUBEY and L.P.SINGH [35] have made and analysis to predict the steady state performance of dc series motor controlled by chopper taking into account the magnetic saturation, armature reaction and eddy current effect. They have used the FROLICH's equation to represent the magnetic saturation. E.G.STRANGAS and H.B.HAMILTON [36] in their paper have utilized finite element technique to solve the electromagnetic field, in the time domain, taking eddy current and saturation effects into account. In 1987 ENAMUL BASHER and A.R.KHAN [37] have worked on a mathematical model for analysis of transients of dc machines which considers complexities of interactions of such phenomena as mutual effect of direct and quadrature fluxes, eddy currents and commutation in a form easy to be handled in computer calculations.

1.3 SCOPE OF THE PRESENT WORK

The objective of the present work is the steady state analysis of chopper-fed dc series motor. So, the scope of this thesis includes the study of the relevant topics and development of a mathematical model suitable for rational representation of dc series motor supplied from the chopper. The thesis deals also with the problem of working out effective method of application of model by suggesting how to determine its parameters.

Nonlinearity caused by the magnetic saturation, armature reaction, eddy current, commutation interval of the chopping cycle etc. complicates the differential equations, that describe the operation of the motor. A published analytical model [35] based on empirical representation of above non-

linearities has been used to calculate the performance curve of a sample motor. This concrete model has been singled out as it considers all the above mentioned nonlinear physical phenomena. The different constants of this model are determined from the available motor data as well as from experiments carried out in the laboratory set up. The large number of coefficients so determined are fitted in the empirical relationships of the model to draw the mechanical characteristic of the chopper-fed dc series motor.

A mathematical model, in which the dc series motor is simulated by a set of nonlinear differential equations has been developed. Numerical technique is to be used to solve the system of differential equations. Fourth order Runge-Kutta method has been used for this purpose, because, it simplifies the computer programming and it is a reasonably accurate numerical method for solving differential equations. A computer program in FORTRAN-77 has been developed to solve the system of equations by digital computer.

The theoretical results obtained by applying the models to a chopper-fed dc series motor have been compared with the experimental results. The results have been analysed critically and the possible way for further work on this context have also been recommended.

1.4 THESIS ORGANIZATION

This thesis consists of eight chapters. As an introductory approach, the thesis objective and literature review are presented in chapter 1. In this thesis primary stress is given on the simulation of chopper-fed dc series motor, therefore, in chapter 2 and 3, a very brief idea is given about electric drive systems and chopper drives. The mathematical models have been formulated in chapter 4. Using these mathematical models numerical evaluation is carried out in chapter 5. Chapter 6 presents the actual steady state performance of a chopper-fed dc series motor. Comparison of the theoretical results with the experimental one is done in chapter 7. Analysis of the

results are also presented in chapter 7. In chapter 8 conclusions are presented on the basis of the results found in chapter 5 and 6. Recommendations for further work are also provided in chapter 8.

CHAPTER 2

ELECTRIC DRIVE SYSTEM

2.1 INTRODUCTION

An electric drive system consists of the following main elements: Main power supply, Converter, Motor, Mechanical system and the Controller. Initially the nature of the mechanical system and the main power supply only will be known, where as the motor, converter and the controller must be designed or chosen. When a preliminary design of a desirable drive system has been carried out it may be discovered that the available electric power supply is, in some way inadequate. It is therefore logical to start with a discussion of the kinds of mechanical system that may be encountered and the demands they will make on the power supply, regardless of the exact nature of the controller and motor.

In this chapter a brief discussion of the general features of a conventional electric drive system is presented. This chapter also presents some basic concepts underlying with the selection of the element of a drive system and ends with a discussion of dc motor applications and its control technique.

2.2 MODEL OF AN ELECTRIC DRIVE SYSTEM

The block diagram in figure 2.1 illustrates the main elements into which an electric drive system may conveniently be divided. The dotted block as shown in figure 2.1 represents the subordinate current loop, to limit the current at the time of transient.

2.3 THE MECHANICAL SYSTEM

The mechanical system is "seen" by the motor as a torque that must be applied to a shaft by the motor coupling. The relation between this load torque and the motor speed must be defined. For steady state operation this

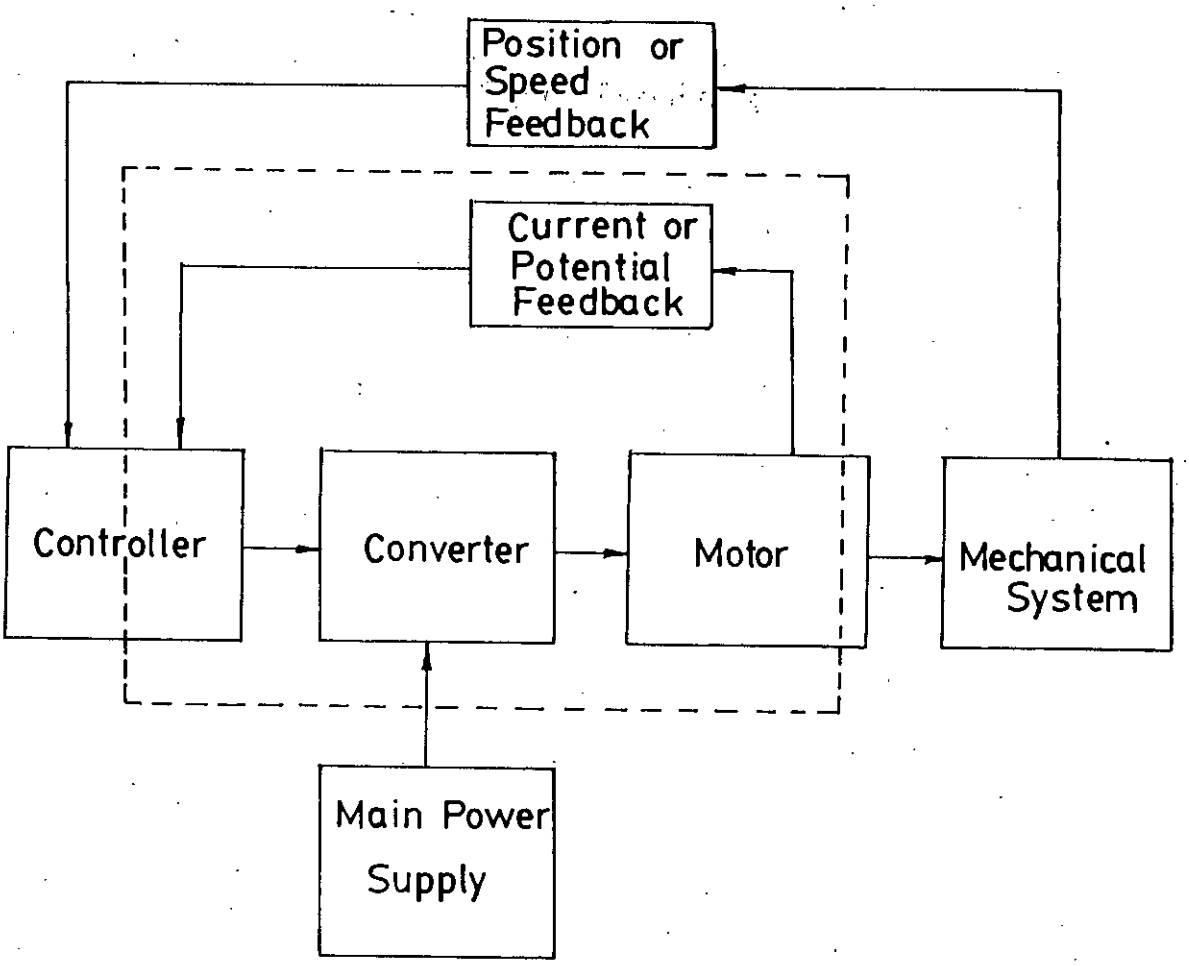

FIG. 2.1 MODEL OF AN ELECTRIC DRIVE SYSTEM.

definition may be made in terms of the four-quadrant, speed-torque diagram in figure 2.2 in which ω is the speed of the rotation of the motor, or the driven shaft, and T_L is the coupling torque developed by the motor or the load presented by the shaft of the mechanical system.

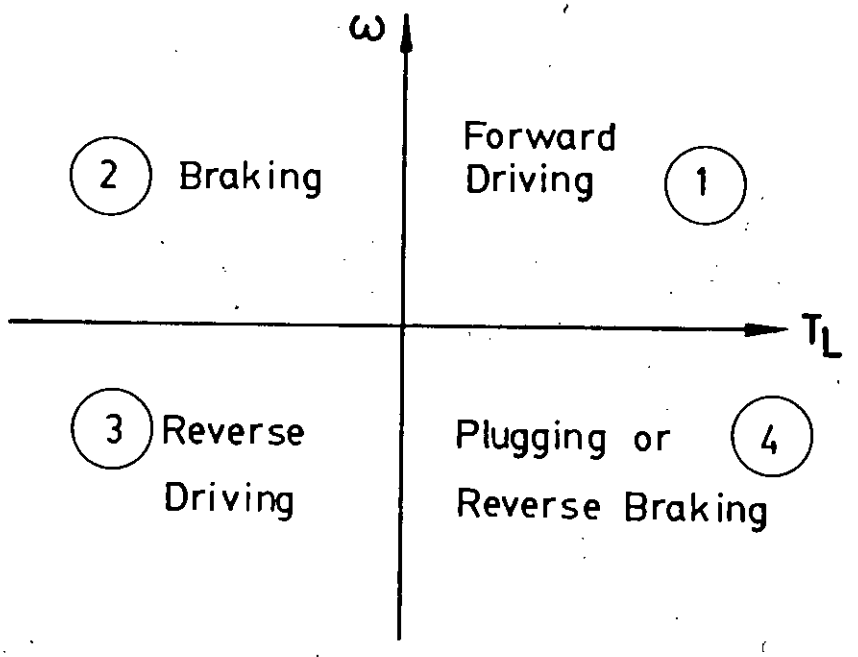

FIG. 2.2 FOUR-QUADRANT SPEED-TORQUE DIAGRAM

1. The first quadrant applies to normal forward driving.
2. In the second quadrant the mechanical system demands a negative torque to provide braking. This braking torque may be produced in a variety of ways: friction braking, eddy current braking, dynamic braking and regenerative braking.
3. In the third quadrant motor torque and direction of rotation are reversed. The operating condition are similar to those in the first quadrant.
4. The fourth quadrant may represent one of two possible conditions. If the electrical conditions are the same as in first quadrant driving, the mechanical system is driving the motor in a direction opposite to that

which would result from its own developed torque. This is another type of braking called "plugging". If the electrical conditions are changed to give reverse driving in the third quadrant, any of the types of braking described for the second quadrant are obtainable in the fourth quadrant.

There are different types of mechanical systems such as Compressor, Centrifugal pump or Fan, Constant Power Drive, Transportation Drive, Winch Drive, Crane Hoist etc. and each one demands different speed-torque characteristics. So before selecting the motor-controller combination, the type of the mechanical load must be studied first.

2.4 ELECTRIC POWER SUPPLY

The choice of the power converter or conditioner and motor can not be arbitrarily made but depends on the nature of the power supply available. Once the driving elements have been chosen and a preliminary design of the system carried out it is possible to determine whether the available power source will satisfy the requirements of the drive system particularly in regard to maximum power rating. The frequency and potential variation of the source should be specified. There may also be restrictions on the harmonic content of currents drawn from the source and the power factor at which the drive system may operate.

It is unusual for a dc source to be available for general purpose in an industrial plant; therefore, if dc is particularly desirable, it must normally be provided by some form of conversion from the ac power system. If rectification is employed the possibility of regeneration from the drive system must be considered because a simple diode cannot regenerate. A motor-generator set that consists of an ac motor and a dc generator is capable of regeneration but is inefficient in comparison with a rectifier.

In traction systems, large scale conversion equipment capable of regeneration may be installed in substations. The advantage of dc for power distribution in a rail-guided traction system is great because the guiding rails and a third rail or overhead wire are conductors, where as the high self inductance of steel rails prohibits their use with ac of standard power frequency.

2.5 SELECTION OF THE DRIVE ELEMENTS

Once the characteristics of the mechanical system and the source are defined it is possible to select a suitable motor and converter. Frequently several combinations are possible.

The converter may be considered to consist of two parts : the power converter or modulator and the logic unit. The logic unit receives command and feedback signals and produces from them the signals that control the operation of the power converter. Figure 2.3 shows a typical converter system. The components of the converter system are as follows:

1. Power Converter : the output of which may be a variable dc or ac potential or may be a variable frequency ac potential.

2. Logic Unit: in response to the signals from the controlling system it switches the thyristors of the power converter on and off at proper instants.

3. Controlled System: this may simply be a rotating machine and driven load with appropriate feedback path.

4. Controlling System: in response to the command and feedback signals it transmits the appropriate control signals to the logic unit.

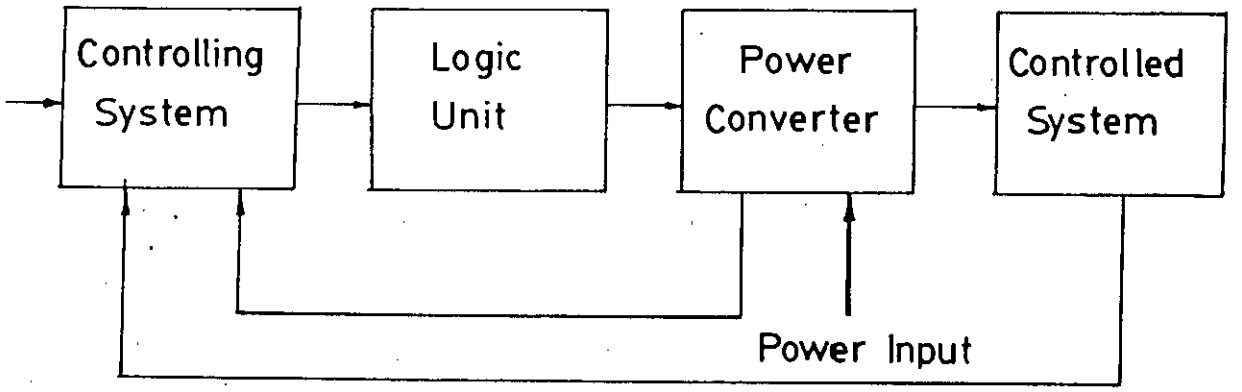

FIG. 2.3 BLOCK DIAGRAM OF A TYPICAL CONVERTER SYSTEM

2.6 TYPES OF CONVERTERS

Table 2.1 lists the main types of converter system. Important information required for each type of converter includes

a. converter transfer characteristic;

b. nature of output harmonics;

c. nature of current harmonics created in the power supply line;

d. ability to accept regenerated energy.

TABLE 2.1

System	Conversion Function
1. AC voltage controllers	Fixed voltage ac to variable voltage ac.
2. Rectifiers (uncontrolled or controlled)	Fixed voltage ac to fixed voltage dc or variable voltage dc.
3. DC-to-dc converters (choppers)	Fixed voltage dc to variable voltage dc
4. Inverters (Uncontrolled or controlled)	Fixed voltage dc to fixed voltage ac or variable voltage ac.
5. Cycloconverters	Fixed frequency ac to variable frequency and variable voltage ac.

2.7 APPLICATION OF DC MOTORS

DC motors are very frequently used in different industrial and electric traction drives due to its high degree of flexibility and ease of control. These features can not be obtained easily in other electro-mechanical energy conversion devices. The dc motors offer a wide range of control of speed and torque as well as excellent acceleration and deceleration. As a result dc motors are often used in applications requiring a wide range of motor speed or precise control of motor output. Shunt motors are used for driving constant speed load, centrifugal pumps, machine tools, blowers and fans, reciprocating pumps etc. Series motors are used for electric locomotives, rapid transit systems, trolley cars, cranes and hoists, conveyers etc. And the compound wound motors are found suitable for elevators, conveyers, heavy planer, rolling mills etc. The speed-torque characteristics of different types of dc motors are shown in figure 2.4, from which some idea may be obtained, about the fields in which these motors are used or may be used.

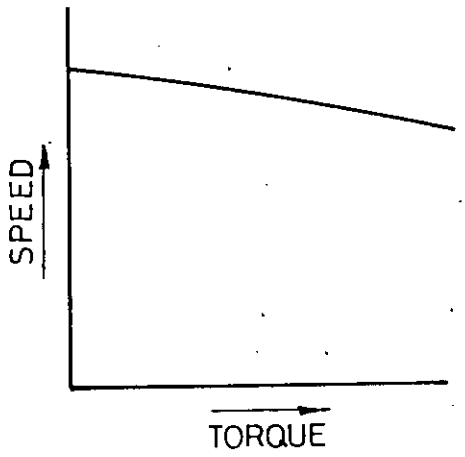

Separately excited motor

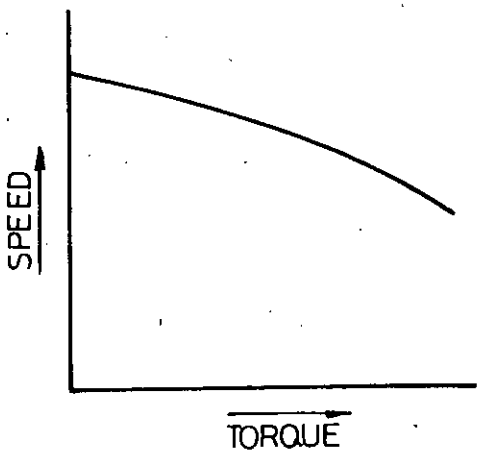

Shunt motor

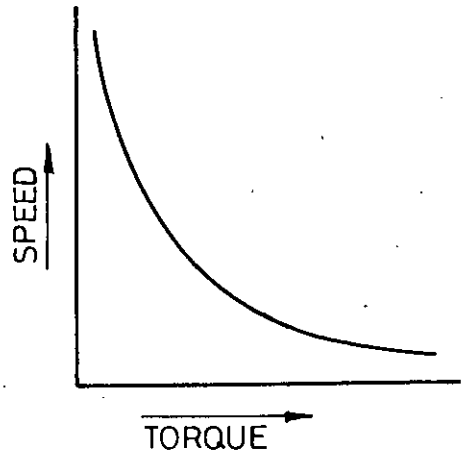

Series motor

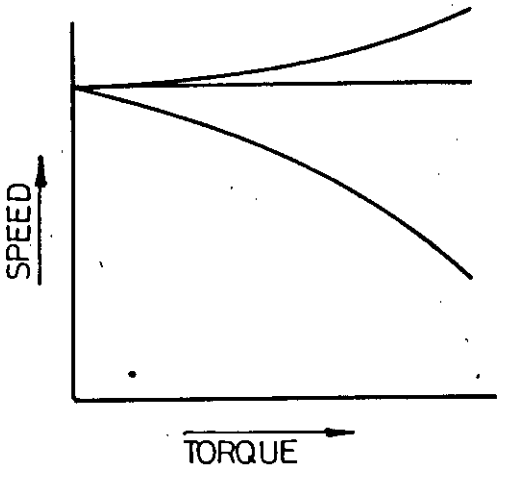

Compound wound motor.

FIG. 2.4 SPEED-TORQUE CHARACTERISTICS OF DIFFERENT TYPES OF D C MOTORS.

2.8 TECHNIQUES OF CONTROL OF DC MOTORS

The most outstanding characteristic of a dc motor is its adaptability of control of its torque and speed. The steady state output characteristics of dc motors are given by

$$T_e = K_a \Phi_d I_a \qquad (2.1)$$

$$\omega_m = \frac{V - I_a R_a}{K_a \Phi_d} \qquad (2.2)$$

where I_a and V are the steady state values of the armature current and terminal voltage, respectively, and K_a is machine constant fixed by the design of the armature winding. These equations, together with the magnetisation curve and method of excitation of the field windings, determine the built-in torque-speed characteristics. When these inherent characteristics do not provide the desired result, control of the torque and speed can be obtained by variation of any of the three quantities R_a, Φ_d and V. These methods of control are as follows:

i. inserting resistance to the armature circuit (Armature or Rheostatic control method).

ii. controlling field excitation (Flux control method).

iii. controlling the armature supply voltage (Voltage control method).

But when high precision, stability and speed of response are important specifications, the controller must be furnished with a measure of the actual performance; in other words, a feedback control system must be employed. Machine output, in the control sense, refers to more than simply the mechanical power delivered by the shaft of a motor or the electrical power delivered by a generator, although the power output is controlled in accomplishing other desired results. Among the more significant machine quantities over which control may be exercised are: speed, torque, position, acceleration, frequency, current, voltage etc. Hence the desired control performance can be achieved in

various ways. However the technique of control may be crudely classified into two categories.

i. Open loop control.

ii. Closed loop control.

2.8.1 Open Loop Control

Open loop control is very simple concept. It consists of some selected components those are inherently accurate. The characteristics of these components are used to obtain the desired control. The output has no effect on the input of the system. The block diagram of an open loop control system is shown in figure 2.5. Here no feedback system is employed. Cumulatively compounded generator, separately excited dc motor etc. are the examples of such system.

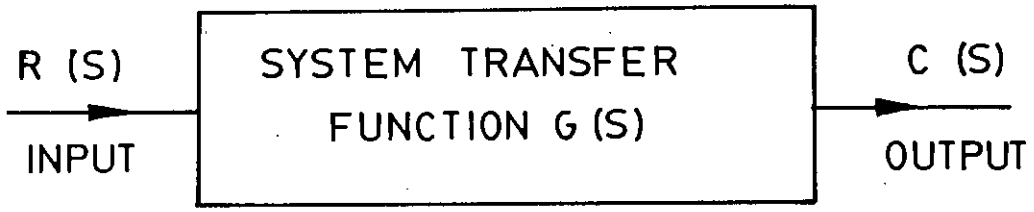

FIG. 2.5 BLOCK DIAGRAM OF OPEN LOOP SYSTEM

2.8.2 Closed Loop Control

In the closed loop control system the response (output) has an effect on the excitation (input). Here the response is sensed and fed back to the input to control the behavior of the system. Figure 2.6 shows the block diagram of a closed loop control system. The closed loop control system provides the advantages of minimum supervision and reduction of manual labour. The examples of such system are hoists and lifts, metadyne generator etc.

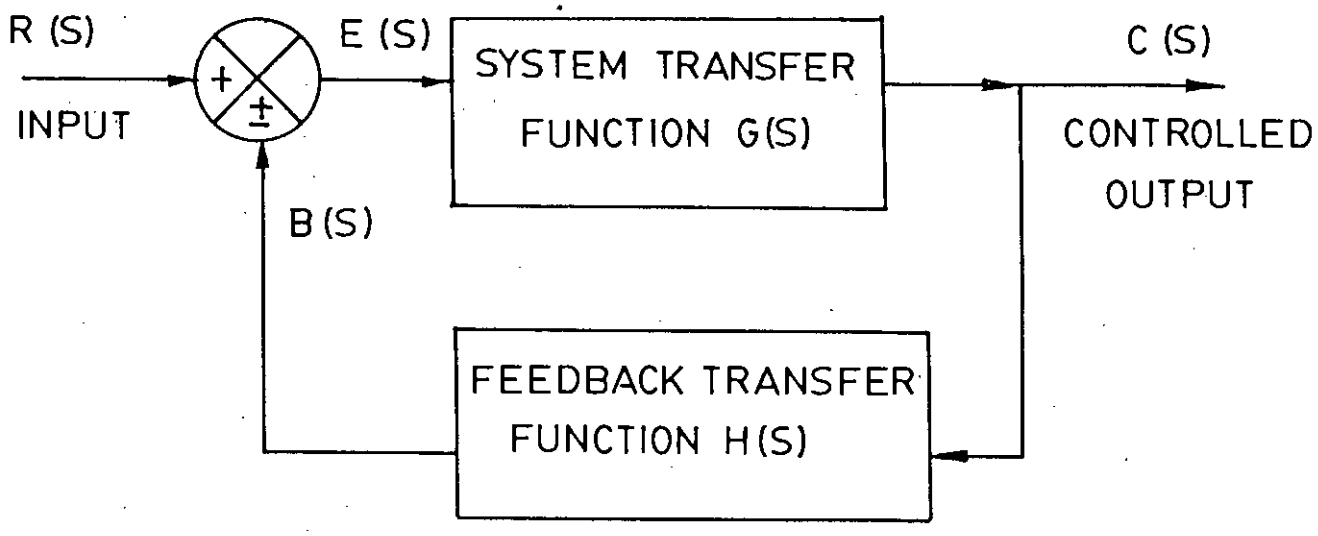

FIG. 2.6 BLOCK DIAGRAM OF CLOSED LOOP CONTROL SYSTEM

CHAPTER 3

CHOPPER DRIVES

3.1 INTRODUCTION

The economical availability of large thyristors has suggested a complete change in the concept of control engineering. Due to their compactness, fast response and higher efficiency most of the conventional control systems such as motor-generator set, thyratrons and mercury arc converters have been replaced by thyristor controlled ones, such as rectifiers, choppers, inverters and cycloconverters. Since in the present work the analysis of a chopper-controlled dc series motor has been carried out, it is necessary to discuss the operation and applications of choppers in some details and this has been done in this chapter.

3.2 CHOPPERS

DC-to-dc converters, commonly called choppers because of their principle of operation, are employed to vary the average value of the direct voltage applied to a load circuit by introducing one or more thyristors between the load circuit and a dc source. The function of a chopper is illustrated by figure 3.1. The manner in which the average load voltage is reduced below that of the source is illustrated in figure 3.2. This shows that the chopper applies a train of unidirectional voltage pulses to the load circuit, the magnitude of these pulses being the same as that of the source voltage. Load voltage V_o may be varied in one of three different ways.

1. Pulse-width modulation; t_{on} may be varied, while periodic time T is held constant.
2. Frequency modulation; t_{on} may be kept constant while T is varied.
3. Combined pulse-width and frequency modulation.

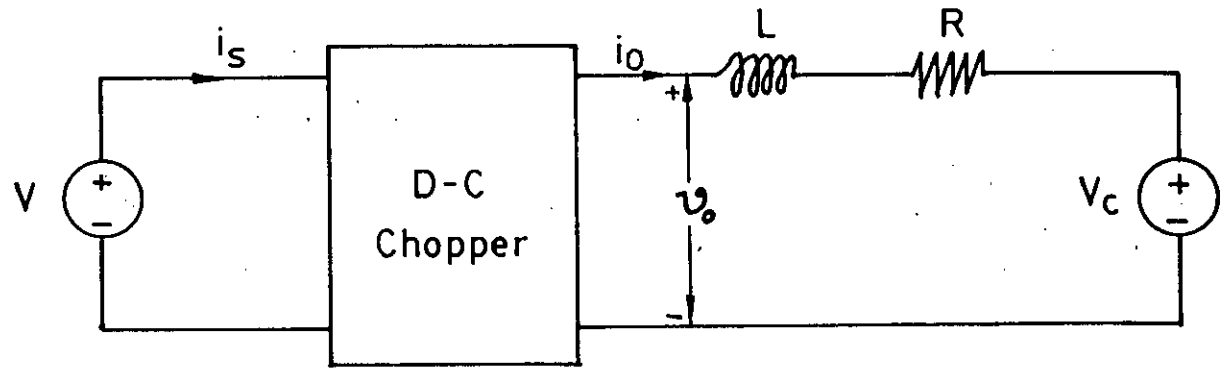

FIG. 3.1 BLOCK DIAGRAM OF A CHOPPER CIRCUIT

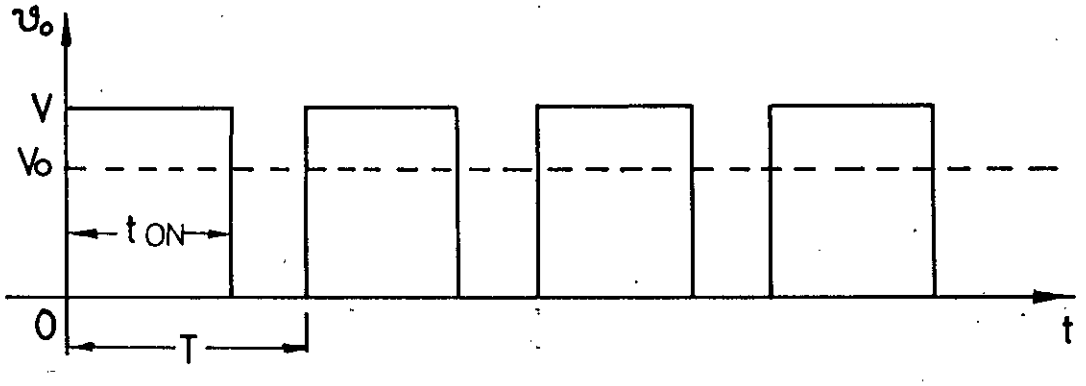

FIG. 3.2 FUNCTION OF A DC CHOPPER

3.3 CLASSIFICATION OF CHOPPERS

Choppers may be classified according to the number of quadrants of the v_o-i_o diagram in which they are capable of operating. A classification that is convenient for the discussion that follows is shown in figure 3.3.

3.3.1 Class A Chopper

Figure 3.4a illustrates the basic power circuit of a step-down single quadrant chopper. The model of the motor armature circuit is shown as three separate circuit elements. The term step-down signifies that the average terminal pd of the armature circuit is less than that of the source. The term single quadrant signifies that the armature circuit variables v_o and i_o occur only in the first quadrant of the v_o-i_o diagram. In the circuit diagram, the thyristor symbol enclosed in a circle represents a thyristor that may be turned on and commutated by means of circuit elements not included in the diagram; D_1 is a free-wheeling diode. Two possible conditions of operation are illustrated in figure 3.4b and 3.4c where it is assumed that the control is by means of frequency modulation.

In figure 3.4b, the load current i_o is discontinuous, so that during the interval for which i_o is zero, $v_o = E_a$. In figure 3.4c, the periodic time T has been reduced to such an extent that i_o has not ceased to flow before Q_1 is again turned on. As a consequence, the output voltage v_o consists of a train of rectangular pulses of magnitude V. An increase of load circuit inductance L_a or a reduction of E_a would also tend to result in a continuous output current.

3.3.2 Class B Chopper

A class B chopper steps up the output terminal pd of a regenerating motor to feed energy back to the dc source. It may be formed from the components of the class A chopper rearranged by switching. A typical application

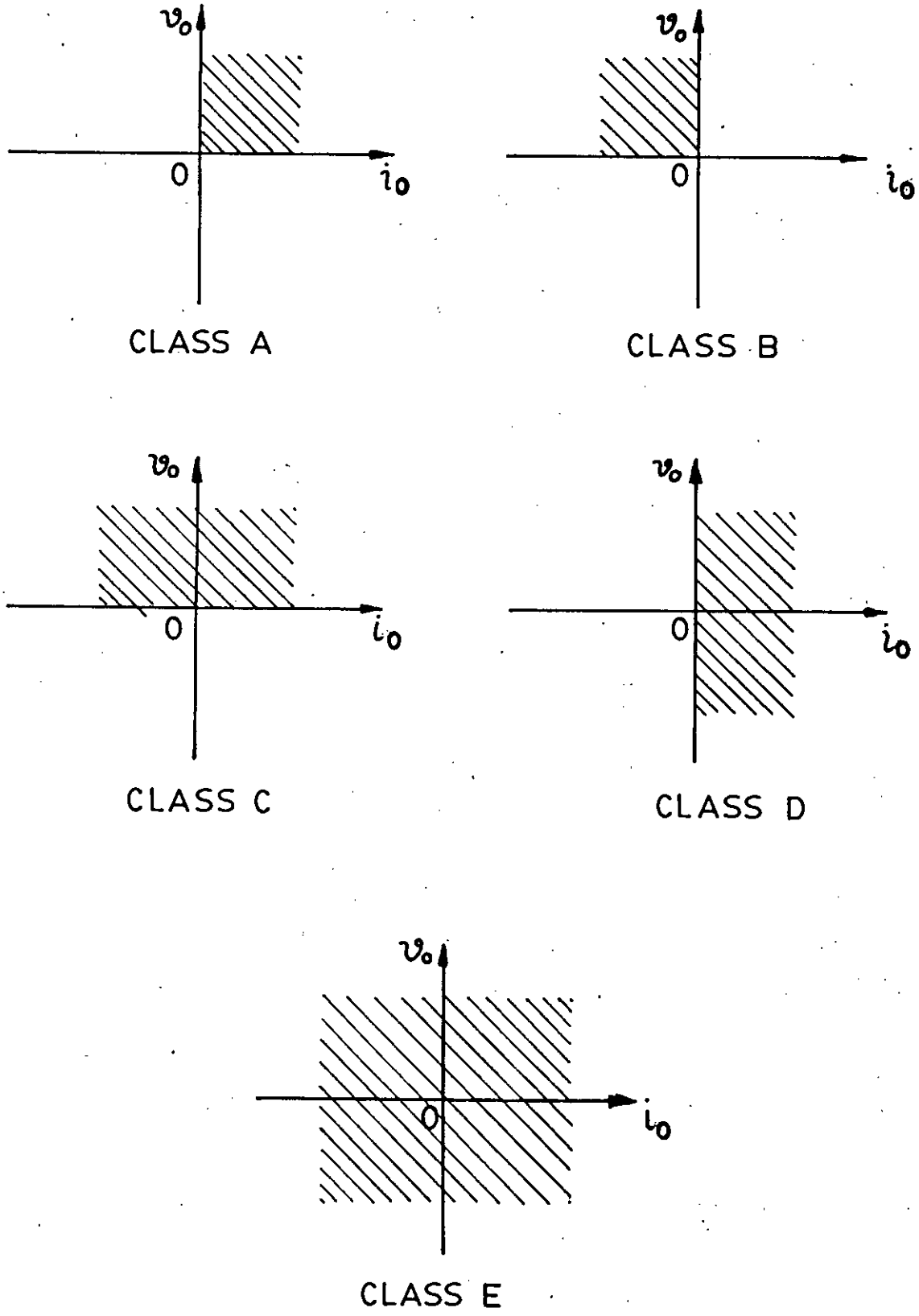

FIG. 3.3 CLASSIFICATION OF CHOPPERS BY QUADRANTS OF OPERATION

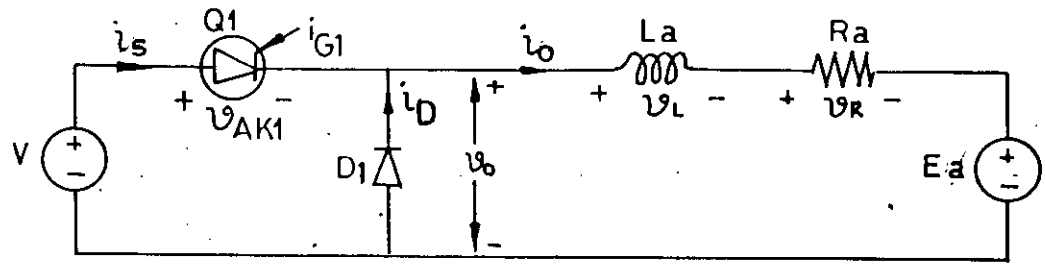

FIG. 3.4a BASIC POWER CIRCUIT OF A CLASS A CHOPPER

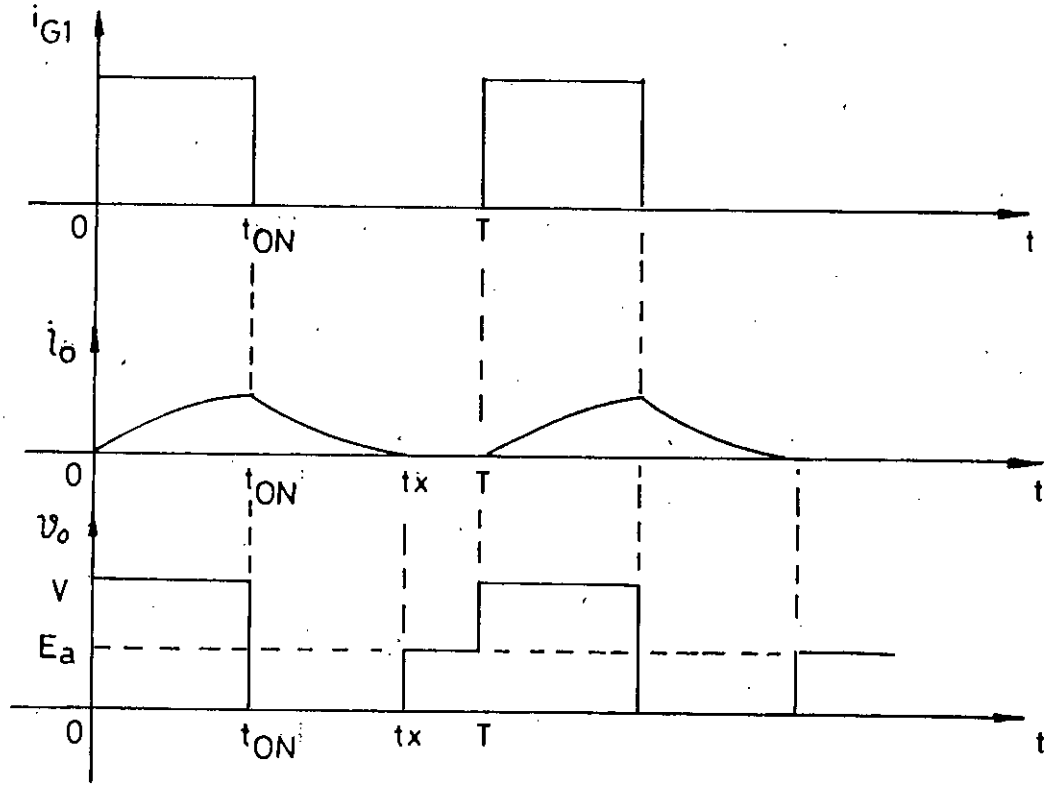

FIG. 3.4b BASIC PRINCIPLE OF OPERATION OF A CLASS A CHOPPER (Discontinuous output current)

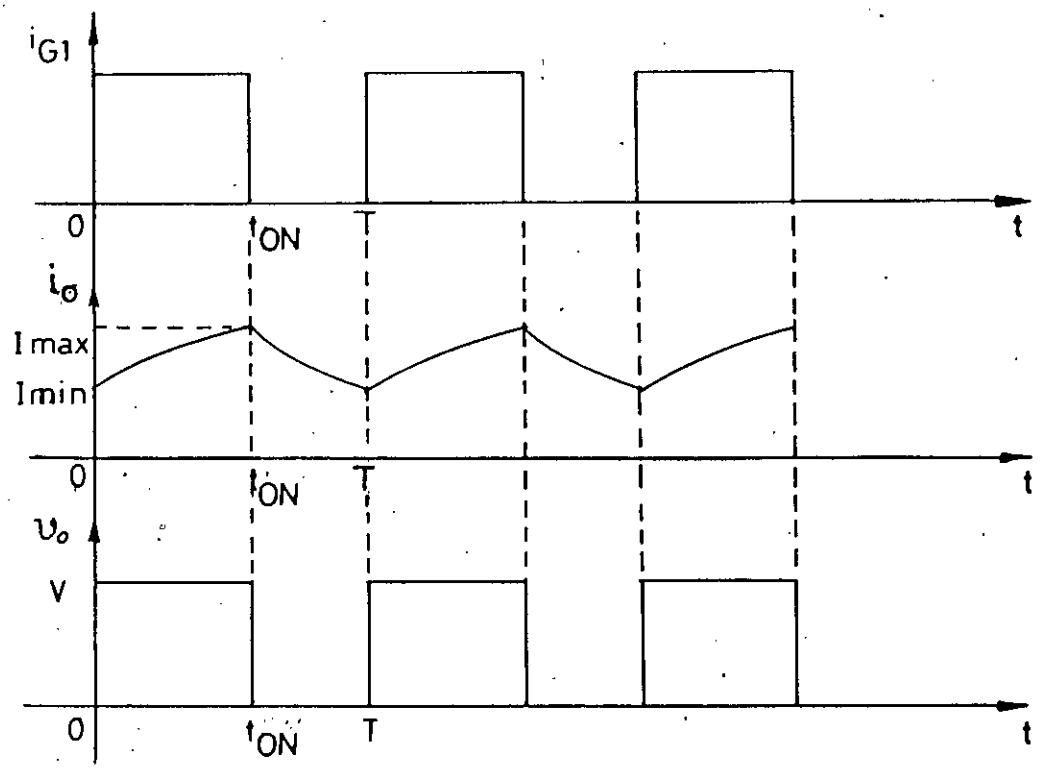

FIG. 3.4c BASIC PRINCIPLE OF OPERATION OF A CLASS A CHOPPER
(Continuous output current)

is the chopper drive of a subway train. The basic power circuit for class B operation is shown in figure 3.5a. The system is operating in the second quadrant of the v_o-i_o diagram. Operation with discontinuous output current is possible, but only continuous current operation in the steady state is shown in figure 3.5b. If thyristor Q_2 is never turned on and $V>E_a$, i_o and i_s are zero; therefore the circuit is completely inactive. If Q_2 is turned on and off during regular intervals of period T_p, emf E_a stores energy in inductance L_a whenever the thyristor is conducting and part of that stored energy is delivered to source V by current through D_2 when Q_2 is commutated. Here the interval during which D_2 conducts is designated as t_{ON}.

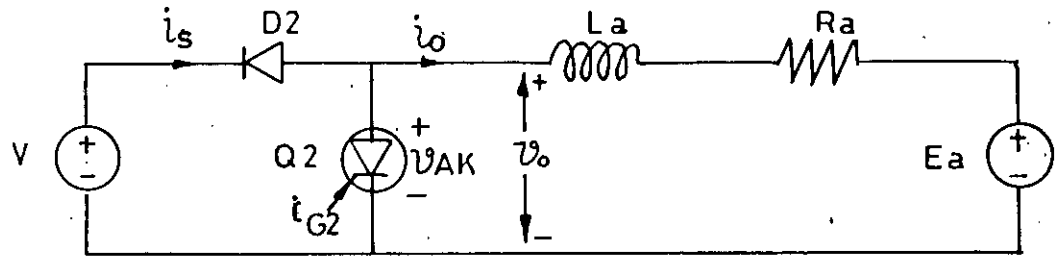

FIG. 3.5a BASIC POWER CIRCUIT OF A CLASS B CHOPPER

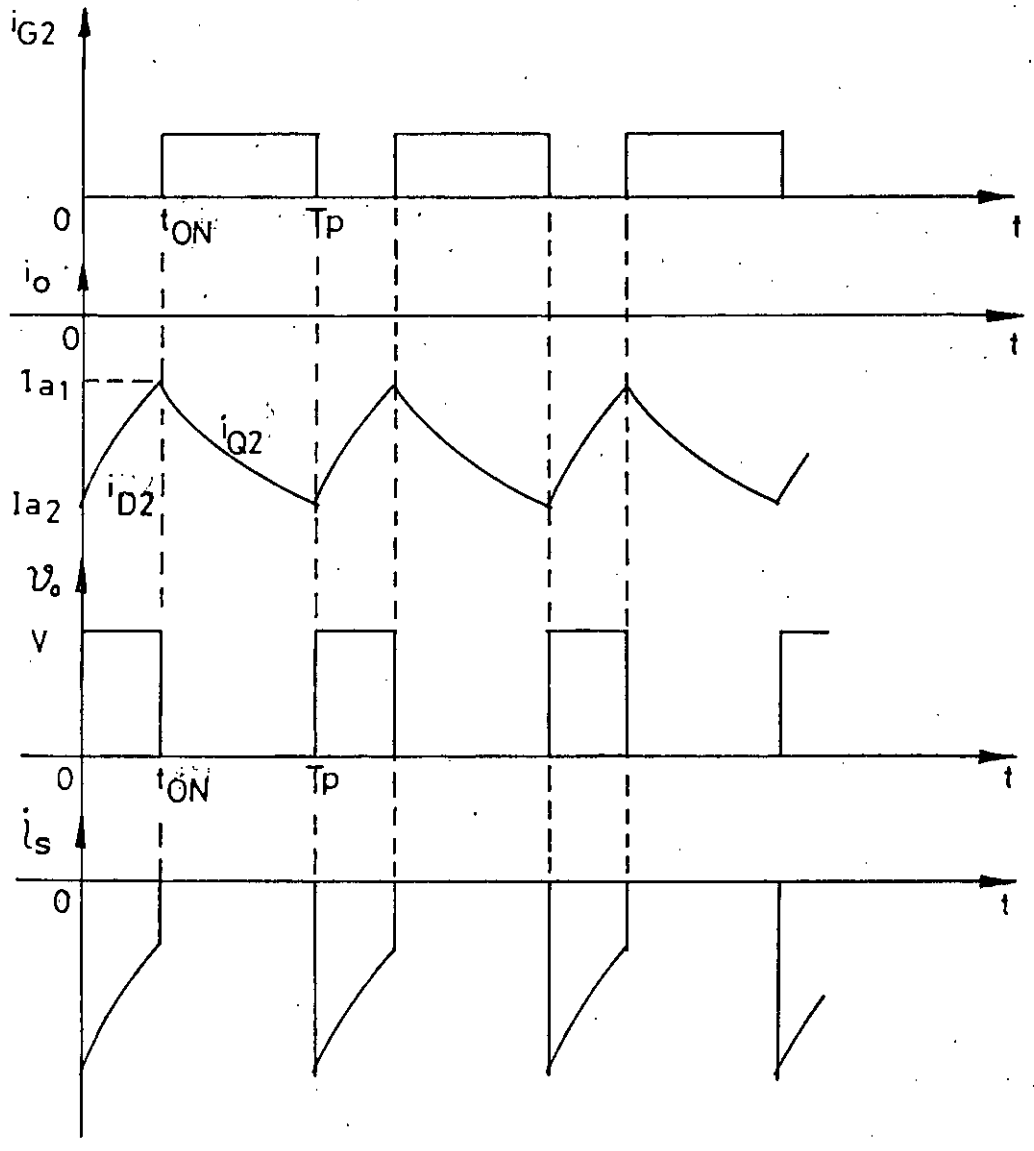

FIG. 3.5b BASIC PRINCIPLE OF OPERATION OF A CLASS B CHOPPER

3.3.3 Class C Two-Quadrant Chopper

Although switching from a class A to a class B configuration is a satisfactory method of obtaining regenerative braking for some applications, in others a smooth transition from driving to braking is essential. This is frequently the case in machine tool drives. A combination of the circuits of figure 3.4a and 3.5a provides the required drive.

Figure 3.6a illustrates a class C chopper, in which I_o may be either positive or negative but V_o can only be positive. A converter of this type may be employed with a load circuit that is capable of regenerating and returning energy to source V. Here, there are two thyristors that can be turned on and commutated. It is clear that both thyristors may not be turned on simultaneously because that would short circuit source V. For operation with positive output current, thyristor Q_1 and diode D_1 are controlled and the function is exactly the same as in class A chopper. For operation with negative output current elements Q_2 and D_2 are employed, while Q_1 is turned off. If $E_a>0$ and Q_2 is turned on, then a negative i_o will flow and energy from source E_a will be stored in inductance L_a. If Q_2 is then commutated, a positive value of v_L will result and, in conjunction with source voltage E_a, will drive current i_o through diode D_2 and the source V, in this way supplying the energy stored in inductance L_a to source V.

The basic principle of operation of a class C chopper is illustrated by figure 3.6b and 3.6c. The operation can be divided into four categories. If the independent variables of figure 3.6a are such that $I_{min}>0$, the converter is operating simply as a class A chopper with continuous output current. Thyristor Q_2 and diode D_2 do not conduct during any part of the cycle. This is first quadrant operation. If the independent variables are such that $I_{max}>0$, and $I_{min}<0$, then the result may be first quadrant operation as illustrated in figure 3.6b, where $I_o>0$. If the independent variables are such that I_{max} has a smaller positive value and I_{min} a larger negative value than are shown in

figure 3.6b, so that $I_o < 0$, then the result will be second quadrant operation. Finally, if the independent variables are such that $I_{max} < 0$, then $I_o < 0$, and the result is second quadrant operation. Under such condition, thyristor Q_1 and diode D_1 do not conduct during any part of the cycle. This condition is illustrated in figure 3.6c.

3.3.4 Class D Two-Quadrant Chopper

The basic power circuit of the class D chopper is shown in figure 3.7a. There is no advantage of using this converter as a source for a dc motor armature because first and second quadrant or four-quadrant operation is required for that purpose. It is of advantage, however, in controlling the field current of a dc or synchronous machine when rapid change of that current is required because it can short circuit its load circuit and rapidly reduce the field current. Thus, although a source of emf is included in the load circuit in figure 3.7a it may not be present.

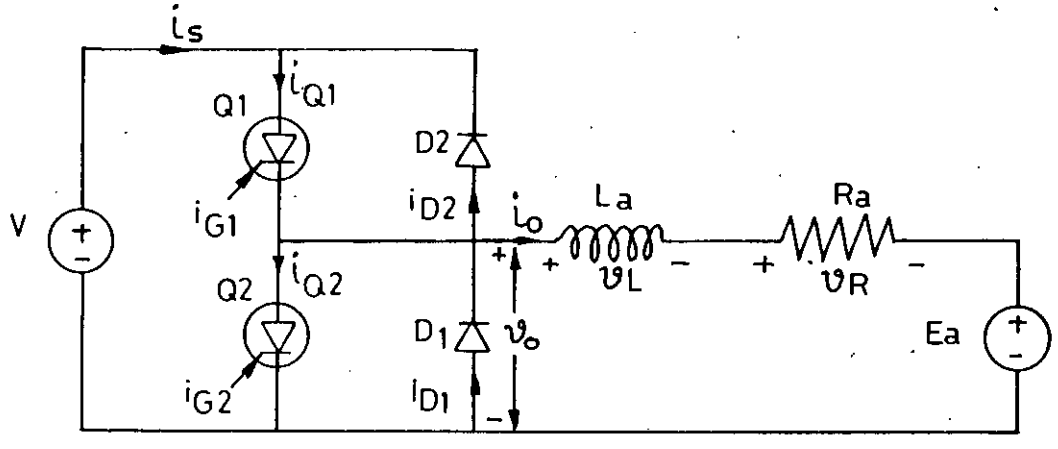

FIG. 3.6 a BASIC POWER CIRCUIT OF A CLASS C CHOPPER

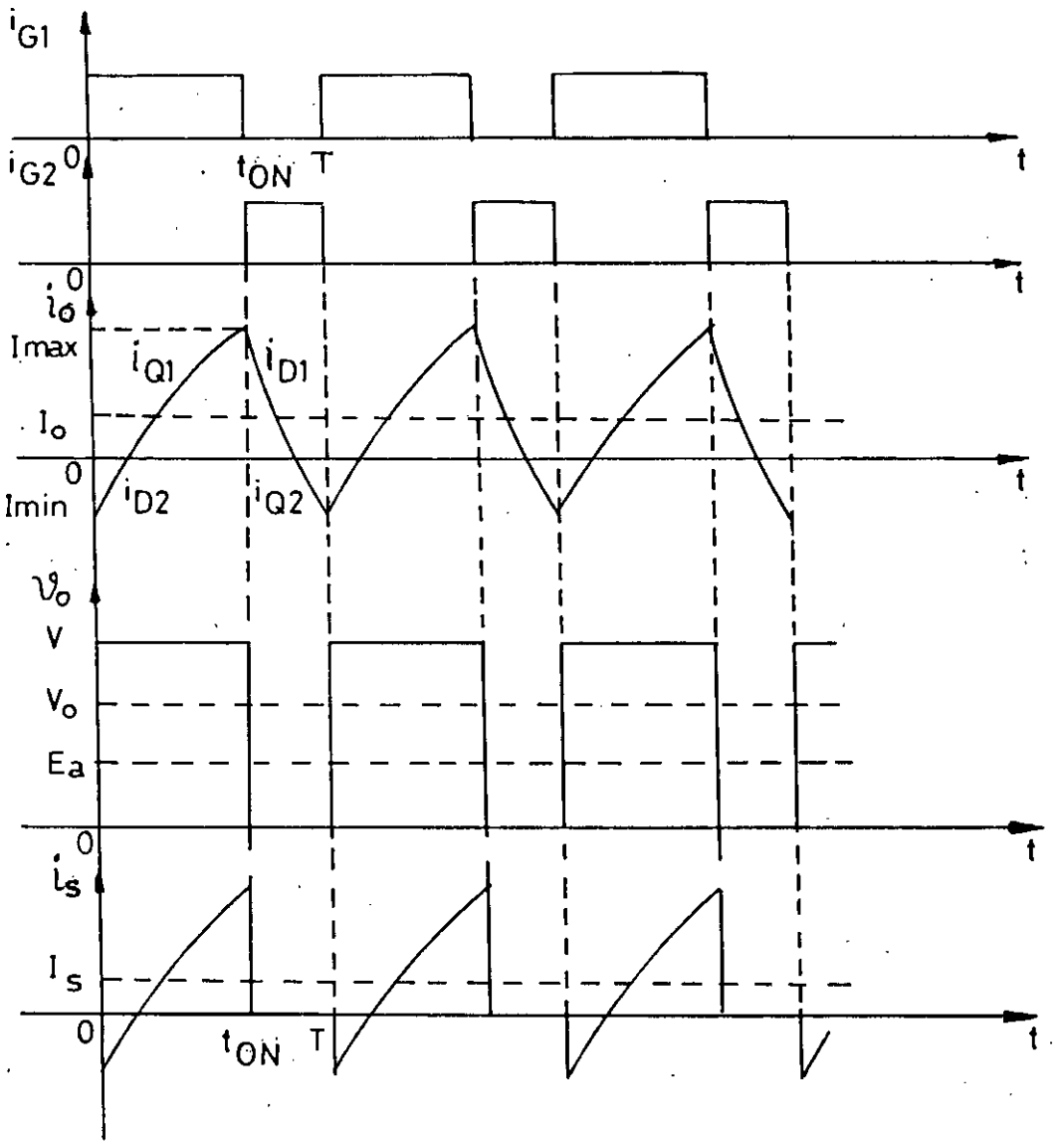

FIG. 3.6 b BASIC PRINCIPLE OF OPERATION OF A CLASS C CHOPPER (First-quadrant operation)

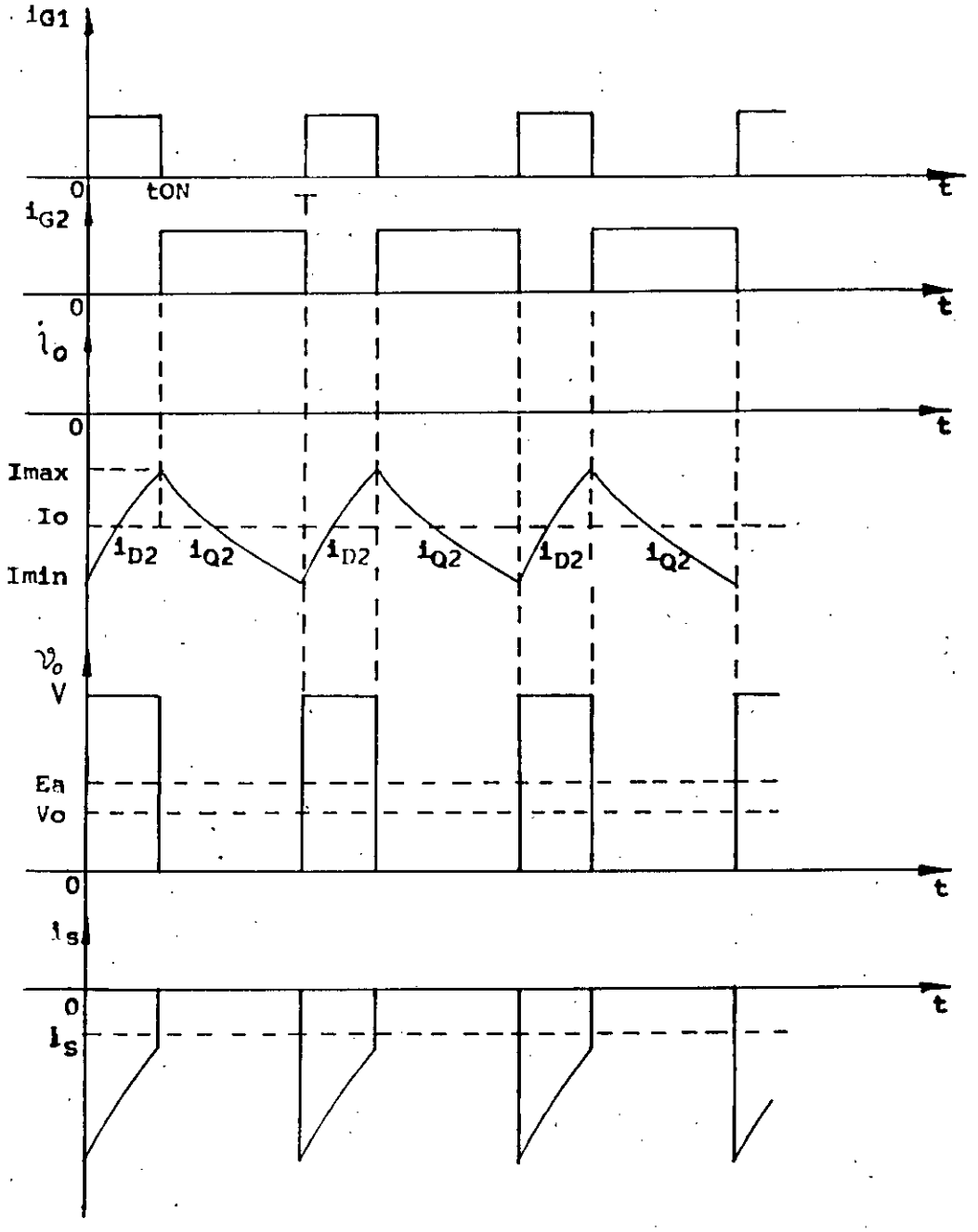

FIG. 3.6 c. BASIC PRINCIPLE OF OPERATION OF A CLASS C CHOPPER
(Second-quadrant of operation)

The operation of the circuit may be understood with the help of the waveforms in figure 3.7b and 3.7c. It is to be noted that the two thyristors are turned on alternately, their gating signals terminating at fixed points on the time axis and commencing at controllable points; the delay time for thyristor Q_1 is designated as t_α. If both thyristors are continuously turned on the load current rises to a constant magnitude expressed by

$$i_o = \frac{V-E}{R}$$

The periodic time of the gating signals is T_p and there are two modes of operation: one for which $t_\alpha < T_p/2$ and the two gating signals overlap; the other for which $t_\alpha > T_p/2$ and only one thyristor is turned on at any instant. These modes of operation are analysed below for continuous current i_o, although each may result in discontinuous current.

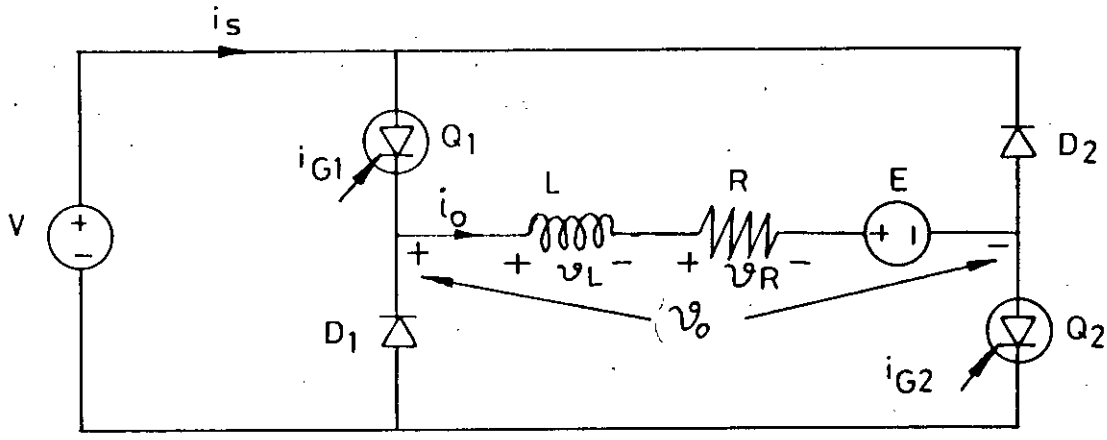

FIG. 3.7a BASIC POWER CIRCUIT OF A CLASS D, TWO-QUADRANT CHOPPER

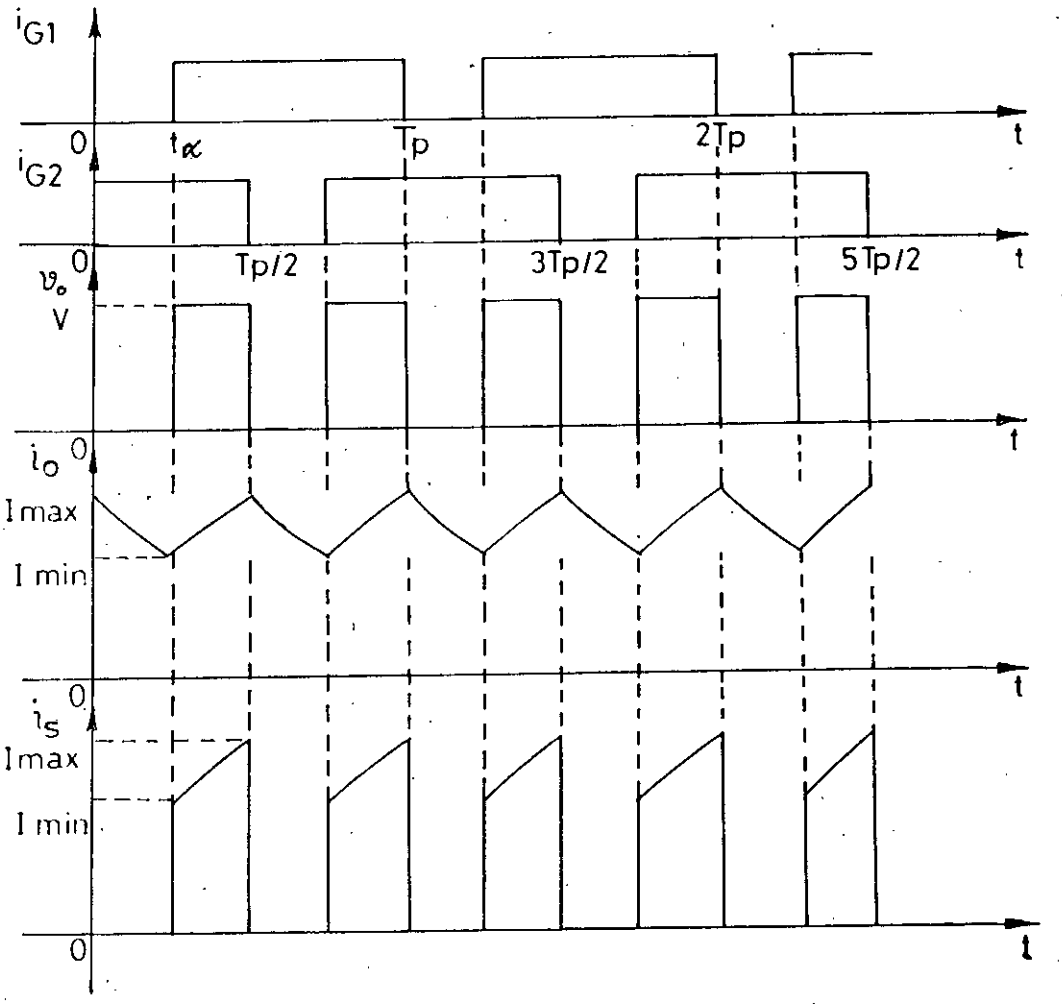

FIG. 3.7b WAVEFORMS OF THE VARIABLES IN FIG. 3.7a; $o < t\alpha < Tp/2$

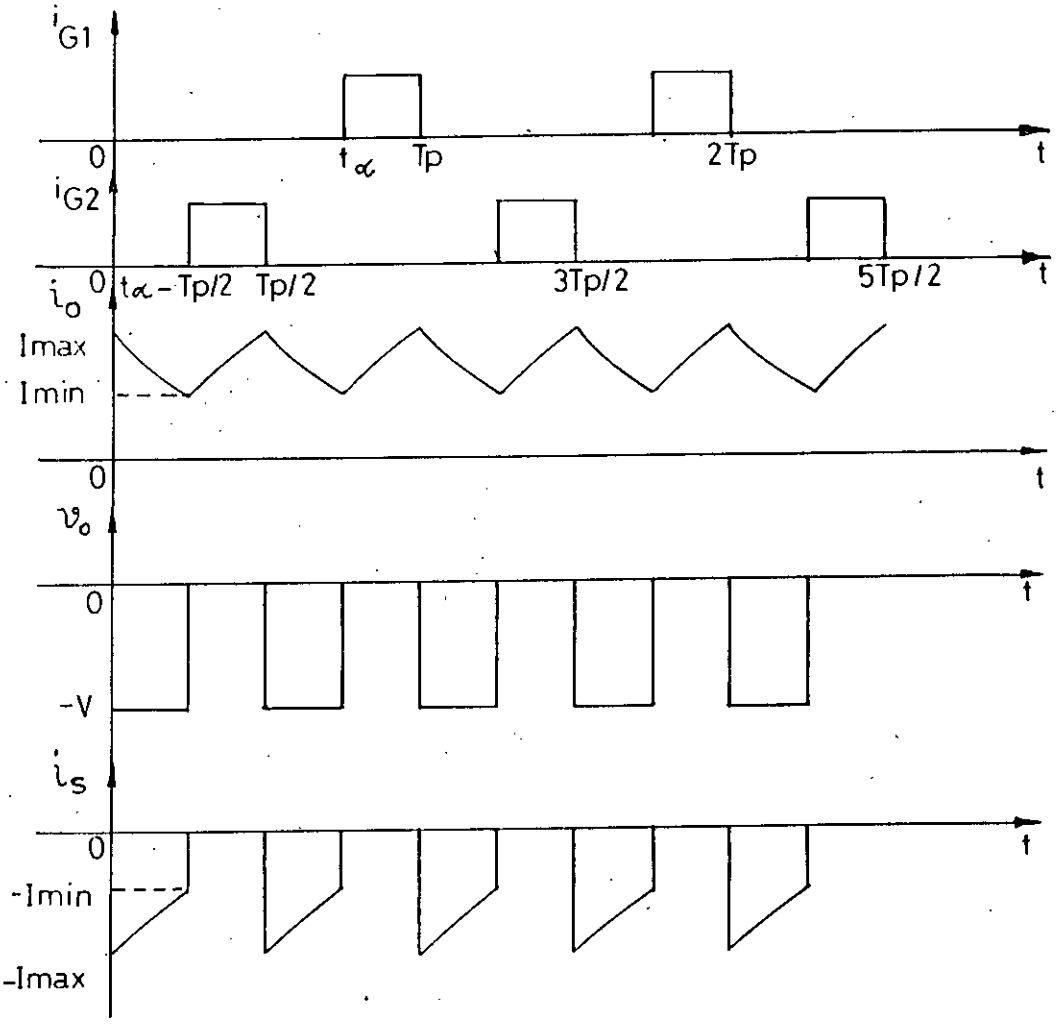

FIG. 3.7 c WAVEFORMS OF THE VARIABLES IN FIG. 3.7a ; $Tp/2 < t_\alpha < Tp$

Mode 1 Operation: $t_{\alpha} < T_p/2$

For steady state operation in this mode it is necessary that V>E. When both the thyristors are turned on source pd V is applied to the load circuit and current i_o increases. When only one thyristor is turned on that thyristor and one of the diodes short circuit the load branch and provide a path in which some of the energy stored in inductance L may be dissipated in maintaining a decreasing load current i_o. This mode of operation is illustrated in figure 3.7b.

Mode 2 Operation: $T_p/2 < t_{\alpha} < T_p$

For steady state operation in this mode it is necessary that E<0 and -E>V. Thus steady state operation with a passive load circuit, such as the field winding of a dc machine, is not possible in this mode. Two thyristors are not turned on simultaneously. When either one is turned on the load circuit terminals are shorted and the load current builds up because E<0. When neither thyristor is turned on the two diodes conduct and the load circuit supplies energy to source V. This mode of operation is shown in figure 3.7c.

3.3.5 Class E Four-Quadrant Chopper

The power circuit of a chopper that can operate in all four quadrants of the v_o-i_o diagram is shown in figure 3.8a. A converter of this type can provide both regeneration and reversal of the supply to the load circuit. If the control is so arranged that reversals of v_o and i_o occur cyclically at the same frequency, then the converter is in fact operating as a nonsinusoidal ac system, and functions as single phase bridge inverter.

If thyristor Q_4 is turned on continuously the antiparallel-connected pair of devices Q_4 and D_3 constitute a short circuit. Thyristor Q_3 may not be turned on at the same time as Q_4 because that would short circuit source V. Moreover, because under these conditions the terminal pd of diode D_4 is always negative, the pair of devices Q_3 and D_4 is equivalent to an open circuit. Con-

tinuous turn on of Q_4 thus produces a circuit equivalent to that of figure 3.6a (Class C) and operation in the first and second quadrants are possible. If on the other hand, thyristor Q_2 is turned on continuously the equivalent circuit in figure 3.8b results. In this circuit v_o is negative and operation in the third and fourth quadrants are possible. In this condition the quadrants of operation is also shown in figure 3.8b.

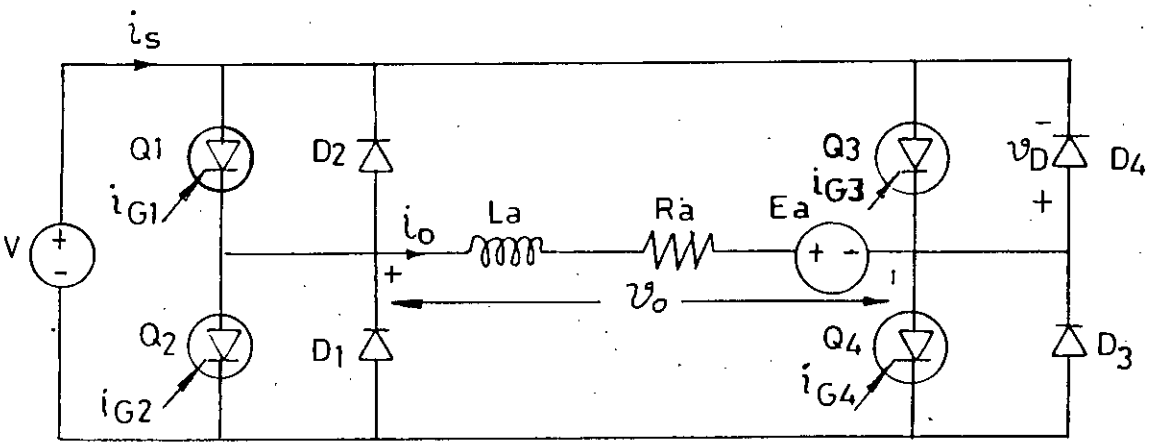

FIG. 3.8a BASIC POWER CIRCUIT OF A CLASS E, FOUR-QUADRANT CHOPPER

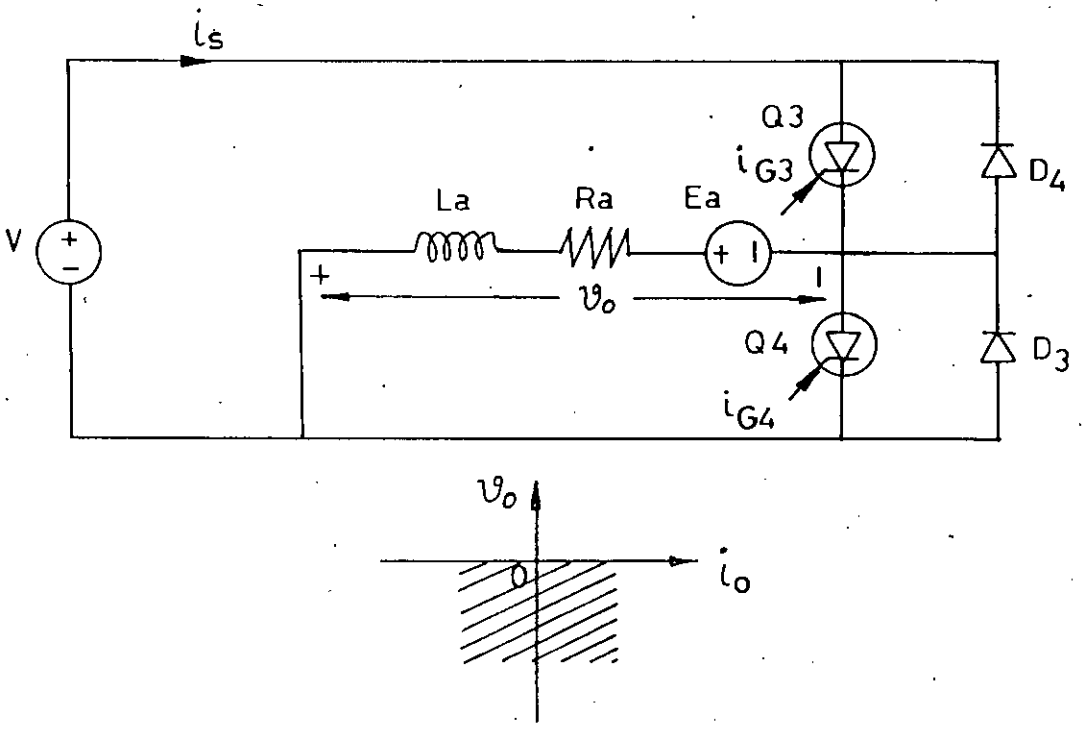

FIG. 3.8b EQUIVALENT POWER CIRCUIT OF A CLASS E CHOPPER, OPERATING IN THE THIRD AND FOURTH QUADRANT TOGETHER WITH ITS QUADRANTS OF OPERATION

3.4 COMMUTATION

In the present work the performance characteristics of a chopper-fed dc series motor is determined from its mathematical model and the analytical results are compared with the experimental one. In the experimental set-up the dc series motor is fed from a class C chopper, in which current commutation is utilized to commutate the thyristors. Hence a brief discussion of chopper commutation is necessary here.

An ideal transistor may be turned off; that is, its resistance to forward current restored to infinity, while forward current is flowing simply by reducing the base current to zero. This is not the case with a thyristor. Once turned on, a thyristor can not recover its resistance to forward current unless that current is reduced to zero and held there for at least the turn off time. A number of different methods may be employed to commutate or turn-off a thyristor and the method employed in a particular case depends on the function of the system embodying the thyristor. The three basic techniques of commutation are:

1. Line Commutation.
2. Load Commutation.
3. Forced Commutation.

Since in this work the Forced Current Commutation of chopper is utilized, so, this type of commutation is only discussed here.

3.4.1 Current Commutation of Class A Chopper

The circuit of a class A chopper with current commutation is shown in figure 3.9. Protective circuits are not shown in figure and inductor L_1 is linear. The additional elements not shown in figure 3.4a are required for current commutation. In particular, capacitor C is charged and employed to initiate the commutation of the main thyristor Q_1. The sequence of operation for the entire circuit is as follows:

i) The converter is connected to the source by closing switch SW and capacitor C is charged up to $v_c = V$ volts via resistor R_1.

ii) When the capacitor is fully charged, thyristor Q_1 is turned on, and load current i_o increases exponentially from zero to its maximum value I_{max}.

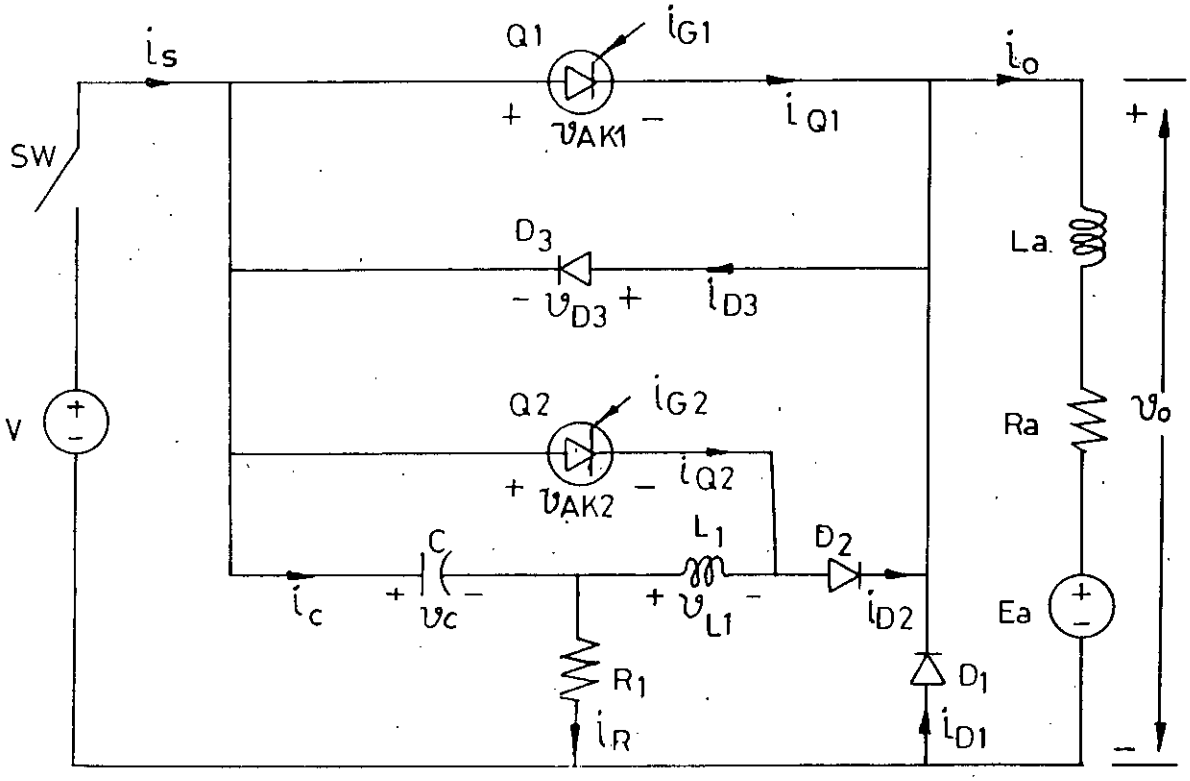

FIG. 3.9 CLASS A CHOPPER-CURRENT COMMUTATION

iii) To commutate the thyristor Q_1, Q_2 is turned on and an oscillatory current flows in the ringing circuit comprising C, L_1 and Q_2; i_c is initially negative. It is assumed here that the commutation interval is so short that i_o remains sensibly constant at the value I_{max} through out the interval. It is also assumed that R_1 is sufficiently large to permit i_R to be neglected in the analysis of commutation circuit, but is small enough to permit v_c to decay to the value V before the next commutation cycle is initiated

iv) When i_c becomes positive, diode D_2 conducts, Q_2 turns off and since i_o is assumed constant, i_c reduces i_{Q1}.

v) When i_{Q1} is reduced to zero by the increasing value of i_c, diode D_3 begins to conduct and the forward voltage drop across this diode commutates thyristor Q_1. Current ($i_c - I_{max}$) then flows through diode D3.

vi) After i_c has passed its maximum positive value and again become less than I_{max}, diode D_1 conducts. A new oscillatory circuit than exists, comprising C, L_1, D_2, D_1 and source V.

vii) The oscillatory cycle of i_c is completed, and i_c becomes zero, leaving $v_c > V$.

viii) i_o decays exponentially through D_1 from the value I_{max}, and simultaneously v_c decays through R_1 to leave $v_c = V$.

ix) When i_o is reduced to I_{min}, Q_1 is again turned on.

3.4.2 Current Commutation of Class C Chopper

The circuit of a class C chopper with current commutation is shown in figure 3.10a. The circuit employed for first quadrant operation is identical with that shown in figure 3.9, provided the following correspondences are observed:

Figure 3.10a		Figure 3.9
Q_1	corresponds to	Q_1
D_1	corresponds to	D_1
Q_{11}	corresponds to	Q_2
D_{11}	corresponds to	D_2
D_2	corresponds to	D_3
C_1	corresponds to	C
L_1	corresponds to	L_1
R_{c1}	corresponds to	R_1

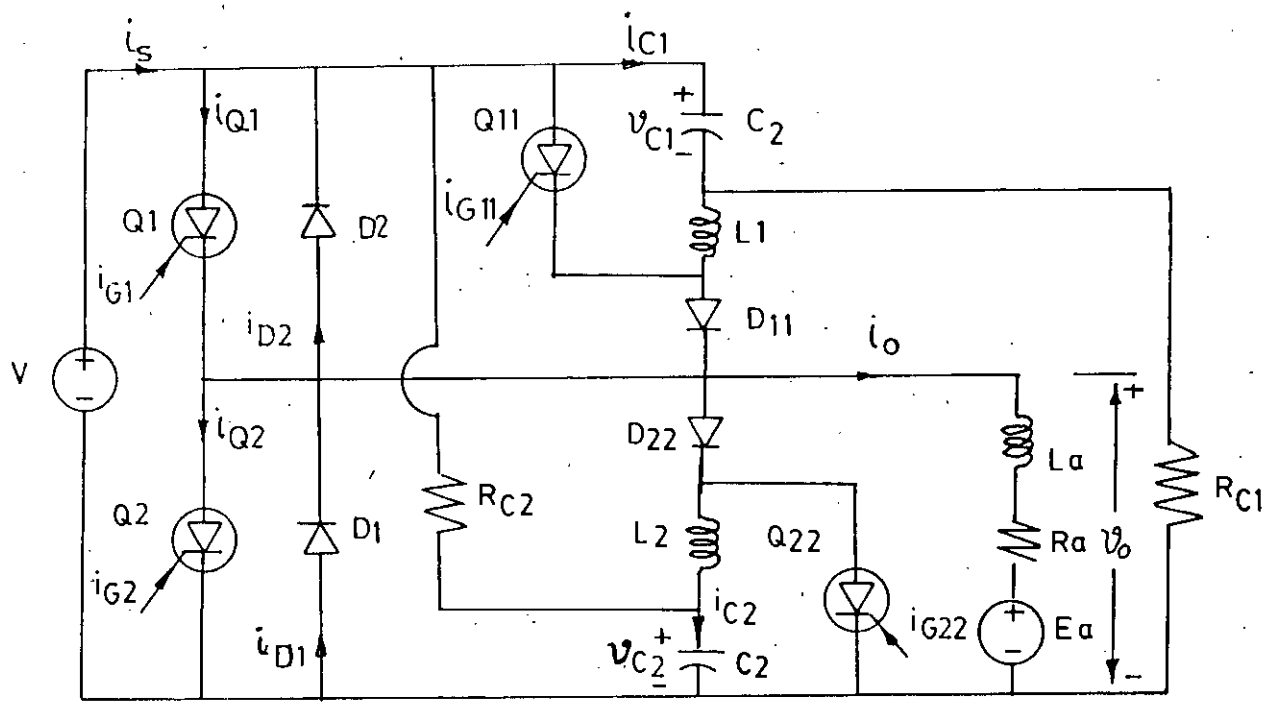

FIG. 3.10 a CLASS C CHOPPER-CURRENT COMMUTATION

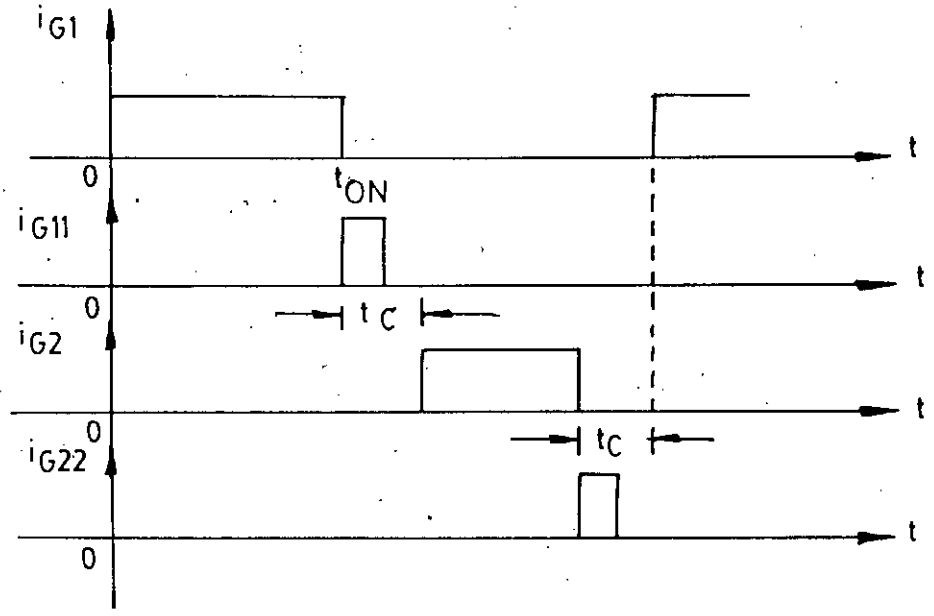

FIG. 3.10 b ARRANGEMENT OF THE GATING SIGNALS FOR CURRENT COMMUTATION OF A CLASS C CHOPPER

If the class C chopper is operating in the first quadrant, and i_o is always positive, then the explanation of the commutation circuit given in section 3.4.1 may be applied directly to the circuit of figure 3.10a. The commutation circuit employed for second quadrant operation is identical with that shown in figure 3.9, provided the following correspondences are observed:

Figure 3.10a		Figure 3.9
Q_2	corresponds to	Q_1
D_2	corresponds to	D_1
Q_{22}	corresponds to	Q_2
D_{22}	corresponds to	D_2
D_1	corresponds to	D_3
C_2	corresponds to	C
L_2	corresponds to	L_1
R_{C2}	corresponds to	R_1

If the class C chopper is operating in the second quadrant, and i_o is always negative, then the explanation of section 3.4.1 may again be applied. The fact that the power circuit configuration for this quadrant of operation differs from that of the class A chopper does not in any way affect the operation of the commutation circuit.

If the class C chopper is operating in the first or second quadrant under such conditions that $I_{max}>0$ and $I_{min}<0$, as illustrated in figure 3.6b, then an interval must be allowed to elapse between the end of the gating signal for one main thyristor and the beginning of the gating signal for the other. The reason for this may be seen by considering the operation of the

circuit at the end of a current pulse from thyristor Q_1. When the gating signal is removed from Q_1 and Q_{11} is turned on to initiate the commutation cycle, it is not permissible to turn on Q_2 until Q_1 has turned off, otherwise the source V would be short circuited. The Q_1 commutation cycle must therefore be completed, before Q_2 may be turned on. It is therefore normal practice to delay the gating signal on each of the main thyristors until the entire commutation interval of the other has elapsed. The necessary arrangement of the gating signals is therefore that illustrated in figure 3.10b.

3.5 CHOPPER DRIVES

The dc chopper regulator as shown in figure 3.11 is widely used to control a dc series motor in traction applications [38-39]. Besides providing continuous and low loss control of the traction motor voltage, the regulator has been conveniently utilized for regenerative braking of the motor as shown in figure 3.12, even at very low speed. With thyristor chopper regulator, the back emf generated need not be greater than the supply voltage for regenerative braking as in the conventional case. Here during braking the motor armature terminals are first short circuited through the regulator and the motor current increases, thereby converting mechanical energy into inductive energy. Subsequent turning off the main thyristor Q_1 of Figure 3.12 by the auxiliary thyristor Q_2 would transfer a part of the stored inductive energy into the supply through the blocking diode D_1 as the current would have a tendency of continuing to flow because of the inductance of the motor circuit. In fact choppers are used to feed the dc motors mainly for two basic operations.

i. Motoring.

ii. Braking.

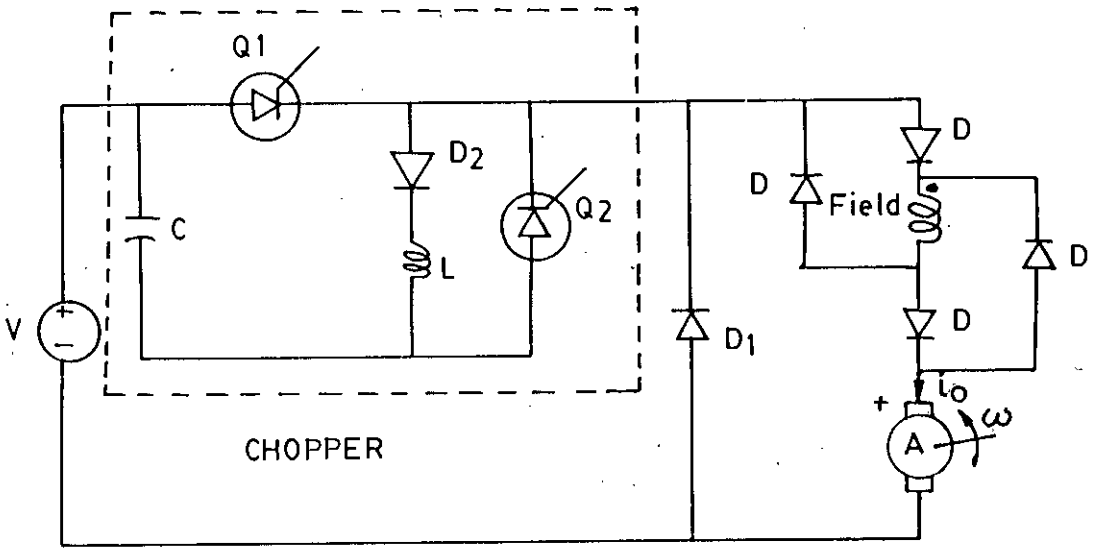

FIG. 3.11 CHOPPER CONTROLLED DC SERIES MOTOR; MOTORING OPERATION

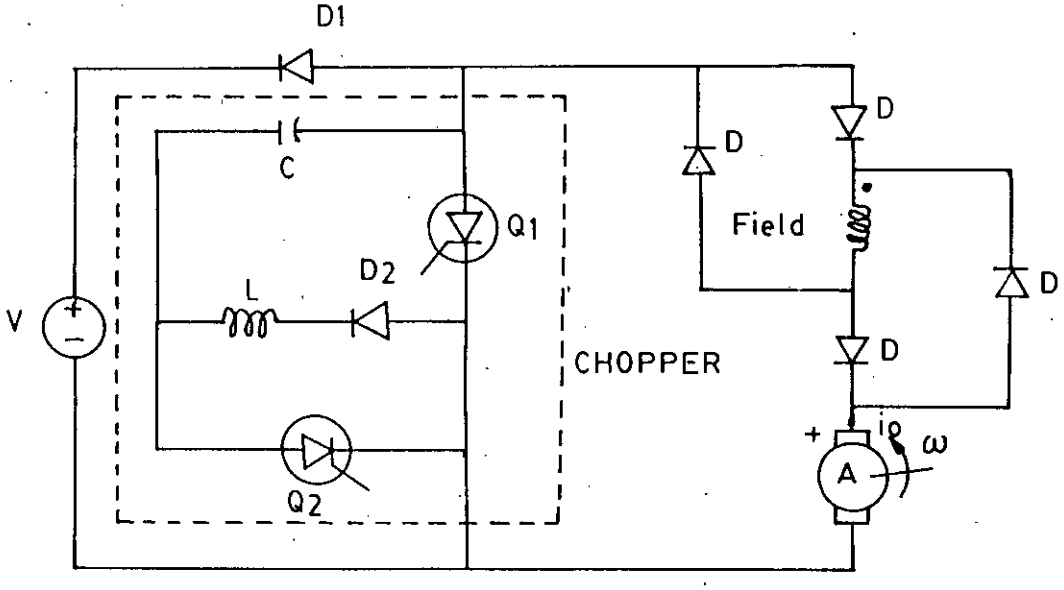

FIG. 3.12 CHOPPER CONTROLLED DC SERIES MOTOR; REGENERATIVE BRAKING OPERATION

3.5.1 Motoring Operation

The connection diagram of the dc series motor fed from chopper for motoring operation is shown in figure 3.11. The motor is by passed by a free-wheeling diode to permit the armature current to circulate after the chopper has been interrupted. During this motoring operation the chopper functions in its first quadrant of the v_o-i_o diagram.

3.5.2 Braking Operation

One of the major advantages of the chopper controlled dc series motor is its adaptability to several methods of braking, particularly regenerative braking with a partial return of power to the source. Three main types of braking that are usually applied to chopper controlled dc series motor are:

1. Dynamic Braking.
2. Regenerative Braking.
3. Plugging.

1. Dynamic Braking

The motor is connected as a self excited dc series generator as shown in figure 3.13. When the thyristor Q_1 is gated, the armature current increases. The mechanical energy supplied by the load partially increases the stored magnetic field energy and the remainder is dissipated in the resistance and the thyristor. When the latter is interrupted, the armature current flows through the relatively large load resistor R_M and the energy supplied by the load and the energy returned by the now decreasing motor field is dissipated in the armature and load resistance. During this period the current decreases. The resistor R_M can be added during the braking process if it should prove to be advantageous to increase the resistance of the armature circuit permanently.

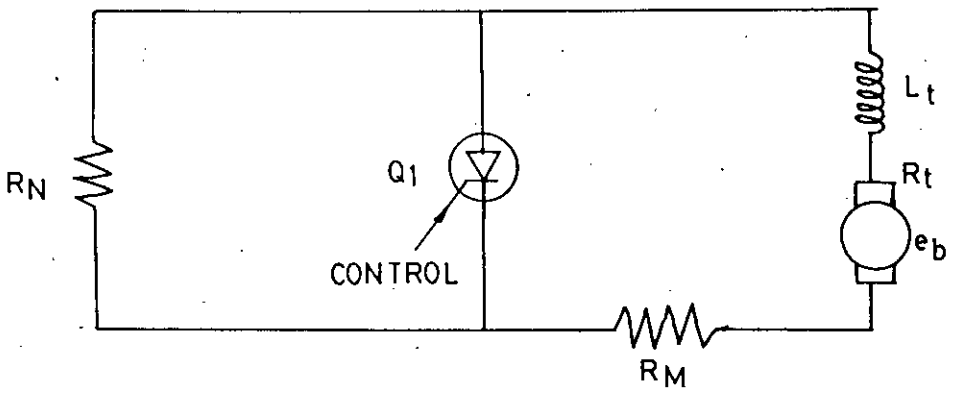

FIG. 3.13 MOTOR DIAGRAM FOR DYNAMIC BRAKING

2. Regenerative Braking

This method of braking is of particular advantage when a battery is used as a power supply. it is assumed that the power source is capable to accept instantaneous reverse power pulses without any increase in terminal voltage. The schematic diagram is shown in figure 3.12. When the thyristor Q_1 is triggered, the motor current will increase in the same manner as during the "on" period of the case of dynamic braking. The thyristor Q_1 is turned off when the current peak has been reached and the electromagnetic field energy of the motor is then returned across the blocking diode D_1 into the power source.

3. Plugging

During this condition, the load forces the motor to turn against its normal direction of rotation and hence its internal emf supports the applied line voltage. The current therefore increases rapidly as soon as the thyristor Q_1 is gated. After it is turned off, the current continues to circulate through the by pass diode D_1 and decays to its minimum value. The connection of the motor for plugging is shown in figure 3.14.

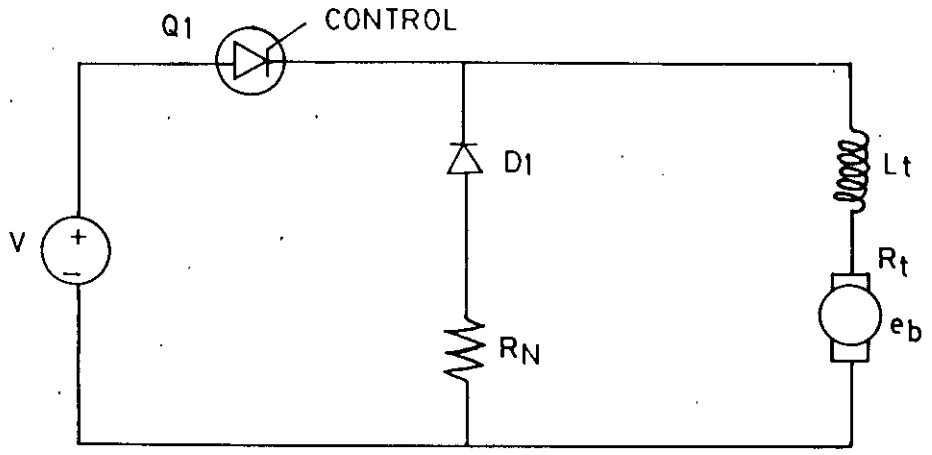

FIG. 3.14 MOTOR DIAGRAM FOR PLUGGING

3.6 APPLICATION OF CHOPPERS

If a supply of direct current at appropriate potential difference is available, it may be controlled by a dc-to-dc converter or chopper and used to supply the armature circuit of a separately excited dc motor or armature and field of a dc series motor. Because the use of dc is widespread in electric traction systems, chopper drives find a ready application in that field. Choppers are employed in variable speed dc drives, where it is desirable to eliminate the waste of energy in the form of heat produced in starting or control resistors, or where the operating characteristics obtained by such methods of control would be unsatisfactory.

Choppers find a particularly rich field of application in electric railways, where the advantages of dc power distribution are great and atleast in underground systems- the elimination of heating from motor control resistors is of first importance. The class C choppers are suitable for transportation drives, since it provides for operation both in the first and second

quadrant of the V_o versus I_o diagram and therefore gives the required smooth transition between motoring and regenerative braking. For the same reason class C choppers are also used widely in machine tool drives. Class D choppers are used to control the field current of dc or synchronous machine when rapid change of that current is required. Again the four quadrant operation of either type of motor may be obtained by means of class E chopper circuit.

CHAPTER 4

MATHEMATICAL MODEL

4.1 INTRODUCTION

For analysing the performance of dc series motor a good mathematical model of the machine should be formulated which should be valid for both dynamic as well as for steady state operating conditions. The dynamics of dc machine system is inherently nonlinear and thus, its complete representation, specially in the transient state, will be too complex for the purpose of formulating a realistic algorithm. It is really a cumbersome job to develop a model of dc series motor taking into account all of its behavior, particularly the nonlinearity arises from the following reasons:

i) Magnetic saturation.
ii) Eddy current.
iii) Commutation.
iv) Armature reaction.

However with some reasonable assumptions, a good mathematical model can be obtained to determine the steady state performances of dc series motor.

In this chapter two different mathematical models are formulated. With the help of the first model [35] the steady state performance of a chopper-fed dc series motor can be determined using some empirical formula which are based on some experimental results. This model leads to some approximate analytical expressions for average values of machine variables. On the other hand the second model requires the numerical solution of some nonlinear differential equations, which describe the operation of the motor.

4.2 MODEL BASED ON EMPIRICAL FORMULA [35]

Choppers can be operated either with time ratio control (TRC) or current limit control (CLC). The present work is concerned with the modelling and analysis of dc series motor controlled by a chopper with time ratio control (TRC). Accurate analysis should take into account the nonlinearity of the magnetic circuit, the variation in the value of motor inductance, armature reaction and eddy current effects. The output voltage of some choppers is either a square wave or can be approximated by a square wave. However, in some chopper circuits, particularly in those with load dependent commutation, this approximation is not valid. In such cases the method of analysis should also take into account the effect of commutation pulse on motor performance. Here an attempt has been made for modelling and analysis of TRC chopper-fed dc series motor taking all these effects into account.

4.2.1 Effect of Magnetic Saturation

It is well known that in a saturated magnetic circuit, the rise of current is relatively faster than in the case of non-saturated magnetic circuit. This is due to decrease of self inductance with saturation. The relationship between flux produced and excitation current is given by

$$\Phi = k_1' \, . i_f \qquad (4.1)$$

where $k_1' = f(i_f)$ (4.2)

Equation (4.1) effectively represents the B-H characteristics of dc machines. Under saturated condition, the field flux may be represented by Frolich's equation

$$\Phi = \frac{k_1 \, . i_f}{(k_2 + i_f)} \qquad (4.3)$$

where k_1 and k_2 are constants to be determined from the saturation characteristic of the machine. The main drawback of equation (4.3) is that, it departs quite widely around the low induction region. To overcome this, an em-

pirical relationship has been suggested by H.SATHPATHI, G.K.DUBEY and L.P.SINGH [35] in the form

$$\Phi = \frac{C.i_f}{(k_2+i_f)} + D.\log_e\left[\frac{k_2+i_f}{k_2}\right] \qquad (4.4)$$

where, constants C and D may be suitably chosen to yield satisfactory results as

$$C = k'\left[1-\frac{1}{D_1}\left(1-\frac{1}{I_o}\right)\right] \quad \text{and}$$

$$D = \frac{k'}{I_o D_1}$$

where k' and D_1 are constants and I_o may conveniently be chosen as the rated current. The expression for dc self inductance follows on differentiation of equation (4.4) as

$$L = N\frac{d\Phi}{di_f}$$

$$= \left[\frac{k_3}{(k_2+i_f)^2} + \frac{k_3(i_f-I_o)}{I_o D_1 (k_2+i_f)^2}\right] \qquad (4.5)$$

The measurement of self inductance of dc machine for different values of steady state current, can be done using a well known bridge method described by C.V.JONES [40]. The method developed by MELLITT and RASHID [41] can be used to measure inductance of machines of higher ratings. However in this work the self inductance of the series field coil for different steady state current is determined in a slightly different way. The self inductance of the coil as determined with the help of universal bridge is assumed to be the unsaturated value which corresponds to the very initial straight line portion of the open circuit characteristic of the machine. The open circuit voltage of a dc machine is given by

$$E_o = \phi Z N_1 (P/A) \qquad (4.6)$$

where E_o = Open circuit voltage.

Φ = Flux per pole.

Z = Number of armature conductors.

N_1 = Revolution per see.

A = Number of parallel paths.

P = Number of poles.

Now since for a particular machine Z, P and A are constants E_o can be written as

$$E_o = CN_1\phi$$

$$\text{or} \quad \frac{dE_o}{di_f} = CN_1\frac{d\phi}{di_f}$$

where $C = (ZP/A)$

$$\text{Again} \quad L = N\frac{d\phi}{di_f}$$

$$\text{or} \quad L = K_1\frac{dE_o}{di_f} \qquad (4.7)$$

where $K_1 = (N/CN_1)$ and considering that linkage of ϕ with exciting coil is hundred percent, N may be taken to be equal to the number of turns of the series coil. Now from the open circuit characteristics (OCC), the value of (dE_o/di_f) at different field current can be determined. The slope of the initial straight line portion of the OCC gives the value of (dE_o/di_f) which corresponds to the measured value of inductance if small value of leakage inductance is neglected. Hence from equation (4.7) the value of the constant K_1 can be determined. Then, determination of the inductances at different field currents requires only the determination of (dE_o/di_f) from the OCC of the machine. The empirical formulation for self inductance given by relationship (4.5) enables one to represent the dc machine self inductance satisfactorily. So, to take into account the effect of magnetic saturation of a particular machine the value of the constants k_2, k_3 and D_1 have to be determined such that the empirical formula for self inductance given by equation (4.5) fits the experimentally determined inductances of the machine.

4.2.2 Representation of Armature Reaction

It is well known that when the armature of the machine carries current, the armature reaction flux affects the main air-gap flux and thus the back emf coefficient K is not a constant and it may be represented as

$$K = f(i_f, i_a) \qquad (4.8)$$

The values of K can be obtained from the internal characteristic of the machine. In the present work the back emf coefficient K is assumed to be a function of average armature current (I_{av}), instead of instantaneous armature current (i_a). To determine the values of K as a function of both field and armature current, the external characteristics of the dc series machine is first determined by operating it as a separately excited dc generator. A series of curves is thus obtained showing the terminal voltage as a function of armature current with field current as a parameter. Then the internal characteristics can be determined from the external characteristics very easily, since the internal voltage or the back emf is simply given by

$$E_b = V + i_a R_a \qquad (4.9)$$

where R_a = Total armature circuit resistance.

Now since $E_b = K\omega_{av} I_{av}$, the back emf coefficient K is given by $E_b/(\omega_{av} . I_{av})$. Hence taking different points on the internal characteristics with known values of ω_{av} the value of K can be determined as a function of both armature and field current.

4.2.3 Effect of Eddy Current

The flux distribution inside a magnetic core excited by a time varying current is given by Maxwell's equation. Eddy currents are induced inside the pole cores, yoke, joints and fittings and also in closed paths formed in packets of armature laminations due to time varying excitation current. These eddy currents produce short duration magnetic fluxes which damp the building up or decay of the air-gap flux. To estimate the effects of eddy current on the ar-

mature induced emf recordings must be taken for measuring the dynamic field current and the armature induced emf for step input voltage to the field and also due to free wheeling of field current. The experimental arrangements are shown in figure 4.1 and 4.2.

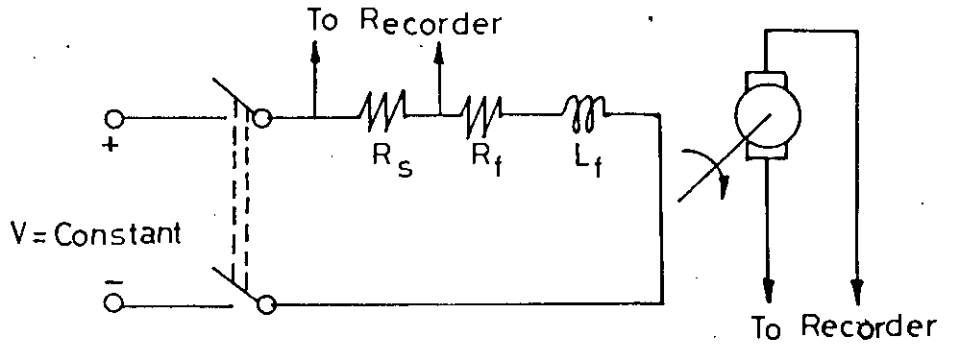

FIG. 4.1 EXPERIMENTAL ARRANGEMENT FOR RECORDING DYNAMIC RESPONSE WITH STEP INPUT VOLTAGE

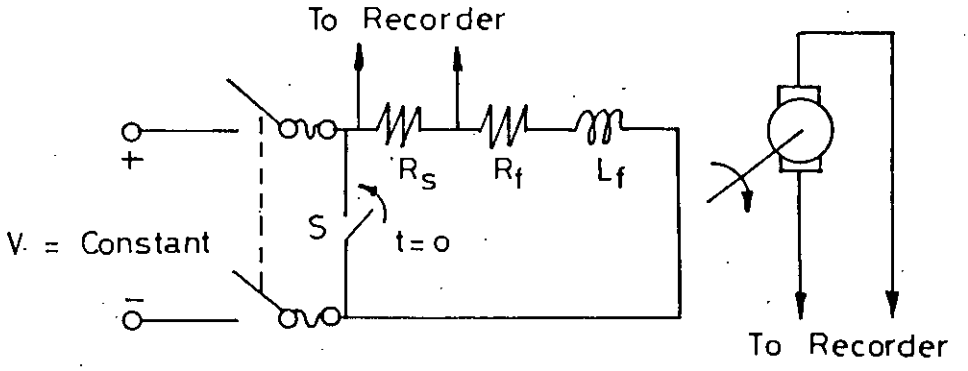

FIG.4.2 EXPERIMENTAL ARRANGEMENT FOR RECORDING DYNAMIC RESPONSE DURING FREE WHEELING OF FIELD CURRENT

The difference between the actual dynamic induced armature emf due to a step input to the field and the emf obtained from the OCC under steady state condition at constant machine speed is just due to the eddy current induced in the magnetic circuit. This difference in voltage may be represented by a functional relationship

$$\Delta V_e = f(i, \frac{di}{dt})$$

A generalized empirical relationship in the form shown below has been developed by trial and error [35] to match the dynamic response characteristics as recorded by the recorder

$$\Delta V_e = \lambda(\frac{\omega}{\omega_o})[\frac{i.\Delta i.sgn(di/dt)}{I_{fo}(k_2+i)} - \frac{k_2.\sigma.(i/I_{fo})^n}{(k_2+i)^2}.\frac{di}{dt}] \qquad (4.10)$$

where sgn = Sign of the derivative.

$\Delta i = (i-I_o)$

I_o = Final steady state current.

= I_{fo} for rising current and

= 0 for falling current during free wheeling.

k_2 = Frolich's constant.

σ = Constant dependent on the machine.

n = An index dependent on the design of the magnetic circuit.

λ = Constant of the machine.

I_{fo} = Maximum Current.

Hence to take into account the effect of eddy currents for a particular machine the dynamic response of the machine as well as the open circuit characteristics must be recorded. Then the constants, λ, n and σ must be determined so that equation (4.10) fits the experimentally determined points. The equation (4.10) thus provides an easy tool to account for the effects of eddy currents on the dynamic machine induced emf due to step input voltage to the field windings.

4.2.4 Steady State Analysis of Chopper-Fed DC Series Motor

The idealised voltage and current waveforms of chopper are shown in figure 4.3. The voltage and current waveforms for choppers using load dependent commutation are shown in figure 4.4. The current of a chopper-fed dc series motor fluctuates between a maximum and a minimum level and as a result, the motor parameter changes with current due to saturation effect. Moreover, eddy currents are induced in the field cores and influence the main field flux. Thus the performance equations of a chopper-fed dc series motor are highly nonlinear and difficult to solve. In the present work chopper-fed dc series motor has been analysed using empirical relationship of equation (4.10) and taking into account magnetic saturation, armature reaction and eddy current effects. The analysis has been carried out with the following assumptions

i) The thyristors and diodes are ideal switches.

ii) The conduction is continuous.

iii) Motor inductances are assumed to be functions of I_{av} instead of i_a.

iv) The back emf coefficient K is assumed to be a function of I_{av} instead of i_a, to take into account the effect of saturation and armature reaction.

v) The core losses and increase in resistance due to skin effect are neglected.

vi) The motor speed remains constant during the period of operation of the chopper.

With the above mentioned assumptions the following equations have been derived in Appendix A from which the performance of the motor can be determined easily.

$$\delta_c T = 2CV/I_{a2} \qquad (4.11)$$

$$I_{a1} = \frac{V}{R_{eq}}\left[\frac{1-e^{\delta T/\tau_a}}{1-e^{(1-\delta_c)T/\tau_a}}\right] - \left[\frac{K'.\omega_{av}}{R_{eq}}\right] \qquad (4.12)$$

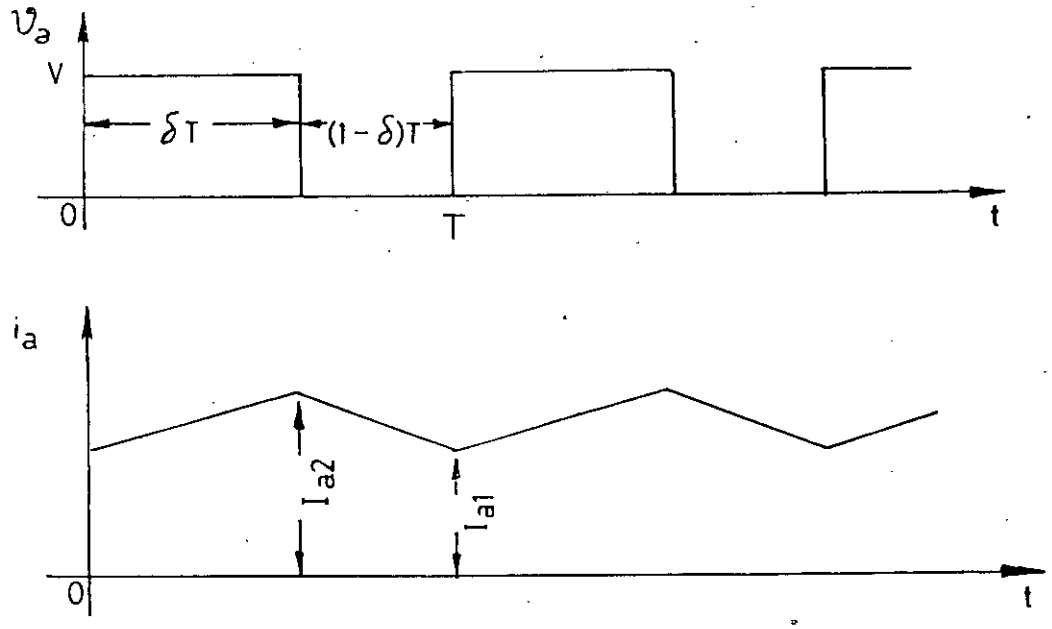

FIG. 4.3 CHOPPER OUTPUT VOLTAGE AND CURRENT WAVEFORMS (IDEAL CONDITION)

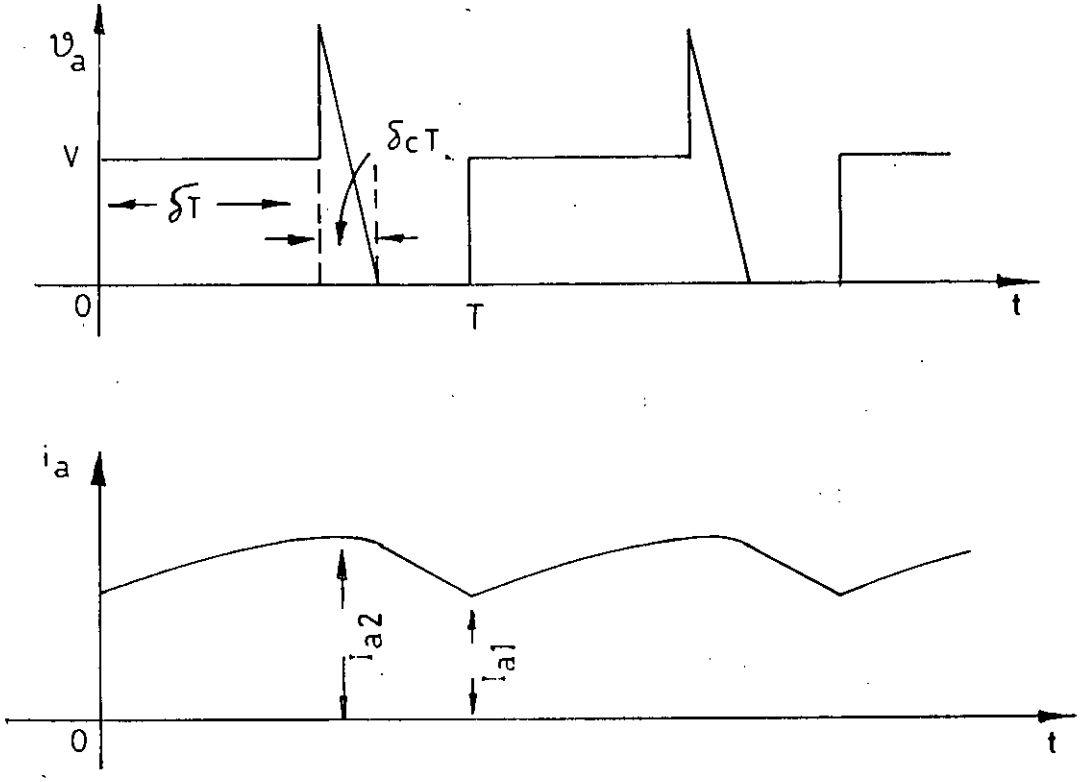

FIG. 4.4 CHOPPER OUTPUT VOLTAGE AND CURRENT WAVEFORMS (LOAD DEPENDENT COMMUTATION)

$$I_{a2} = \frac{V}{R_{eq}}\left[\frac{1-e^{-\delta T/\tau_a}}{1-e^{-(1-\delta_c)T/\tau_a}}\right] - \left[\frac{K'.\omega_{av}}{R_{eq}}\right] \qquad (4.13)$$

$$\omega_{av} = \frac{R_{eq}}{K'}\left[\frac{V}{R_{eq}}\left(\frac{1-e^{-\delta T/\tau_a}}{1-e^{-(1-\delta_c)T/\tau_a}}\right) - \left(\frac{2CV}{\delta_c T}\right)\right] = \frac{E_{av}}{K'} \qquad (4.14)$$

$$I_{av} = \frac{V}{R_{eq}}\left[\delta - (1-\delta_c).\left(\frac{E_{av}}{V}\right)\right] + \frac{2CV}{T} \qquad (4.15)$$

$$T_e = \frac{E_{av}.I_{av}}{\omega_{av}} = K'.I_{av} \qquad (4.16)$$

The values of δ_c for a given E_{av}/V can be determined from equation (4.11) on substitution of I_{a2} from equation (4.13), expanding the terms containing exp $(-\delta_c T/T_a)$ in terms of its power series and neglecting the third and higher order terms in δ_c. For known values of E_{av}/V and (T/T_a), the positive realistic value of δ_c can be obtained, I_{av} can be calculated from equation (4.15), and the corresponding value of K' can be obtained from the internal characteristic of the machine which includes both the saturation and armature reaction effect. The machine speed ω and the electromagnetic torque T_e can then be calculated from equation (4.14) and (4.16). Thus the steady state torque-speed characteristics of a chopper-fed dc series motor taking the effect of magnetic saturation, armature reaction and eddy currents into account can easily be determined with the aid of the equations (4.11)-(4.16).

4.3 MODEL BASED ON NUMERICAL SOLUTION

The performance equation of a chopped-fed dc series motor taking the effect of armature reaction, magnetic saturation and eddy current into account can be represented by some nonlinear differential equations. These nonlinear differential equations can be solved numerically with the help of fourth order Runge-Kutta method. The determination of steady state performance of a chopper-fed dc series motor neglecting the effect of eddy currents requires only the numerical solution of a first order nonlinear differential equation. But with considering the effect of eddy currents the system of equations rep-

resenting the chopper-fed dc series motor becomes a little bit complicated. In that case for determining the performance of the motor nonlinear simultaneous differential equations need to be solved. In formulating the mathematical model the following assumptions are made:

i) The output voltage of the chopper is assumed to be a square wave.

ii) The motor is controlled by the chopper with time ratio control (TRC).

iii) As the period of ON-OFF time of the chopper is very small in comparison with the mechanical time constant of the motor, variation of speed is not more than 1%-3% of its average value. So speed may be taken as constant.

iv) The hysteresis effects may be neglected.

v) The leakage inductances may be considered constant.

With the above mentioned assumptions the equation of the armature circuit of a chopper-fed dc series motor is given by

$$(L_{al}+L_{sl})\frac{di_a}{dt} + \frac{d\psi_{aq}}{dt} + \frac{d\psi_s}{dt} + K\phi_{ma}\omega + i_aR_a + \Delta v_b = v_a \qquad (4.17)$$

where, v_a = instantaneous applied voltage from the chopper.

L_{al}, L_{sl} = leakage inductances of the armature and series field coils respectively.

Δv_b = brush voltage drop.

ϕ_{ma} = the air-gap flux.

ψ_{aq}, ψ_s = flux linkages of the armature and series field coils respectively.

Now, since the output voltage of the chopper is assumed to be a square wave, equation (4.17) takes the form for ON time

$$(L_{al}+L_{sl})\frac{di_a}{dt} + \frac{d\psi_{aq}}{dt} + \frac{d\psi_s}{dt} + K\phi_{ma} + i_aR_a + \Delta v_b = V \qquad (4.18)$$

and for OFF time

$$(L_{al}+L_{sl})\frac{di_a}{dt} + \frac{d\psi_{aq}}{dt} + \frac{d\psi_s}{dt} + K\phi_{ma} + i_aR_a + \Delta v_b = 0 \qquad (4.19)$$

(4.18) and (4.19) are the two fundamental equations which are to be solved in order to predict the steady state performances of dc series motor controlled by chopper.

The air-gap flux ϕ_{ma} is a nonlinear function of total magnetomotive force(mmf) in the direct axis F_d as well as of the armature reaction F_a. F_d and F_a can be expressed as

$$F_d = N_s i_a + F_{ed} \qquad (4.20)$$

$$= N_e i_d$$

and $$F_a = \alpha_i N_a i_a / 2ap \qquad (4.21)$$

$$= N_a' . i_a$$

where, N_s, N_e = number of turns per pole pair of the series field coil and some arbitrarily chosen base exciting coil.

F_{ed} = mmf of the eddy currents in the direct axis.

i_d = total exciting current referred to the base exciting coil.

α_i = pole arc/pole pitch.

N_a = number of turns of the armature coil.

p = number of pole pairs.

a = number of pair of parallel paths.

N_a' = equivalent number of turns of armature coil.

The flux linkages ψ_s and ψ_{sq} are also nonlinear functions of F_d and F_a. ψ_s may be expressed as

$$\psi_s = (N_s/N_e).\psi_e \qquad (4.22)$$

where

$$\psi_e = pN_e \phi_{ma} \qquad (4.23)$$

= flux linkage of the arbitrarily chosen base coil.

The derivatives of the flux linkages of equation (4.17) may be expressed as

$$\frac{d\psi_s}{dt} = \frac{N_s}{N_e}\left(\frac{d\psi_e}{dt}\right) = \frac{N_s}{N_e}\left[\frac{\partial\psi_e}{\partial i_a}.\frac{di_a}{dt} + \frac{\partial\psi_e}{\partial i_d}.\frac{di_d}{dt}\right]$$

and

$$\frac{d\Psi_{aq}}{dt} = \left[\frac{\partial\Psi_{aq}}{\partial i_a}\cdot\frac{di_a}{dt} + \frac{\partial\Psi_{aq}}{\partial i_d}\cdot\frac{di_d}{dt}\right]$$

where Ψ_e is given by equation (4.23) and i_d is given by equation (4.20).

The dynamic inductances may be expressed through the symbols of inductances as

$$\left.\begin{aligned} \frac{\partial\Psi_e}{\partial i_a} &= M_{ea} \quad , \quad \frac{\partial\Psi_e}{\partial i_d} = L_e \\ \text{and} \\ \frac{\partial\Psi_{aq}}{\partial i_a} &= L_{aq} \quad , \quad \frac{\partial\Psi_{aq}}{\partial i_d} = M_{ae} \end{aligned}\right\} \qquad (4.24)$$

The above inductances are also functions of F_d and F_a. Considering equation (4.23)

$$\left.\begin{aligned} M_{ea} &= pN_e(\partial\phi_{ma}/\partial i_a) = pN_eN_a'(\partial\phi_{ma}/\partial F_a) \\ \text{and} \\ Le &= pN_e(\partial\phi_{ma}/\partial i_d) = pN_e^2(\partial\phi_{ma}/\partial F_d) \end{aligned}\right\} \qquad (4.25)$$

So, we see that the air-gap flux ϕ_{ma} and the flux linkage of the armature coil Ψ_{aq} must be calculated out as a function of F_d and F_a in order to solve the differential equation (4.17).

4.3.1 Calculation of Air-gap Flux, ϕ_{ma}

The air-gap flux ϕ_{ma} may be written as

$$\phi_{ma} = L\int_{-\pi/2}^{\pi/2} B(\theta)\,d\theta \qquad (4.26)$$

where

L = axial length of armature.

$B(\theta)$ = Flux density (in wb/m/rad) expressed as a function of angle θ, where θ is zero on the pole axis and +ve in the clockwise direction (figure 4.5).

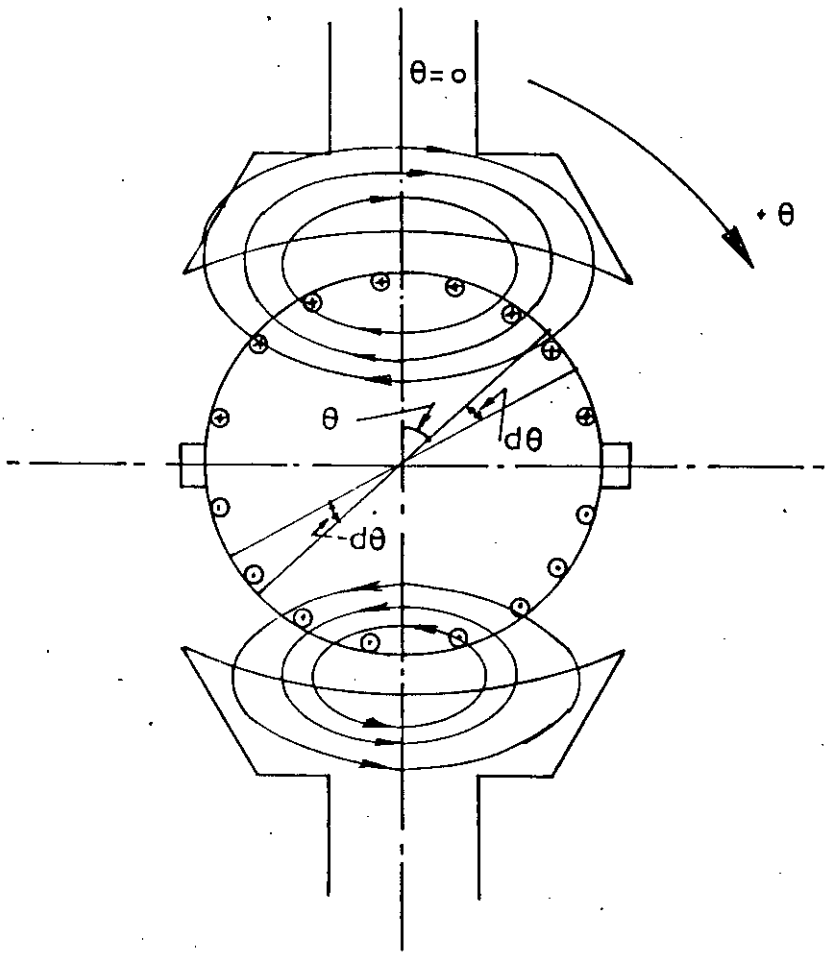

FIG. 4.5 DISTRIBUTION OF ARMATURE REACTION mmf OF 2 POLE MACHINE

But flux density at a point θ is also the function of the mmf F acting at that point. So it is possible to express the integral (4.26) in the following form

$$\phi_{ma} = L \int_{F-\pi/2}^{F+\pi/2} B(F) f'(F) dF \qquad (4.27)$$

where

$f(F)$ = function expressing θ as a function of F.

$f'(F)$ = first derivative of $f(F)$ with respect of F.

$B(F)$ = flux density expressed as a function of mmf F at different θ.

$F_{-\pi/2}$ and $F_{+\pi/2}$ are the mmfs at $\theta = -\pi/2$ and $\theta = \pi/2$ respectively.

The function B(F) may be found out using the magnetising curve of the motor which expresses the air-gap flux at no load as a function of field amp-turns. Using the concept that for dc motors the actual air-gap flux density curve at no load can be replaced by an equivalent one with constant value of flux density (which is equal to the value at the pole centre) over pole arc and zero flux density outside it, the magnetising curve may be shown in a modified form expressing pole centre flux density B_c as a function of field amp-turns as shown in figure 4.6. This curve can be treated as B(F) curve, which gives the value of flux density at different points if the amp-turns at these points are known.

Again the armature current produces the ampere turns linearly distributed on its surface as shown in figure 4.7. Armature reaction attains its maximum value F_a on the interpolar axis, reduces linearly to zero at the pole centre and reverses its sign to attain the -ve maximum value on the other interpolar axis. So armature reaction may be expressed as

$$F_a(\theta) = (2\theta/\pi)F_a .$$

The total ampere turns F then can be expressed as the following function

$$F = F_d + (2\theta/\pi)F_a \quad , \quad -\pi/2 \leqslant \theta \leqslant \pi/2 \qquad (4.28)$$

The value of F_d is independent of θ. Expressing θ as a function of F

$$\theta = [(F-F_d)/2F_a]\pi = f(F)$$

So, $f'(F) = (\pi/2F_a)$.

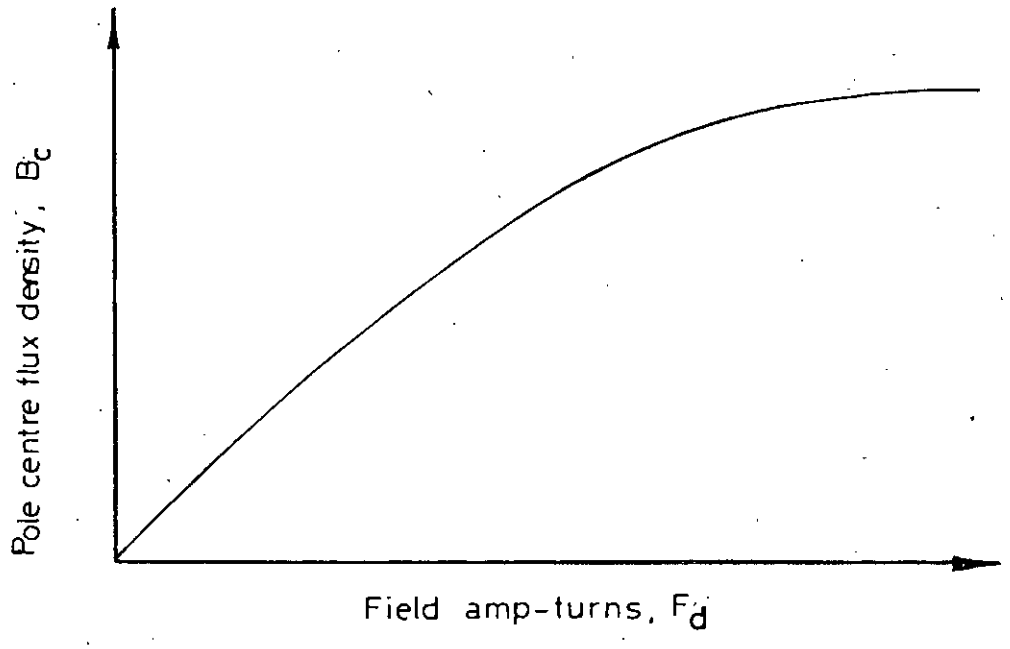

FIG. 4.6 MODIFIED FORM OF MAGNETISING CURVE, EXPRESSING POLE CENTRE FLUX DENSITY B_c AS A FUNCTION OF F_d

Hence equation (4.27) follows

$$\phi_{ma} = \frac{L\tau}{2F_a}\int_{F_d-F_a}^{F_d+F_a} B(F)dF = \frac{1}{2F_a}\int_{F_d-F_a}^{F_d+F_a} (F)dF \qquad (4.29)$$

where

$\phi(F)$ can be obtained from the usual magnetising curve expressing the air-gap flux at no load as the function of field ampere turns. For finding the integral (4.29) it is conveninent to express the magnetising curve analytically through the following formula [34]

$$\phi(F) = a_1 \tan^{-1}(b_1 F) + d_1 F \qquad (4.30)$$

This formula expresses the magnetising curve with high accuracy and contiguity of analytical curve with the actual one is satisfactory. Besides that it leads to handy expressions for machine parameters and the fluxes. Using formula (4.29) and (4.30) the expression of ϕ_{ma} has been derived in Appendix B as

$$\phi_{ma} = \frac{a_1}{2F_a}[F_2 \tan^{-1}(b_1 F_2) - F_1 \tan^{-1}(b_1 F_1) - \frac{1}{2b_1}\ln(\frac{1+b_1^2 F_2^2}{1+b_1^2 F_1^2})] + d_1 F_d \qquad (4.31)$$

where

$$F_2 = F_d + F_a .$$

and $$F_1 = F_d - F_a .$$

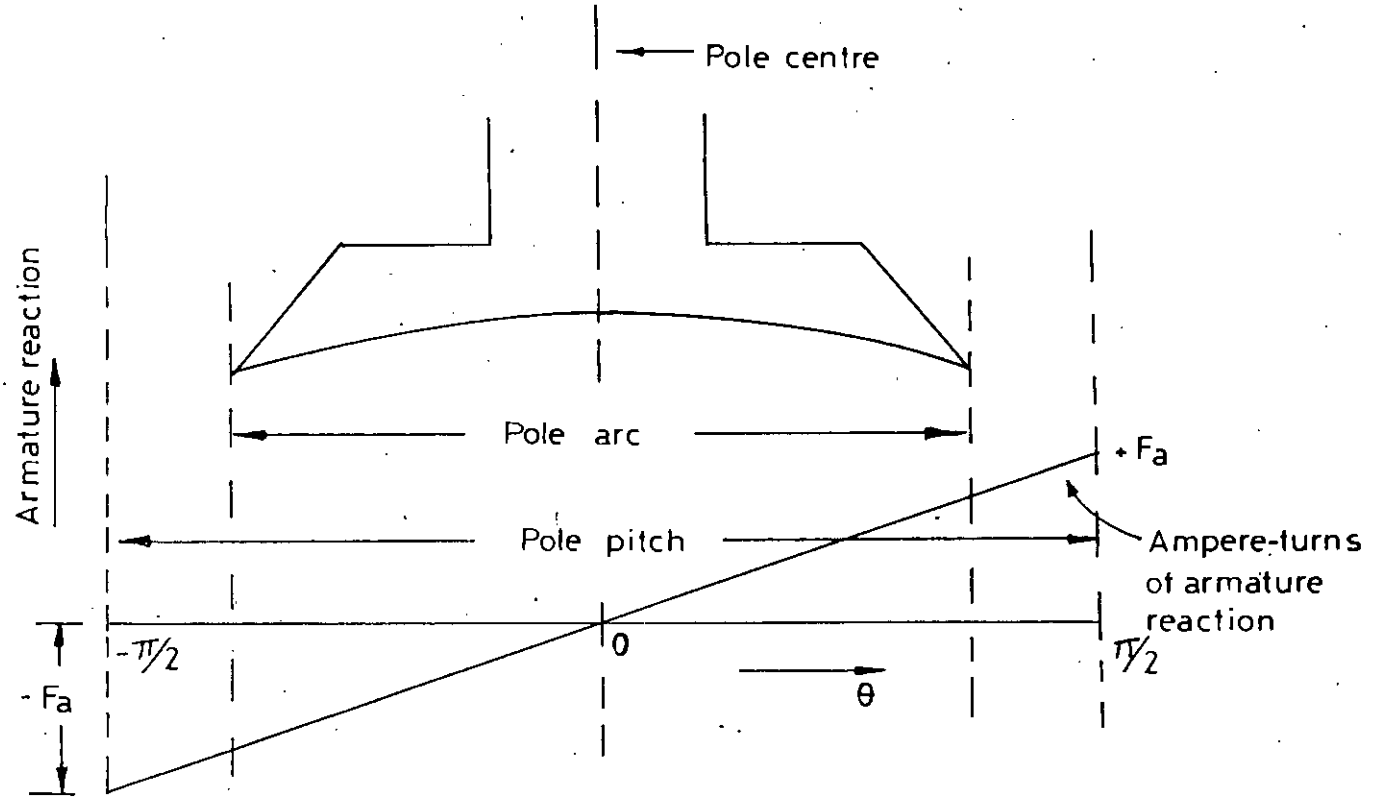

FIG. 4.7 LINEAR DISTRIBUTION OF ARMATURE REACTION AMPERE-TURNS ON ITS SURFACE.

4.3.2 Calculation of Flux Linkage of Armature Coil, Ψ_{aq}

For finding out the expression for Ψ_{aq} an armature of a two pole machine may be analysed. Figure 4.5 shows the armature reaction mmf of a two pole machine. To find out the flux linkage for the portion above the interpolar axis let us separate an elementary flux tube of armature flux at a distance of θ having the thickness $d\theta$ in angular measurement. If $B(\theta)$ is the flux density expressed as function of θ then the elementary flux in the tube is

$$d\Phi_1 = LB(\theta)d\theta \qquad (4.32)$$

This tube encloses a total number of armature conductors given by $(N\theta/\pi)$, where N is the number of armature conductors in the two pole machine. The flux linkage of the tube is then given by

$$d\Psi_1 = (N.L/\pi)\,\theta.B(\theta)d\theta \text{ wb-conductors.}$$

The total flux linkage in the portion above the interpolar axis is given by

$$\Psi_1 = \frac{NL}{\pi}\int_{-\pi/2}^{\pi/2}\theta B(\theta)d\theta \text{ wb-conductors.} \qquad (4.33)$$

For finding the flux linkage in the armature conductors below the interpolar axis, θ in formula (4.33) should be replaced by $-\theta$ and $d\theta$ by $-d\theta$. Then the second portion of flux linkage is

$$\Psi_2 = -\frac{NL}{\pi}\int_{-\pi/2}^{\pi/2}\theta B(-\theta)d\theta \text{ wb-conductors.}$$

so, $$\Psi_1 + \Psi_2 = \frac{NL}{\pi}\int_{-\pi/2}^{\pi/2}\theta[B(\theta)-B(-\theta)]d\theta \text{ wb-conductors.}$$

The total armature flux linkage in wb-turns is therefore

$$\Psi_{aq} = \frac{\Psi_1+\Psi_2}{2} = \frac{NL}{2\pi}\int_{-\pi/2}^{\pi/2}\theta[B(\theta)-B(-\theta)]d\theta \qquad (4.34)$$

Changing the parameter θ by F

$$\psi_{aq} = \frac{NL}{2\pi}\int_{F_d-F_a}^{F_d+F_a} \frac{F-F_d}{2F_a}\pi[B(F-F_d) - B(-(F-F_d))].\frac{\pi}{2F_a}dF$$

$$= \frac{\pi NL}{8F_a^2}\int_{F_d-F_a}^{F_d+F_a}(F-F_d)[B(F-F_d) - B(-(F-F_d)]dF$$

Substituting $F^* = F-F_d$ or $F = F^*+F_d$

$$\psi_{aq} = \frac{\pi NL}{8F_a^2}\int_{-F_a}^{F_a} F^*[B(F^*) - B(-F^*)]dF^*$$

But since $-F^*[B(-F^*)-B(+F^*)] = F^*[B(F^*)-B(-F^*)]$, that is the integrand is an even function, so

$$\psi_{aq} = \frac{\pi NL}{4F_a^2}\int_{o}^{F_a} F^*[B(F^*)-B(-F^*)]dF^*$$

If there are "a" pair of parallel paths in the armature then

$$\psi_{aq} = \frac{\pi NL}{8aF_a^2}\int_{o}^{F_a} F^*[B(F^*)-B(-F^*)]dF^*$$

$$= \frac{N}{8aF_a^2}\int_{o}^{F_a} F^*[\phi(F^*)-\phi(-F^*)]dF^*$$

This is true if number of pole pair is one, in general case when number of pole pairs is p then

$$\psi_{aq} = \frac{pN}{8a}.\frac{1}{F_a^2}\int_{o}^{F_a} F^*[\phi(F^*)-\phi(-F^*)]dF^*$$

But N is given by $(2N_a/p)$ and if it is kept in mind that armature reaction flux virtually confines in the region of pole arc then

$$\psi_{aq} = \frac{pN_a'}{2}.\frac{1}{F_a^2}\int_{o}^{F_a} F^*[\phi(F^*)-\phi(-F^*)]dF^* \qquad (4.35)$$

In equation (4.35) F^* has its zero value when $F=F_d$. The integral (4.35) may now be calculated by dividing it into two parts and in the first part F^* will be replaced by $F-F_d$ and in the second part by F_d-F. So,

$$\psi_{aq} = \frac{pN_a'}{2}.\frac{1}{F_a^2}[\int_{o}^{F_a} F^*\{\phi(F^*)\}dF^* - \int_{o}^{F_a} F^*\{\phi(-F^*)\}dF^*]$$

$$= \frac{pN_a'}{2}.\frac{1}{F_a^2}[\int_{F_d}^{F_a+F_d}(F-F_d)\{\phi(F)\}dF - \int_{F_d}^{F_d-F_a}(F-F_d)\{\phi(F)\}dF]$$

$$= \frac{pN_a'}{2}\cdot\frac{1}{F_a^2}\left[\int_{F_d}^{F_a+F_d}(F-F_d)\{\phi(F)\}dF + \int_{F_d-F_a}^{F_d}(F-F_d)\{\phi(F)\}dF\right]$$

$$= \frac{pN_a'}{2}\cdot\frac{1}{F_a^2}\int_{F_d-F_a}^{F_d+F_a}(F-F_d)\,\phi(F)dF$$

$$\text{or, } \Psi_{aq} = \frac{pN_a'}{2}\cdot\frac{1}{F_a^2}\int_{F_1}^{F_2}(F-F_d)\,\phi(F)dF \qquad (4.36)$$

Now substituting the value of $\phi(F)$ from equation (4.30) into (4.36) and performing the integration, the expression of Ψ_{aq} can be determined easily. With this value of Ψ_{aq} and ϕ_{ma} as given by equation (4.31) the dynamic inductances as given by equations (4.24) and (4.25) can be evaluated as

$$L_e = pN_e^2\left[\frac{a_1}{2F_a}(\tan^{-1}b_1F_2 - \tan^{-1}b_1F_1) + d_1\right]$$

$$M_{ae} = M_{ea} = -pN_eN_a'\frac{a_1}{2F_a^2}\left[F_d(\tan^{-1}b_1F_2 - \tan^{-1}b_1F_1) - \frac{1}{2b_1}\ln\frac{1+b_1^2F_2^2}{1+b_1^2F_1^2}\right] \qquad (4.37)$$

$$L_{aq} = pN_a'^2\left[\frac{a_1}{b_1F_a^2}\left\{1+\frac{b_1^2F_d^2-1}{2b_1F_a}(\tan^{-1}b_1F_2 - \tan^{-1}b_1F_1) - \frac{F_d}{2F_a}\ln\frac{1+b_1^2F_2^2}{1+b_1^2F_1^2}\right\} + \frac{d_1}{3}\right]$$

4.3.3 Model Neglecting the Effect of Eddy Currents

If the effect of eddy current is neglected the total mmf in the direct axis F_d is given by

$$F_d = N_s i_a + F_{ed}$$

$$= N_s i_a$$

$$= N_e i_d$$

From which

$$i_d = (N_s/N_e)i_a \qquad (4.38)$$

Again $(d\Psi_s/dt)$ and $(d\Psi_{aq}/dt)$ can be expressed with the help of equation (4.38) as

$$\frac{d\Psi_s}{dt} = \frac{N_s}{N_e}\cdot\frac{d\Psi_e}{dt} = \frac{N_s}{N_e}\left[\frac{\partial\Psi_e}{\partial i_a}\cdot\frac{di_a}{dt} + \frac{\partial\Psi_e}{\partial i_d}\cdot\frac{di_d}{dt}\right]$$

$$= \frac{N_s}{N_e}\left[M_{ea}\frac{di_a}{dt} + L_e\frac{di_d}{dt}\right]$$

$$= \frac{N_s}{N_e}\left[M_{ea}\frac{di_a}{dt} + \frac{N_s}{N_e}L_e\frac{di_a}{dt}\right] \qquad (4.39)$$

and

$$\frac{d\psi_{aq}}{dt} = \left[\frac{\partial \psi_{aq}}{\partial i_a}\cdot\frac{di_a}{dt} + \frac{\partial \psi_{aq}}{\partial i_d}\cdot\frac{di_d}{dt}\right]$$

$$= \left[L_{aq}\frac{di_a}{dt} + M_{ae}\frac{di_d}{dt}\right]$$

$$= \left[L_{aq}\frac{di_a}{dt} + \frac{N_s}{N_e}M_{ae}\frac{di_a}{dt}\right] \qquad (4.40)$$

where L_e, M_{ea}, M_{ae} and L_{aq} are given by equation (4.37). Now substitution of equation (4.39) and (4.40) in (4.17) gives

$$\left[(L_{a1}+L_{s1})+L_{aq}+\frac{N_s}{N_e}M_{ae}+\frac{N_s}{N_e}M_{ea}+\frac{N_s^2}{N_e^2}L_e\right]\frac{di_a}{dt} = v_a - \Delta v_b - i_a R_a - K\Phi_{ma}\omega.$$

or,

$$\frac{di_a}{dt} = \frac{(v_a - \Delta v_b - i_a R_a - K\Phi_{ma}\omega)}{\left[(L_{a1}+L_{s1})+L_{aq}+2\frac{N_s}{N_e}M_{ae}+\frac{N_s^2}{N_e^2}L_e\right]} \qquad (4.41)$$

Equation (4.41) is a first order nonlinear differential equation which can be solved easily be fourth order Runge-Kutta method. Before performing that we have to determine the constants a_1, b_1 and d_1 such that the analytical magnetising curve given by equation (4.30) fits the experimentally determined magnetising curve. Also some parameters of the motor need to be determined.

4.3.4 Model Considering the Effect of Eddy Currents

Eddy currents are induced inside the pole cores, yoke, joints and fittings and the armature laminations of a chopper-fed dc series motor.These eddy currents produce short duration magnetic fluxes which opposes the change in the air-gap flux. A detailed analysis for flux distribution inside a torroidal core due to step input excitation have been given in reference [42] and it is shown that it is possible to derive an equivalent circuit model to represent the eddy current effect. Each eddy current path can be treated as shorted secondary of a transformer. Hence the equivalent circuit will be as shown in figure 4.8.

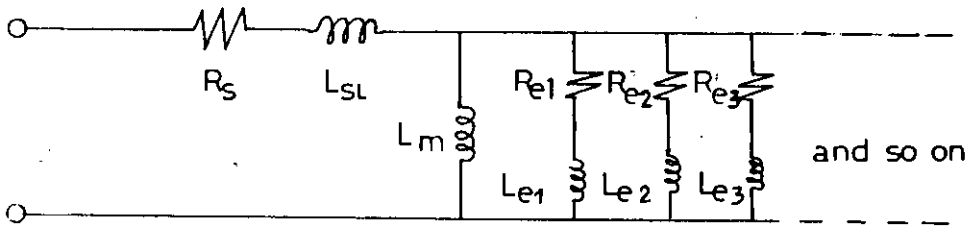

FIG. 4.8 DYNAMIC EQUIVALENT CIRCUIT OF DC MACHINE FIELD TO REPRESENT THE EFFECT OF EDDY CURRENT

The different eddy current paths in figure 4.8 are for different harmonics. Since the magnitude of current of the higher harmonics gradually decreases it is sufficient to consider only the first two or three branches. In case of chopper fed motor the variations of mmfs and fluxes are such that a single branch simulates the effects of eddy current quite satisfactorily. Let R_{ed} and L_{ed} are equivalent resistance and inductance of the eddy current path. To include the eddy current effects, a second differential equation of the eddy current path must also be considered in addition to the equation (4.17). The differential equation representing the eddy current path is

$$(d\psi_{ed}/dt) = -i_{ed}R_{ed}$$

where

$$\psi_{ed} = L_{ed}i_{ed}+pN_s\phi_{ma} \qquad (4.42)$$

or, $$i_{ed} = [(\psi_{ed}-pN_s\phi_{ma})/L_{ed}]$$

In the above equation it is considered that the eddy current coil has a number of turns equal to that of the series coil . Now

$$F_d = N_s i_a + F_{ed}$$
$$= N_s(i_a+i_{ed})$$
$$= Neid$$

$$\text{so,}\quad i_d = \frac{N_s}{N_e}(i_a + i_{ed}) \qquad (4.43)$$

From equation (4.17) and (4.42) with the substitution of equation (4.43), a simultaneous differential equation of the form shown below has been derived in Appendix C which is the fundamental equation to take into account the effect of eddy currents.

$$\frac{di_a}{dt} = \frac{\left[\left(L_{ed}+p\frac{N_s^2}{N_e}L_2\right)\left(v_a-\Delta v_b-i_aR_a-K\phi_{ma}\omega\right)+\left(\frac{N_s}{N_e}M_{ae}+\frac{N_s^2}{N_e^2}L_e\right)i_{ed}R_{ed}\right]}{\left[\left(L_{ed}+p\frac{N_s^2}{N_e}L_2\right)\left(L_{a1}+L_{s1}+L_{aq}+2\frac{N_s}{N_e}M_{ae}+\frac{N_s^2}{N_e^2}L_e\right)-\left(\frac{N_s}{N_e}M_{ae}+\frac{N_s^2}{N_e^2}L_e\right)\left(pN_sL_1+p\frac{N_s^2}{N_e}L_2\right)\right]} \qquad \ldots\ldots(4.44)$$

and

$$\frac{di_{ed}}{dt} = \frac{\left[-\left(pN_sL_1+p\frac{N_s^2}{N_e}L_2\right)\left(v_a-\Delta v_b-i_aR_a-K\phi_{ma}\omega\right)-\left(L_{a1}+L_{s1}+L_{aq}+2\frac{N_s}{N_e}M_{ae}+\frac{N_s^2}{N_e^2}L_e\right)i_{ed}R_{ed}\right]}{\left[\left(L_{ed}+p\frac{N_s^2}{N_e}L_2\right)\left(L_{a1}+L_{s1}+L_{aq}+2\frac{N_s}{N_e}M_{ae}+\frac{N_s^2}{N_e^2}L_e\right)-\left(\frac{N_s}{N_e}M_{ae}+\frac{N_s^2}{N_e^2}L_e\right)\left(pN_sL_1+p\frac{N_s^2}{N_e}L_2\right)\right]} \qquad \ldots\ldots(4.45)$$

where

$$L_1 = -\frac{a_1N_a'}{2F_a^2}\left[F_d\left(\tan^{-1}b_1F_2-\tan^{-1}b_1F_1\right)-\frac{1}{2b_1}\ln\frac{1+b_1^2F_2^2}{1+b_1^2F_1^2}\right]$$

and

$$L_2 = \frac{a_1N_e}{2F_a}\left[\tan^{-1}b_1F_2-\tan^{-1}b_1F_1\right]+d_1N_e \qquad (4.46)$$

The above expressions of L_1 and L_2 have been derived in Appendix D.

4.3.5 Method of Determination of L_{ed} and R_{ed}

The resistance and inductance of the eddy current paths can be determined in different ways. Let us consider only one eddy current path. The experimental set-up to determine R_{ed} and L_{ed} is shown in figure 4.9. Low ac voltage is applied so that saturation can be neglected and L_m can be considered as constant. From the equivalent circuit

$$Z_{eq} = (R_s+j\omega L_{s1}) + \frac{(R_{ed}+j\omega L_{ed})(j\omega L_m)}{(R_{ed}+j\omega L_{ed}+j\omega L_m)} \qquad (4.47)$$

where

R_s = Series field resistance.

L_s = Inductance of the series field coil.

L_m = Magnetising inductance, $(L_s - L_{sl})$.

Again from test :

Z_{eq} = (V/I) = (Voltmeter reading/Ammeter reading)

and

$$R_{eq} = \frac{P}{I^2} = \frac{\text{Wattmeter reading}}{(\text{Ammeter reading})^2} \qquad (4.48)$$

$$X_{eq} = \sqrt{Z_{eq}^2 - R_{eq}^2} \qquad (4.49)$$

Now solving equations (4.47)-(4.49) the value of R_{ed} and L_{ed} can be determined.

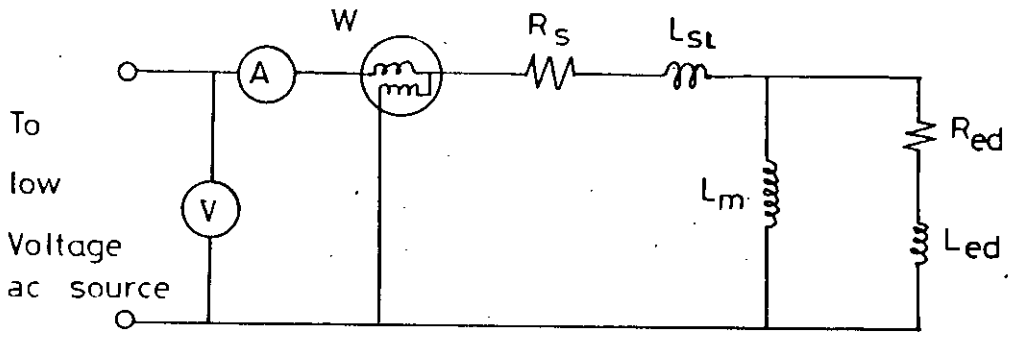

FIG. 4.9 EXPERIMENTAL SET-UP TO DETERMINE THE PARAMETER OF THE EDDY CURRENT PATH

Another method of determination of the eddy current parameters requires the recordings of the dynamic field current. Suddenly a dc voltage V is applied on the field circuit and after sometimes it is switched off and at the same time the terminals are shorted to give a path so that the field currents

can die out. Simultaneously the dynamic field current is recorded. The experimental set-up is as shown in figure 4.1 and 4.2. If only one eddy current branch is considered, the total current for charging period will be the sum of two exponentially rising currents as given by

$$\begin{aligned} i &= I_1(1-e^{-t/T_1}) + I_2(1-e^{-t/T_2}) \\ &= (I_1+I_2) - (I_1e^{-t/T_1} + I_2e^{-t/T_2}) \\ &= I_s - (I_1e^{-t/T_1} + I_2e^{-t/T_2}) \end{aligned} \qquad (4.50)$$

Similarly for discharging period

$$i = (I_1e^{-t/T_1} + I_2e^{-t/T_2}) \qquad (4.51)$$

where, T_1 and T_2 are the time constants of the field coil and the eddy current path respectively. The constants I_1, I_2 and T_1, T_2 can be determined as follows:

From the decaying curve, the $\log_e i$ as a function of time can be plotted. Since the eddy current term will die out very quickly, the latter portion of the curve is due to the series field coil only. That is the latter portion is given by

$$\begin{aligned} y &= \log_e(I_1e^{-t/T_1}) \\ &= \log_e I_1 - t/T_1 \end{aligned}$$

which is the equation of a straight line. The y-axis intercept of this straight line gives the value of $\log_e I_1$ and the slope gives the time constant, T_1. This is shown in figure 4.10. Now from equation (4.51) and with the calculated values of I_1 and T_1, $\log_e(I_2e^{-t/T_2})$ can also be plotted as a function of time. This will also be a straight line and in a similar way from the y-axis intercept and slope of the straight line the constants I_2 and T_2 can be determined. Proceeding with the same technique the other constants can also be determined if more than one eddy current branch is considered.

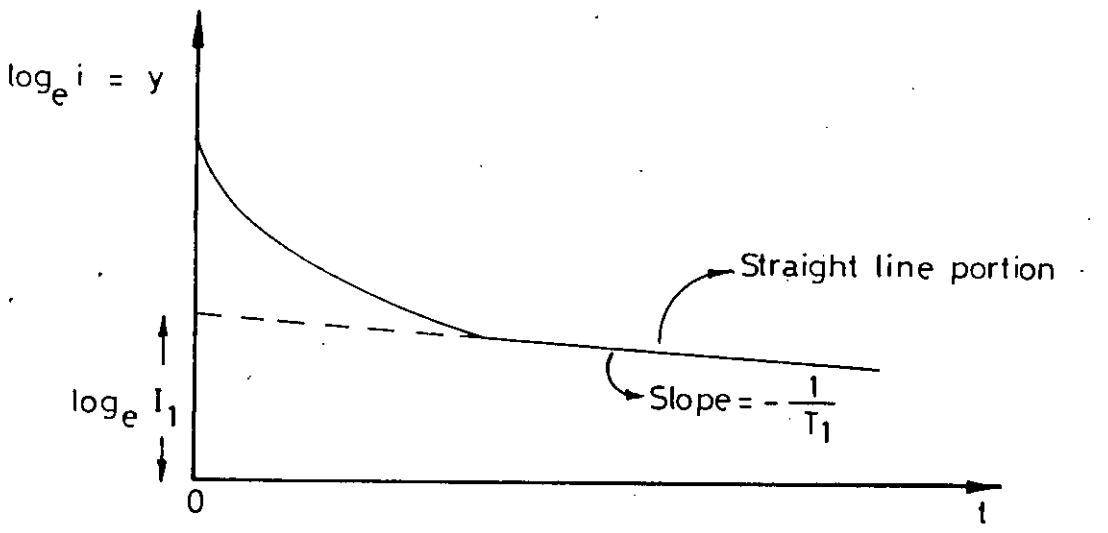

FIG. 4.10 LOGARITHM OF DYNAMIC FIELD CURRENT AS A FUNCTION OF TIME

To determine the value of R_{ed} and L_{ed} let us take laplace transform of the equation (4.50), this gives

$$I(S) = \frac{I_s}{S} - \frac{I_1}{S+1/T_1} - \frac{I_2}{S+1/T_2}$$

where I_s is the steady state current given by (V/R_s). Therefore

$$I(j\omega) = \frac{I_s}{j\omega} - \frac{I_1 T_1}{1+j\omega T_1} - \frac{I_2 T_2}{1+j\omega T_2}$$

Again $V(S)=(V/S)$, that is $V(j\omega)=(V/j\omega)$. Hence the frequency response of transfer function

$$Z(j\omega) = \frac{V(j\omega)}{I(j\omega)}$$

$$= Re(\omega) + jIm(\omega) \qquad (4.52)$$

But $Z(j\omega)$ is given by equation (4.47), which can be written as

$$Z(j\omega) = Re(\omega, L_{ed}, R_{ed}) + jIm(\omega, L_{ed}, R_{ed}) \quad (4.53)$$

Equating equations (4.52) and (4.53)

$$Re(\omega) = Re(\omega, L_{ed}, R_{ed})$$

and (4.54)

$$Im(\omega) = Im(\omega, L_{ed}, R_{ed})$$

For a particular value of ω from equation (4.54) the two unknowns R_{ed} and L_{ed} can be calculated out. The main advantage of this method is that if more than one eddy current branch is considered, say two, then to determine the four constants L_{e1}, L_{e2}, R_{e1} and R_{e2} the same equation (4.54) can be used. In this case equation (4.54) will be used twice, with two different values of ω so that the four necessary equations can be obtained to determine the four unknown quantities.

4.3.6 Steady State Performance

To determine the steady state performance of a chopper-fed dc series motor without considering the effect of eddy currents the first order non-linear differential equation given by (4.41) must be solved. On the otherhand to determine the performance with taking the effect of eddy currents into account the nonlinear simultaneous differential equations given by (4.44) and (4.45) must be solved. Both the equations can be solved quite easily by fourth order Runge-Kutta method. This method gives the steady state armature current as a function of time for a particular angular speed ω. Once the current as a function of time is determined, the air-gap flux ϕ_{ma} can also be determined using equation 4.31. Now the electromagnetic torque is given by

$$T_e = K.I_{av}.\phi_{av} \quad (4.55)$$

Average value of armature current and air-gap flux can be evaluated graphically from the steady state armature current versus time and air-gap flux versus time curve. Hence T_e can be calculated from equation (4.55) which corresponds to a particular ω. Then choosing other values of ω and repeating

the whole process the electromagnetic torque T_e can be calculated and plotted as a function of speed. Thus the steady state torque-speed characteristics of a chopper-fed dc series motor can be obtained.

CHAPTER 5

NUMERICAL EVALUATION

5.1 INTRODUCTION

For the simulation of a chopper-fed dc series motor two different mathematical models have been formulated in chapter 4. These two models are applied to a low power dc series motor in order to determine its steady state performance characteristics. The simulation results are presented in this chapter. The results include steady state torque-speed characteristics of the motor, neglecting as well as considering the effect of eddy currents.

5.2 DETERMINATION OF FROLICH'S CONSTANTS

The effect of magnetic saturation has been included in the first model by frolich's equation as

$$L = \left[\frac{k_3}{(k_2+i_f)^2} + \frac{k_3(i_f-I_o)}{I_o D_1 (k_2+i_f)^2}\right] \qquad (5.1)$$

In order to determine the value of the constants of this equation, for the test machine, particulars of which are given in Appendix E, it must be tested first so that the self inductance of the field coil as a function of its current can be determined. This has been done from the OCC of the machine. The open circuit voltages at different field currents for the test machine are given in table 5.1. Figure 5.1 shows the OCC of the machine from which the value of (dE_o/di_f) at different field currents have been determined. Then the inductance at different field currents have been calculated using equation (4.7), where K_1 is a constant. The value of K_1 has been determined from the initial portion of the OCC and the measured value of inductance of the field coil. Here it has been assumed that the measured value of inductance of the field coil gives the unsaturated value of inductance.

TABLE 5.1

Field current I_f amp.	O.C. Voltage E_o volt.
0.0	12
0.1	32
0.2	70
0.3	103
0.4	138
0.5	172
0.6	198
0.7	216
0.8	230
0.9	242
1.0	253
1.1	262
1.2	269
1.3	274
1.4	278
1.5	280

The experimentally determined self inductance versus current curves for the test machine together with the analytically determined values by equation (5.1), (with $k_2=1.284423$, $k_3=203.4443$ and $D_1=-2.25344$) is shown in figure 5.2. This figure clearly shows that the empirical formulation for self inductance given by relationship (5.1) enables one to represent the dc machine self inductance quite satisfactorily.

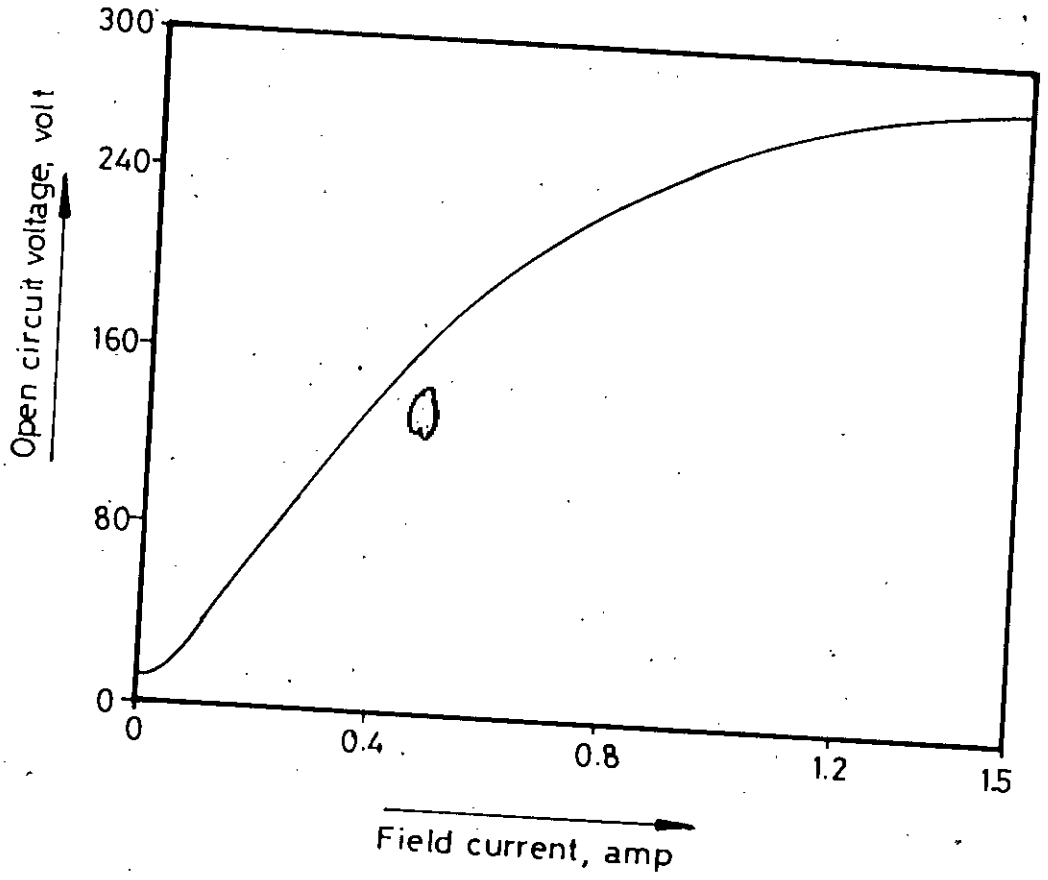

Figure- 5.1 Open circuit characteristics of the test machine

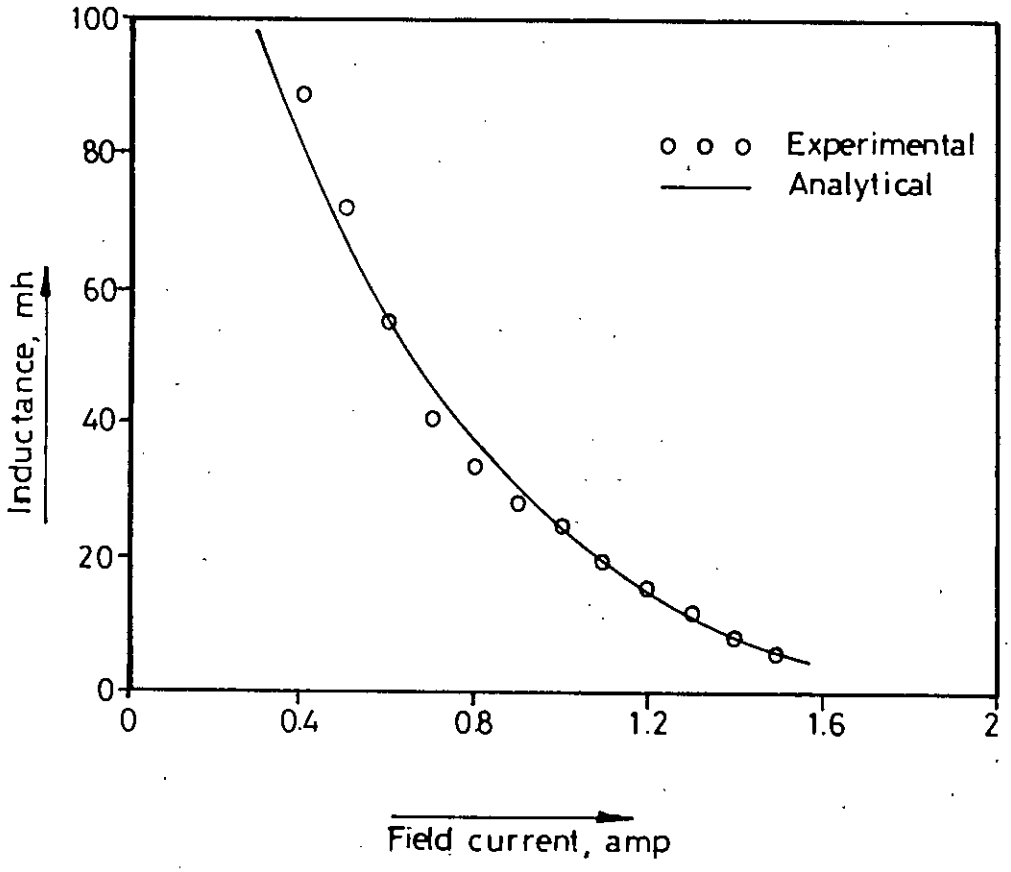

Figure- 5.2 Variation of self inductance with saturation

5.3 DETERMINATION OF BACK EMF COEFFICIENT, K

The steady state armature current of a chopper-fed dc series motor changes between a maximum and a minimum value. The armature reaction flux also varies with the armature current. As a result the back emf coefficient, K is not a constant. However, it may, effectively be represented by equation (4.8) to take into account the effect of armature reaction. The value of the coefficient K has been determined from the internal characteristics of the machine as follows :

The external characteristics of the test machine are given in Appendix F. From the external characteristics a series of curves have been drawn as shown in figure 5.3(a) - 5.3(c). These curves show the variation of back emf E_b with the armature current, taking the field current as a parameter. These series of curves have been constructed using equation (4.9). From these internal characteristics the value of the back emf coefficient K as a function of both the armature and the field current has been determined using the relationship

$$K = (E_b / \omega . i_a) \qquad (5.2)$$

The value of K at different field and armature currents is listed in Appendix G. But since in a series motor the same current flows through the field coil and the armature coil, only those values of K are of practical importance which corresponds to the same field and armature current. Figure 5.4 shows the values of K for same field and armature current.

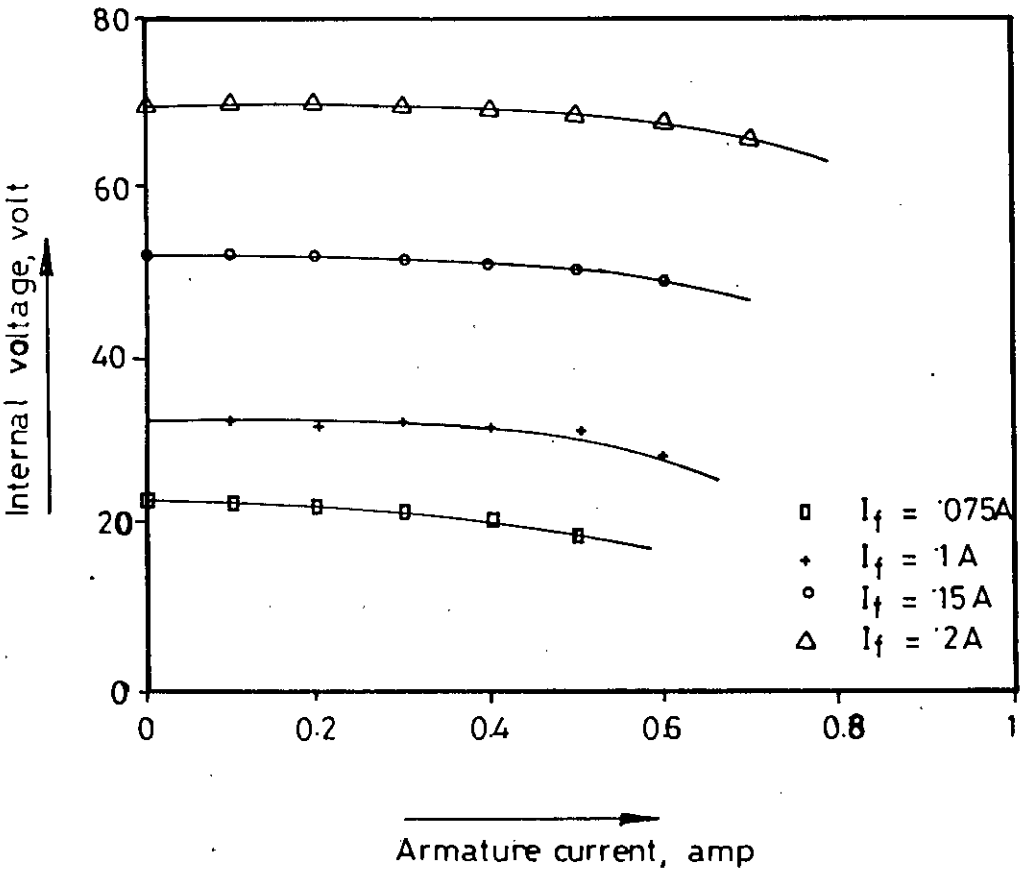

Figure– 5.3(a) Internal characteristics of the test machine with field current as a parameter

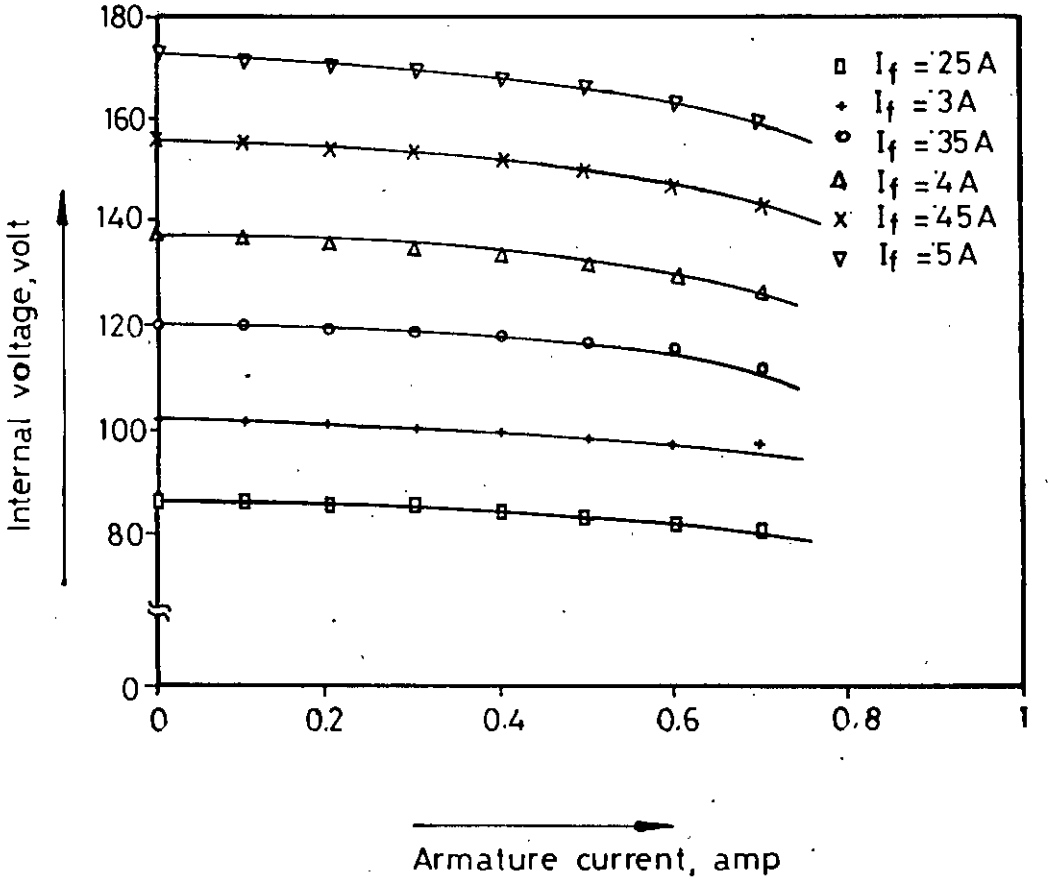

Figure-5.3(b) Internal characteristics of the test machine with field current as a parameter.

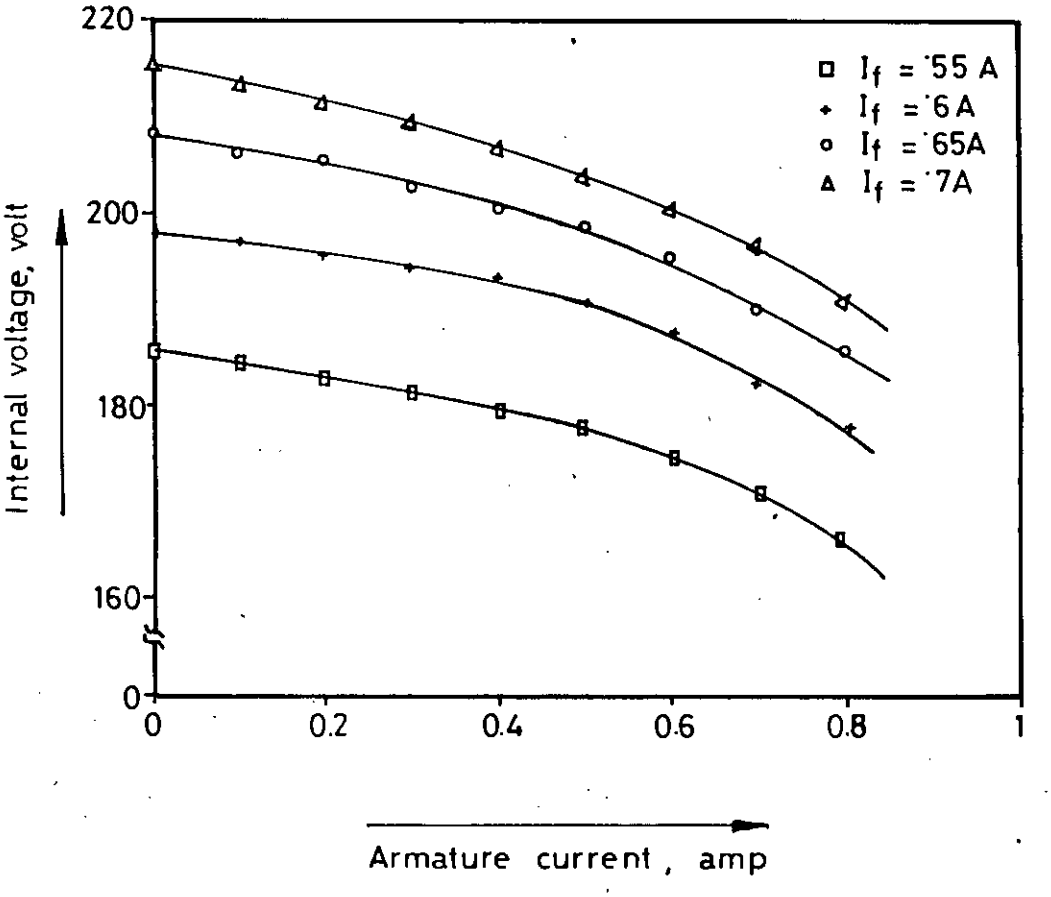

Figure- 5.3(c) Internal characteristics of the test machine with field current as a parameter.

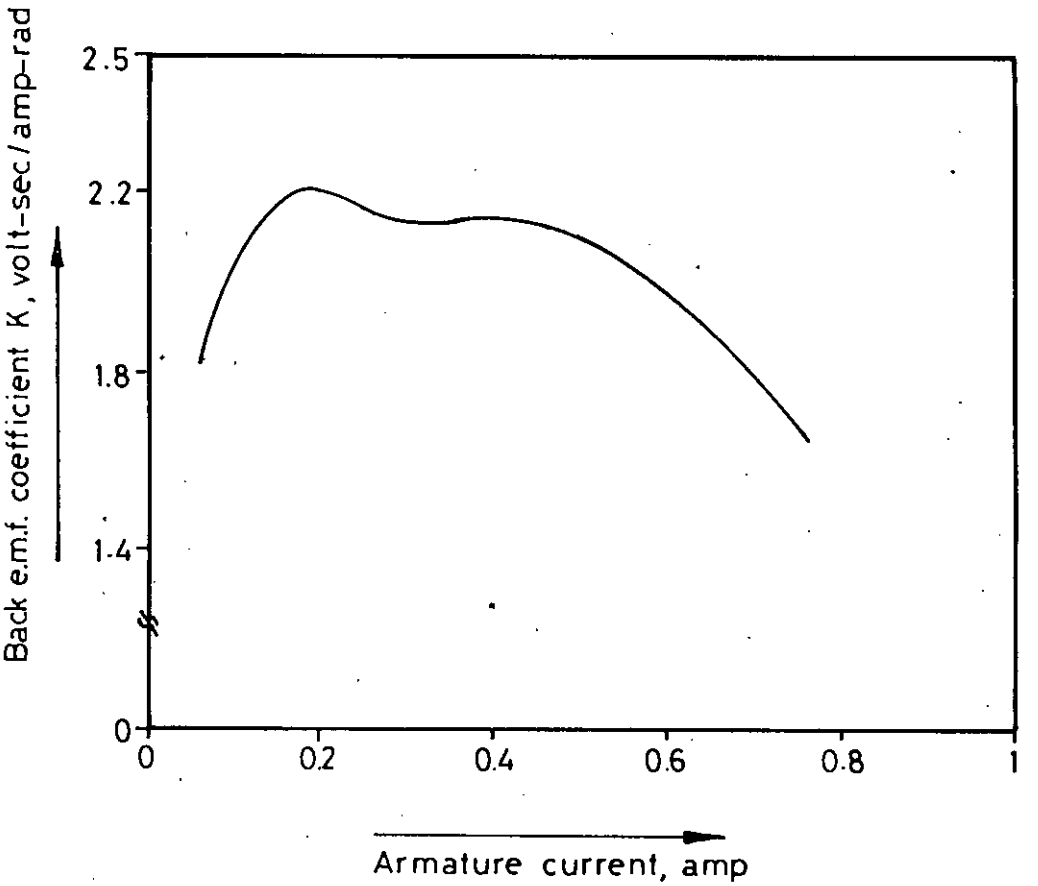

Figure-5.4 Variation of K with armature current.

5.4 DETERMINATION OF EDDY CURRENT CONSTANTS, σ, n and λ

The dynamic open circuit voltage and field current of the test machine, as recorded by the pen recorder, during free wheeling of field current is shown in figure 5.5. Figure 5.6 shows the difference between the actual dynamic induced armature emf and the emf obtained from the OCC under steady state condition . This difference in voltage is just due to the induced eddy currents in the magnetic circuit and may suitably be represented by equation (4.10).

A computer program to determine the constants of the empirical relationship (4.10), so that it fits the experimentally determined $\triangle V_e$ is given in Appendix H. The analytically determined $\triangle V_e$ (with σ =.202451, n=.269691 and λ =71.57106) is also shown in figure 5.6. Figure 5.7 shows the calculated response from empirical model together with the calculated steady state response (OCC) and the experimentally recorded response of the open circuit induced voltage. The satisfactory agreement between calculated and measured curves, as revealed from figure 5.7, justifies that for the machine under consideration, equation (4.10) provides an easy tool to account for the effects of eddy currents.

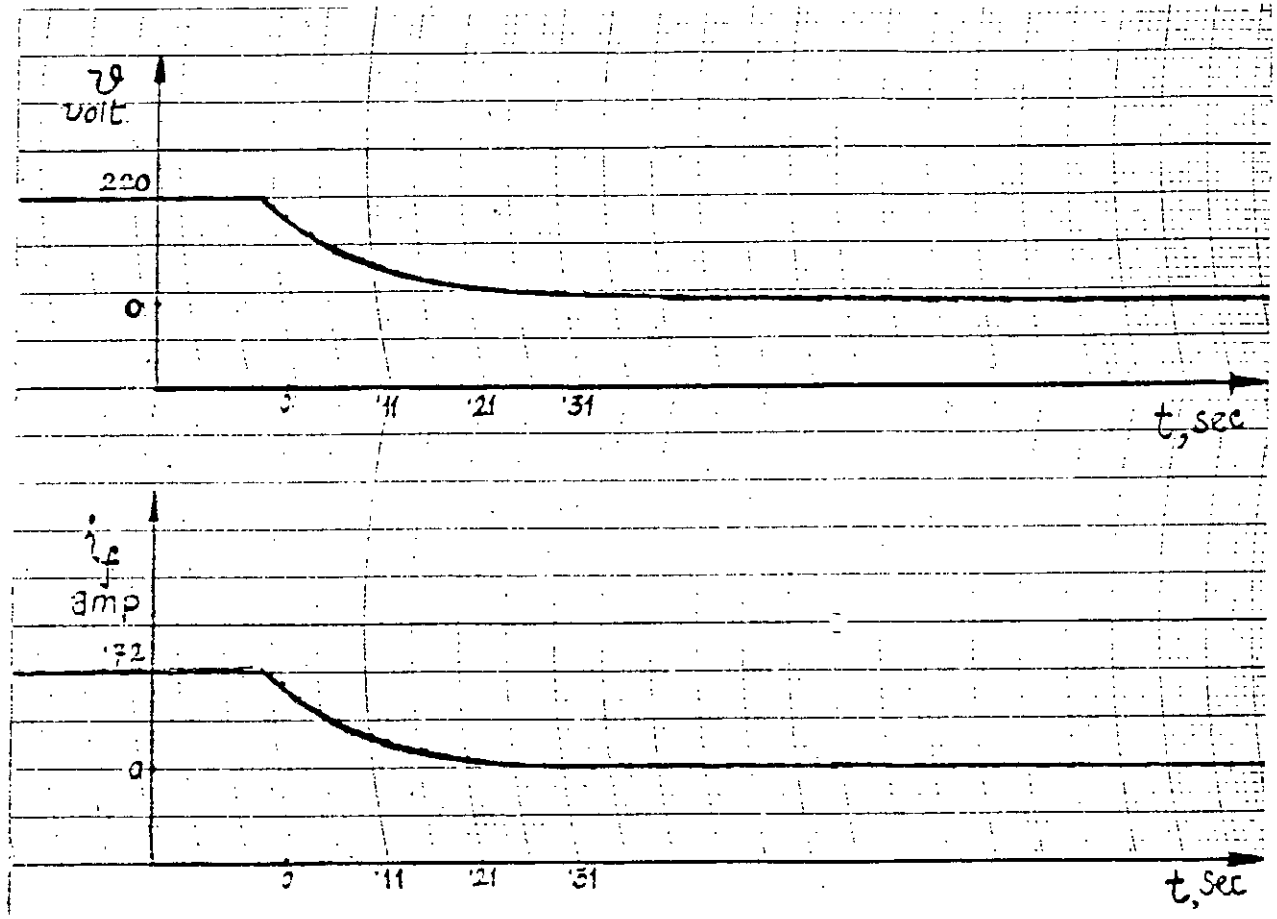

Figure- 5.5 Dynamic response as recorded by the pen recorder.

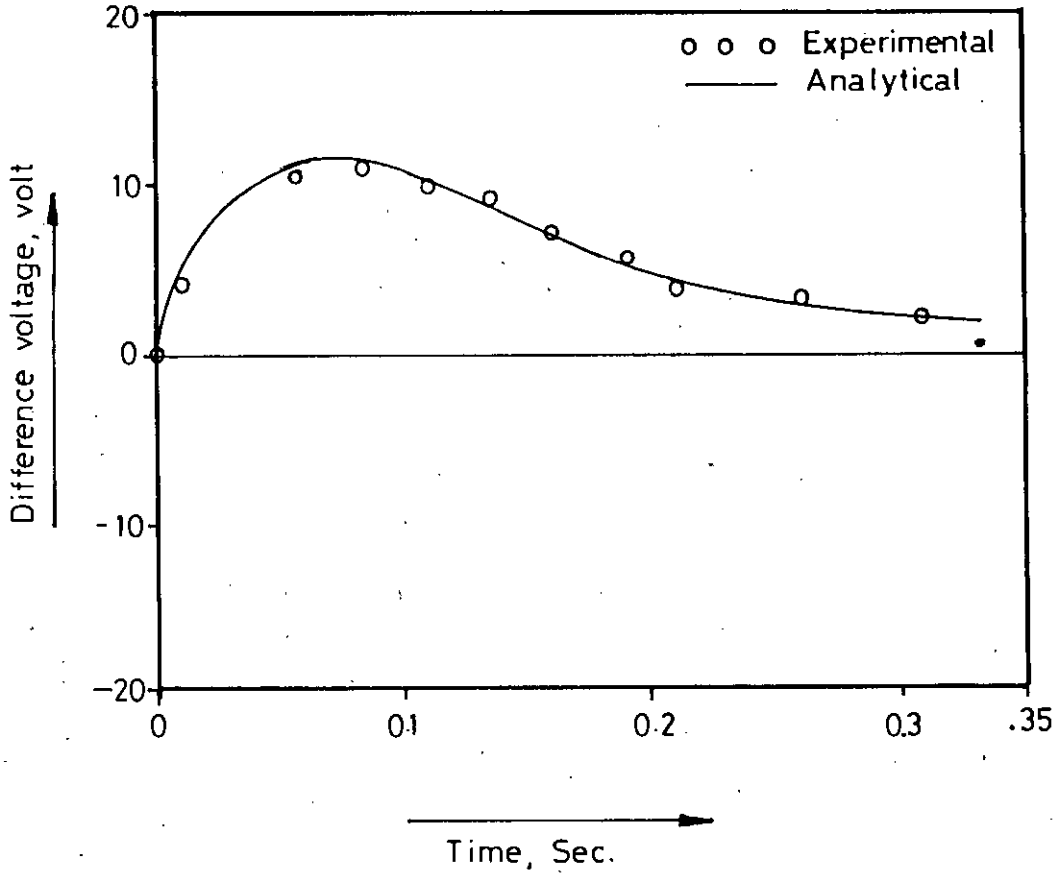

Figure- 5.6 ΔVe as a function of time

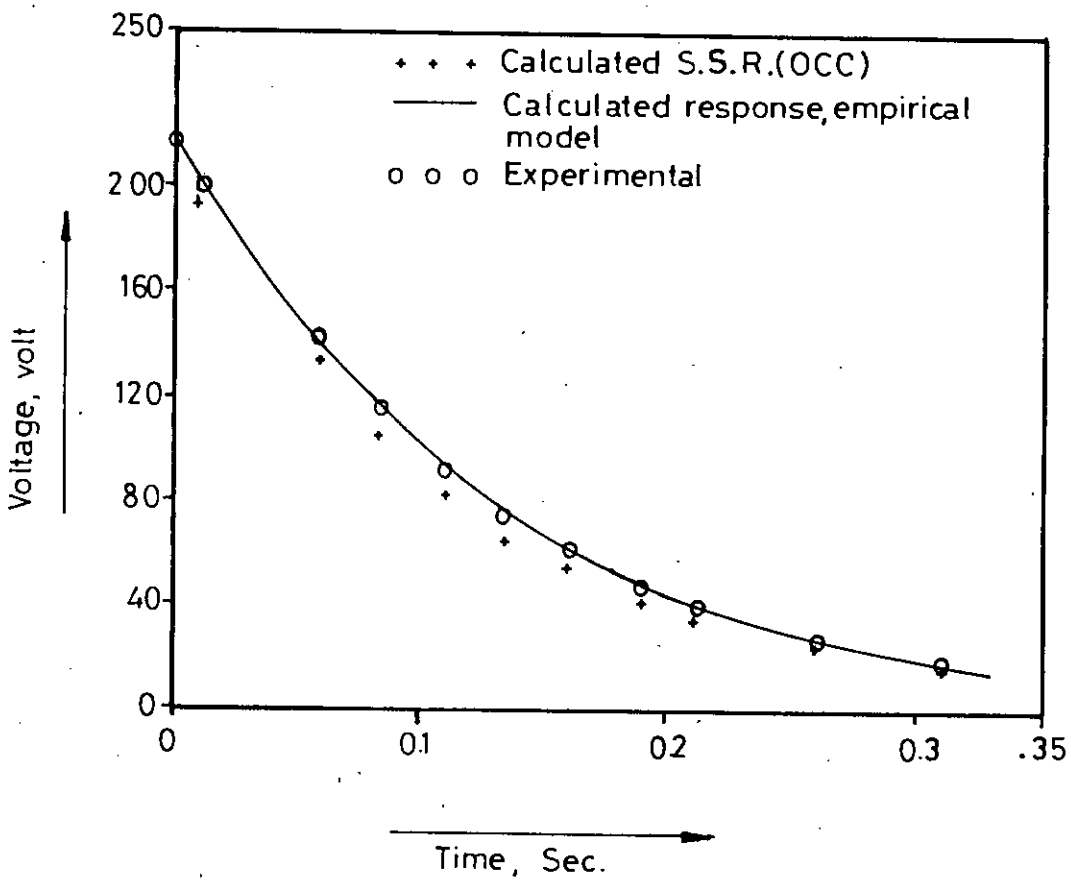

Figure-5.7 Dynamic response of armature e.m.f. due to step input voltage to field (free wheeling)

5.5 STEADY STATE TORQUE-SPEED CHARACTERISTICS

In the first model, the steady state performance of a chopper-fed dc series motor, can be determined using equations (4.11) - (4.16). Neglecting the commutation interval of the chopper circuit (δ_c=0), the average steady state machine speed and the electromagnetic torque, as derived in Appendix A, is given by

$$\omega_{av} = \omega = \frac{V\delta - I_{av}R_a}{I_{av}\left[K - \frac{\lambda.\alpha}{\omega_o(k_2+I_{av})}\right]}$$

and

$$T_e = \frac{E_{av}.I_{av}}{\omega}$$

where $E_{av} = K.\omega.I_{av}$

When the effect of eddy current is neglected the average steady state machine speed takes the form

$$\omega_{av} = \omega = \frac{V\delta - I_{av}R_a}{KI_{av}}$$

The steady state torque-speed characteristics for the test machine (with input voltage V=100 volts and α = 0.1) have been determined from the above equations, for different values of the mark period patio, δ . Figure 5.8 shows the steady state torque-speed characteristics of the machine under consideration, assuming the output voltage wave of the chopper to be square and neglecting the effect of eddy current, while Figure 5.9 shows the same when the effect of eddy current has been taken into consideration.

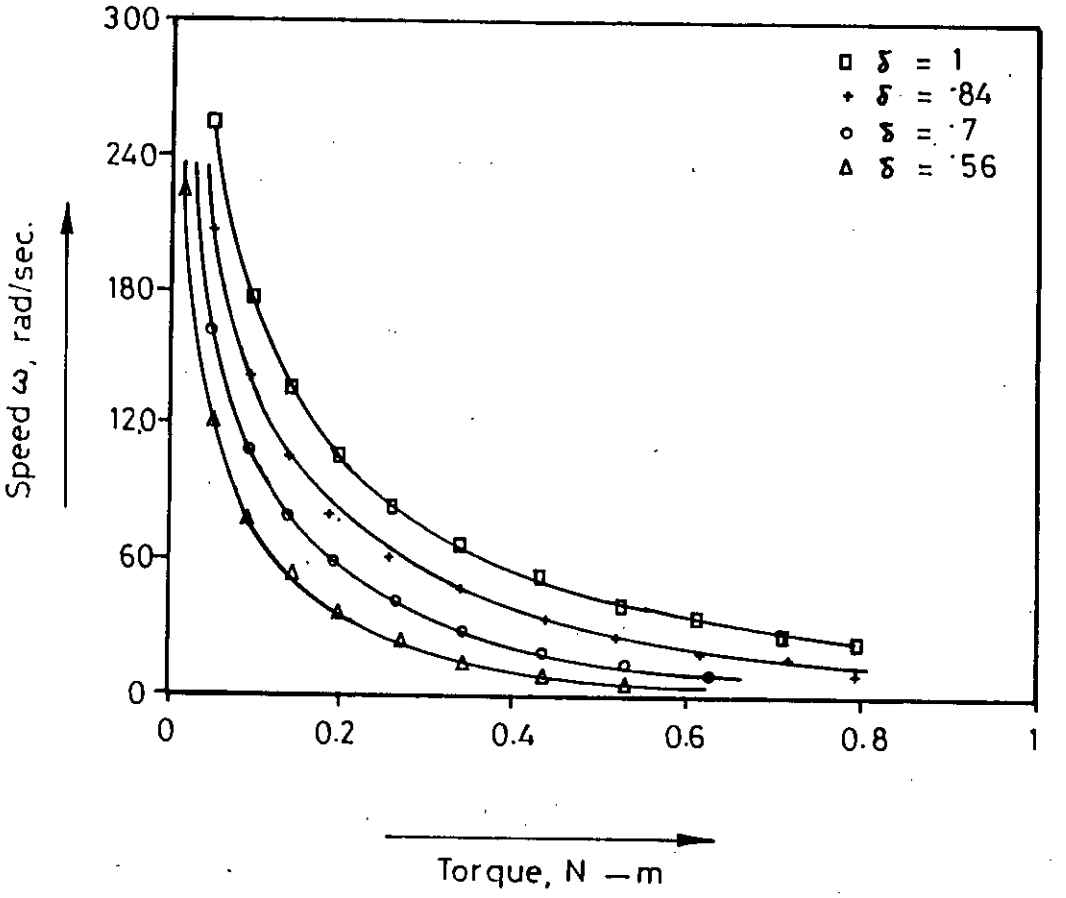

Figure-5.8 Torque-speed characteristics neglecting eddy current effect (Empirical model).

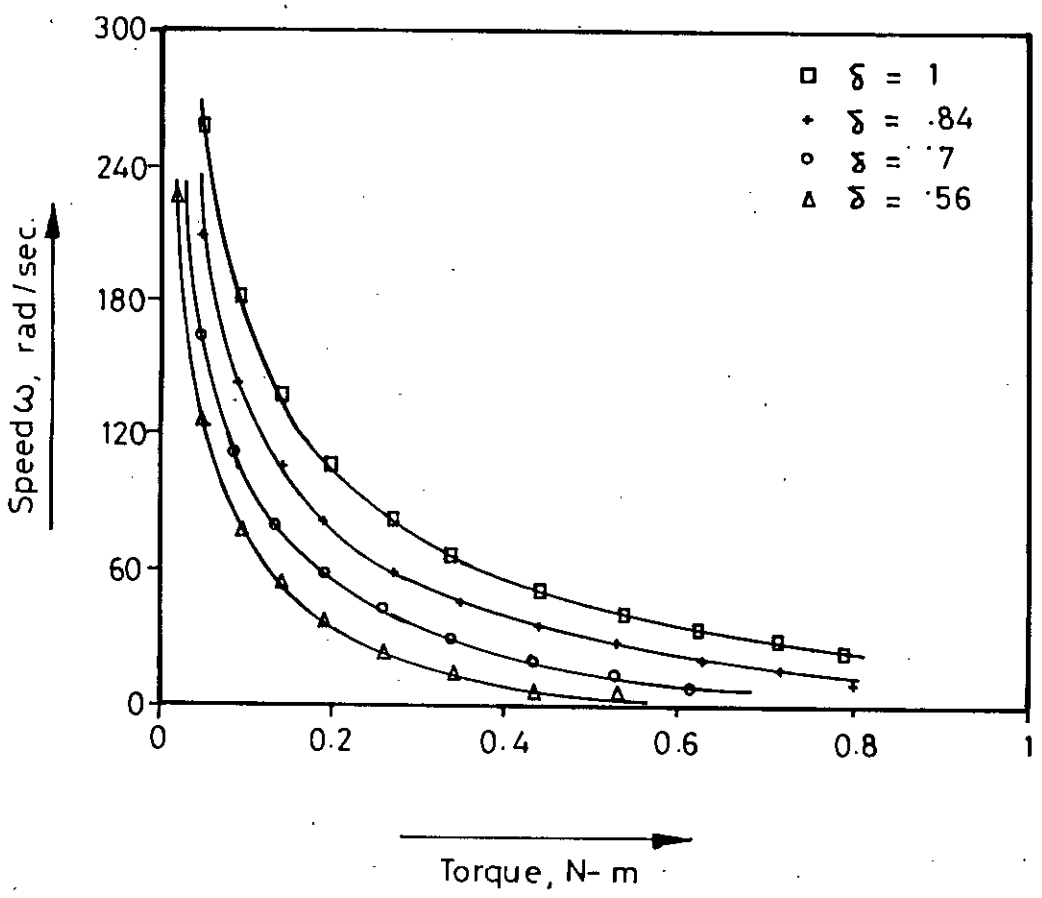

Figure-5.9 Torque-speed characteristics taking eddy current effect (Empirical model).

5.6 REPRESENTATION OF THE MAGNETISING CHARACTERISTICS

For computations using the second model it is necessary to represent the magnetisation characteristics of the machine by the so called arc-tan curve as given by equation (4.30). The magnetisation characteristics of the test machine have been determined from its open circuit characteristics. The open circuit voltage is given by $E_o = (\phi ZNP/A)$. With the known values of the machine parameters Z, P, A and N, the flux ϕ, at different field currents have been determined. The ampere turns corresponding to different field currents have been calculated using the relationship $F = N_s i_f$. Thus the magnetising curve of the test machine (ϕ vs. F) is obtained. The value of the constants a_1, b_1 and d_1 of equation (4.30) have been determined so that $\phi(F)$ given by relationship (4.30), fits the experimentally determined values. The experimentally determined magnetising curve together with the analytically determined one (with $a_1 = 0.115$, $b_1 = 0.095$ and $d_1 = -0.0007$) is shown in figure 5.10.

5.7 COMPUTER PROGRAM

Determination of the torque-speed characteristics by the second model requires the numerical solution of the motor performance equation. In steady state condition a chopper-fed dc series motor may be simulated by a set of nonlinear differential equations as discussed in chapter 4. For numerical evaluation a computer program is developed in Fortran. Standard Runge-Kutta numerical method have been used. The program is general in nature and it is capable of determining the transient performance also with some modifications in the model. The computer program is given in Appendix H.

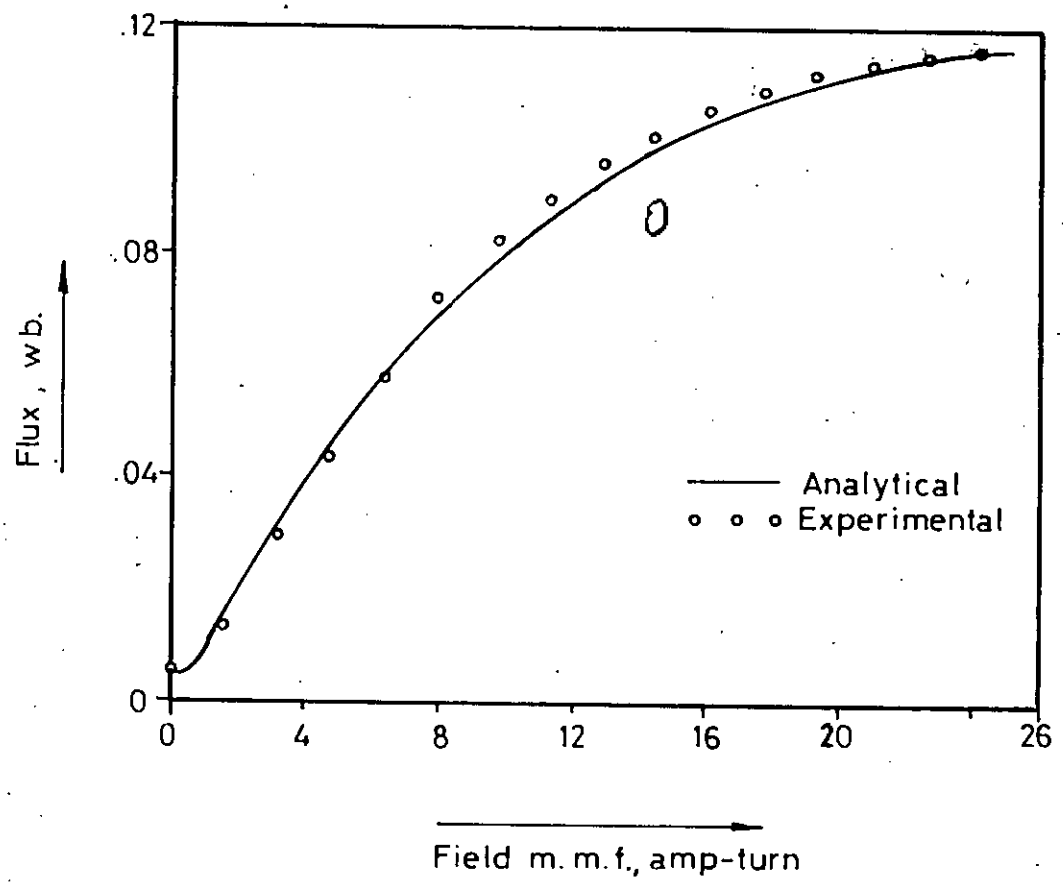

Figure-5.10 Magnetisation characteristics of the test machine

5.8 STEADY STATE PERFORMANCE, DETERMINED BY SECOND MODEL

The computer program in Fortran (Appendix H) enables to determine the steady state armature current and air-gap flux as a function of time for different angular speed ω. As a sample, the variation of the steady state armature current and air-gap flux with time, for a particular angular speed ω is shown in figure 5.11 when the eddy current effect is neglected. The output voltage of the chopper is taken as 100 volts and the mark period ratio, δ , as 0.84. Figure 5.12 shows the same when the effect of eddy current is taken into account. The steady state eddy current is also shown in the same figure. The average armature current and air-gap flux have been determined graphically from these curves. The torque corresponding to different values of angular speed have been determined using equation (4.55). Figure 5.13 shows the steady state torque-speed characteristics of the test machine for two different values of δ, neglecting the effect of eddy current; while figure 5.14 shows the same considering the eddy current effect.

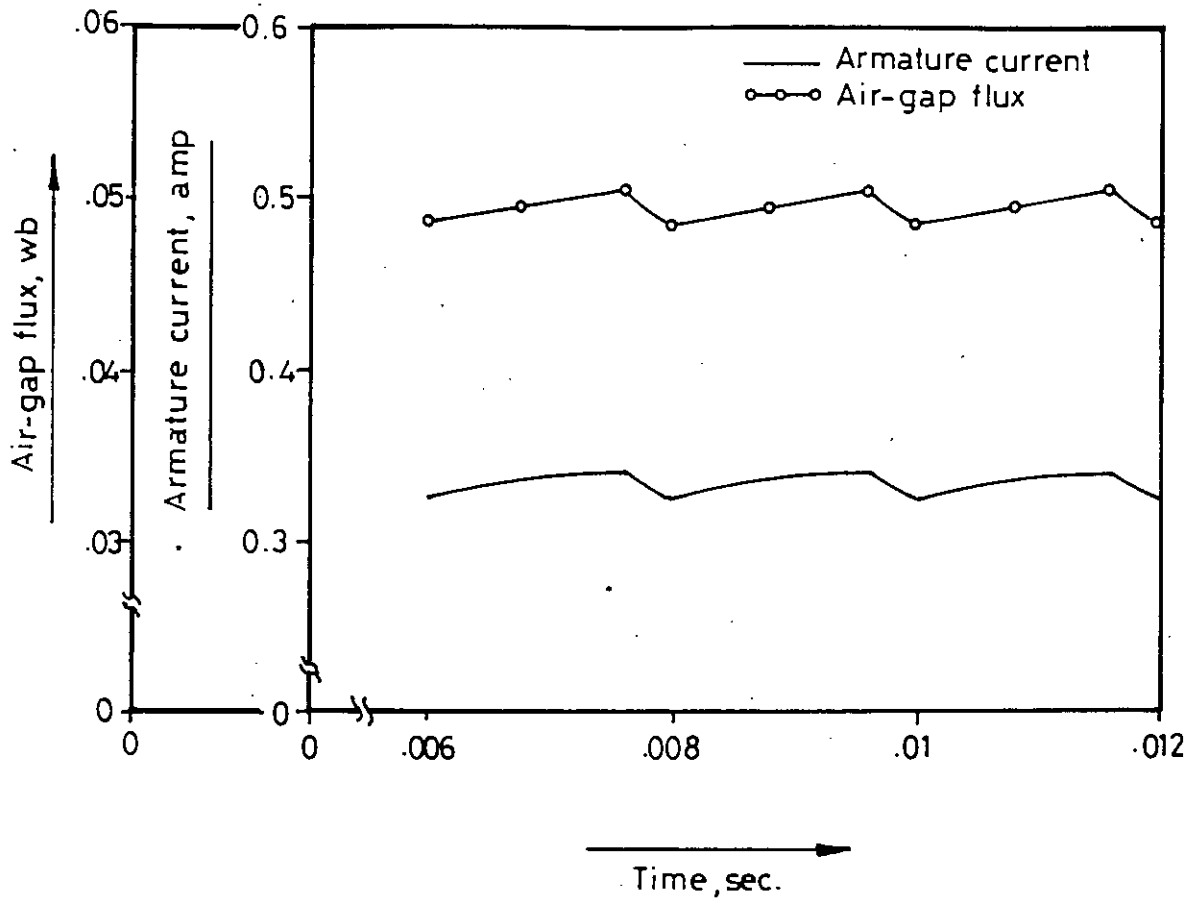

Figure–5.11 Variation of steady state armature current and air-gap flux with time (neglecting eddy current effect) for ω=80 rad/sec., δ=.84

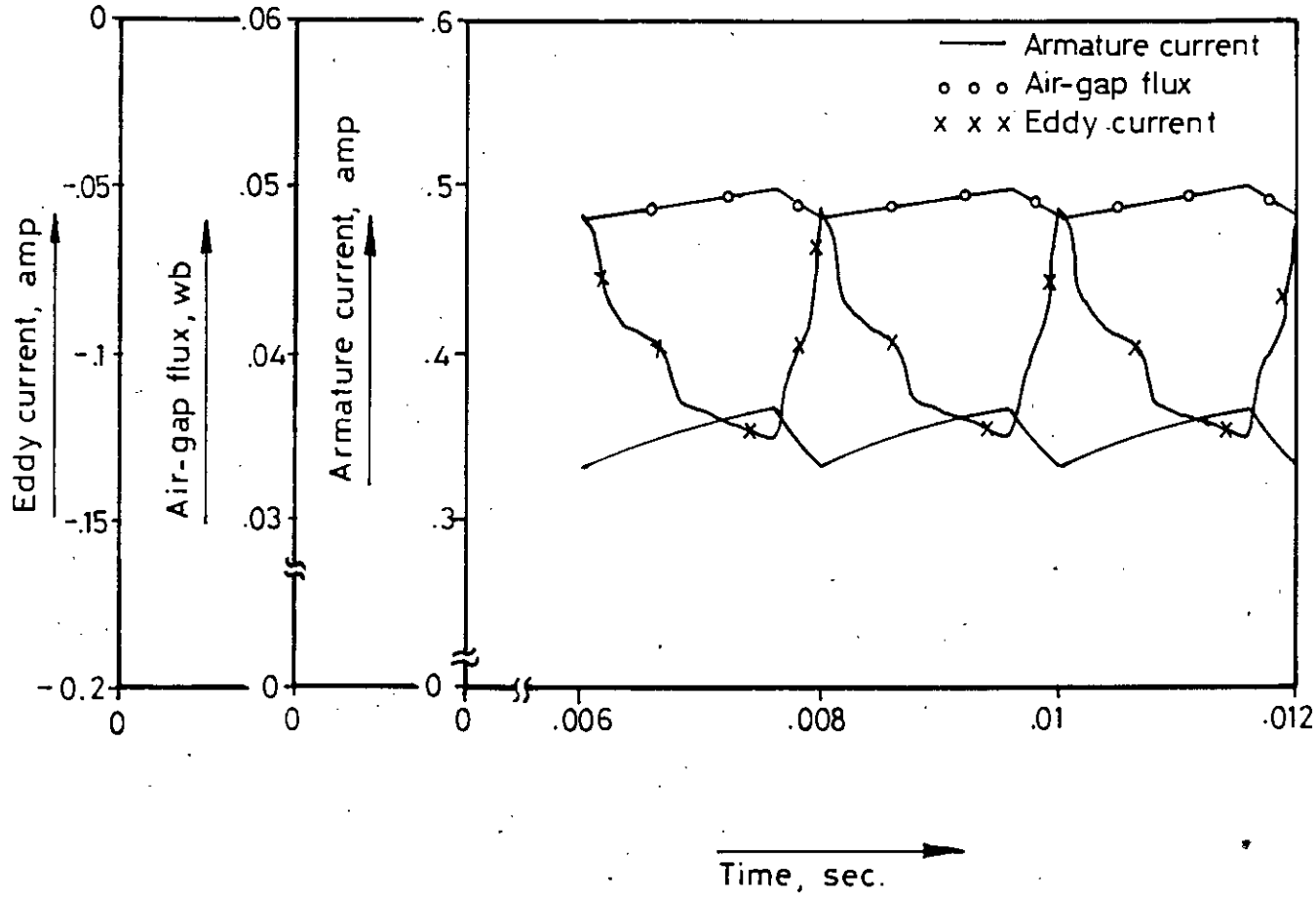

Figure-5.12 Variation of steady state armature current, eddy current and air-gap flux with time (taking eddy current effect) for $\omega = 80$ rad/sec., $\delta = .84$

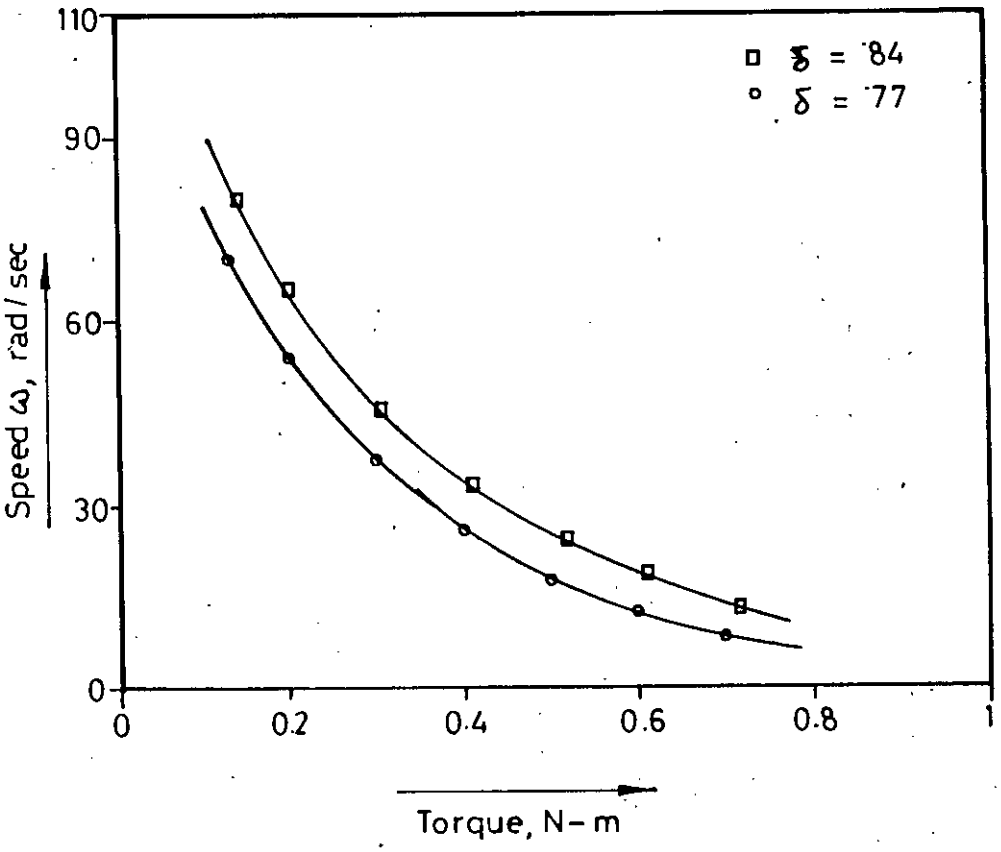

Figure-5.13 Torque-speed characteristics neglecting eddy current effect (Numerical model)

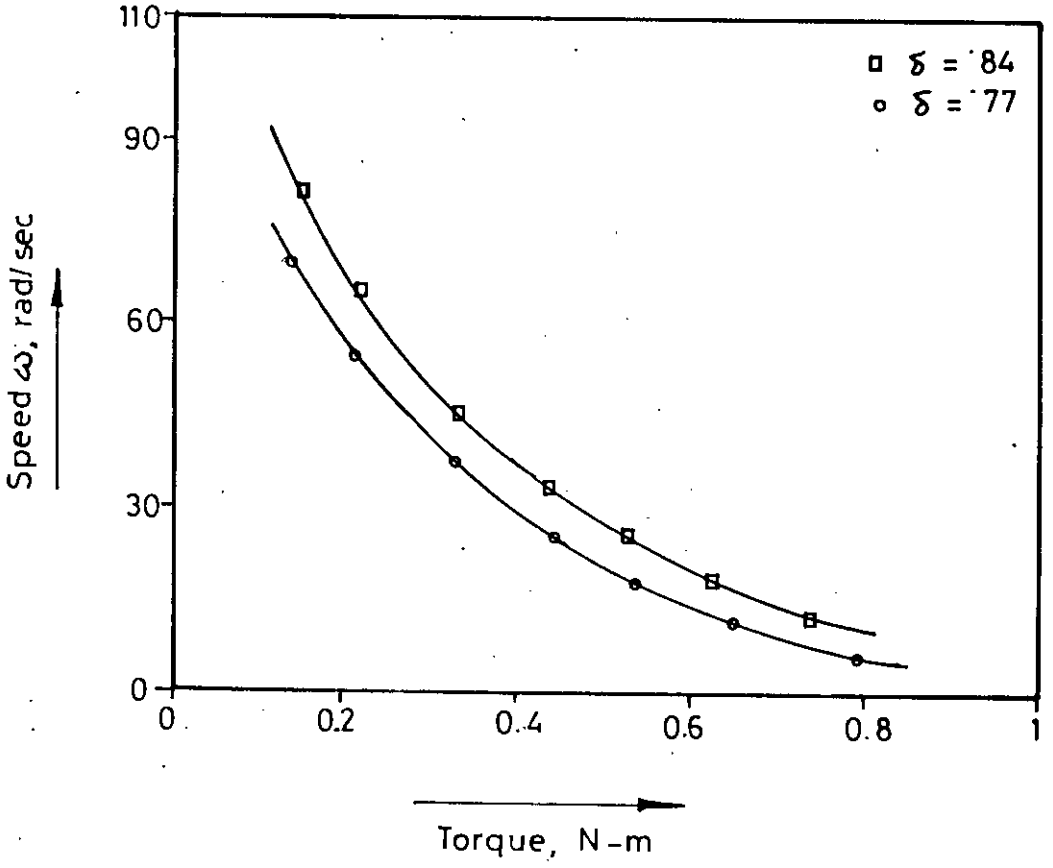

Figure-5.14 Torque-speed characteristics taking eddy current effect (Numerical model)

CHAPTER 6

EXPERIMENTAL RESULTS

6.1 INTRODUCTION

The accuracy of the mathematical models formulated in chapter 4 can be determined by comparing the results given in chapter 5 with the actual results. This requires determination of the actual steady state performance of the test machine when supplied from a chopper, which has been done experimentally. This chapter presents the experimental set-up and its brief description. The experimentally determined steady state torque-speed characteristics has also been given at the end of the chapter.

6.2 EXPERIMENTAL SET-UP

The actual steady state performance of the test motor when fed from chopper has been determined experimentally by supplying the motor from the output of a class C chopper, in which current commutation is used. The circuit diagram of the chopper together with the arrangements for current commutation is shown in figure 3.10a. The experimental set-up in block diagram is shown in figure 6.1. Figure 6.2 shows the interconnection of logic modules. The mark period ratio δ, is varied by the two quadrant dc/dc converter logic. Pulse width modulation has been utilized, that is , t_{ON} has been varied keeping the chopping frequency constant. The steady state torque has been measured with the help of an eddy current brake. The photograph of the whole experimental set-up is given in Appendix I.

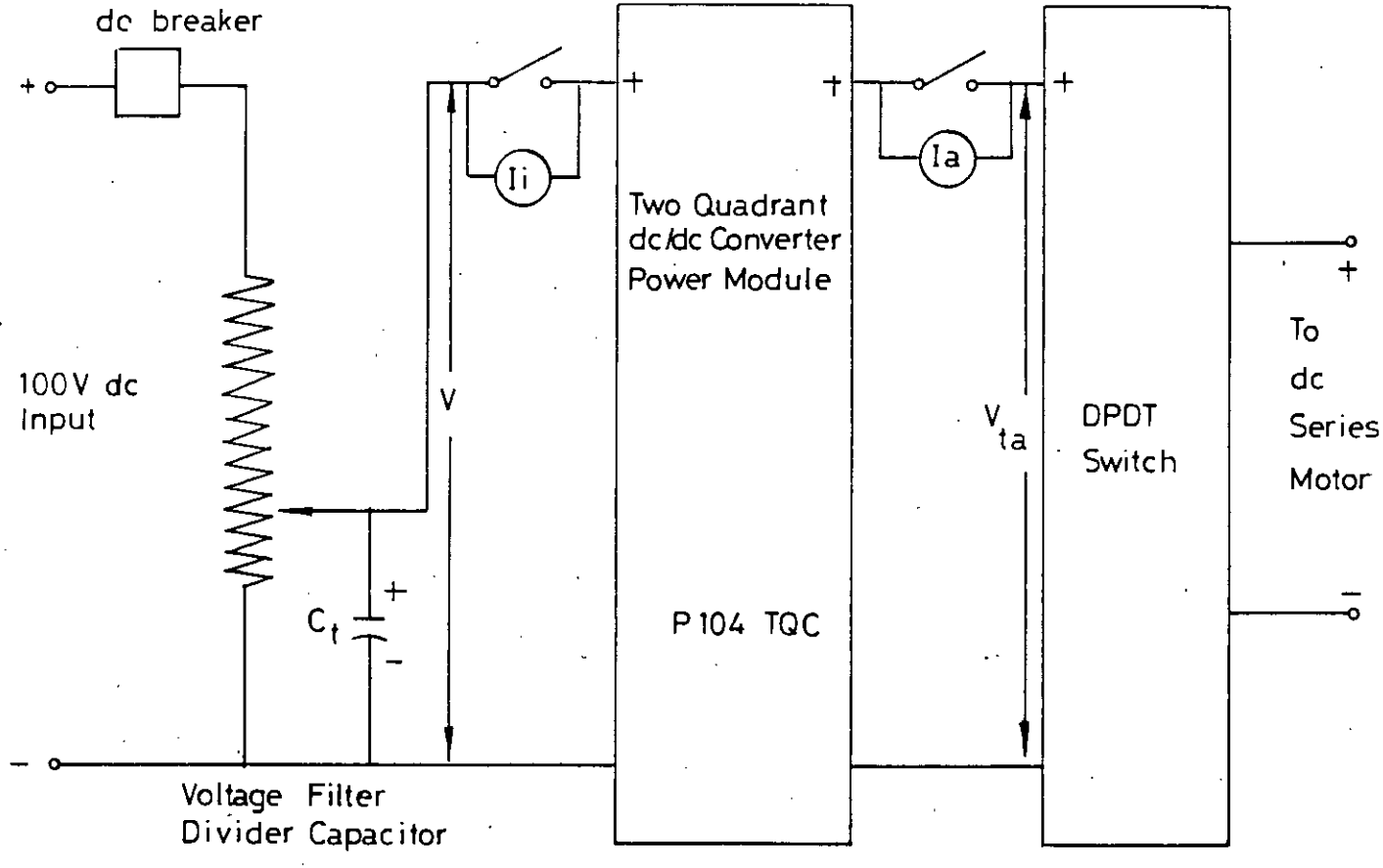

FIGURE - 6.1 TWO QUADRANT DC/DC CONVERTER POWER AND INSTRUMENTATION CIRCUIT

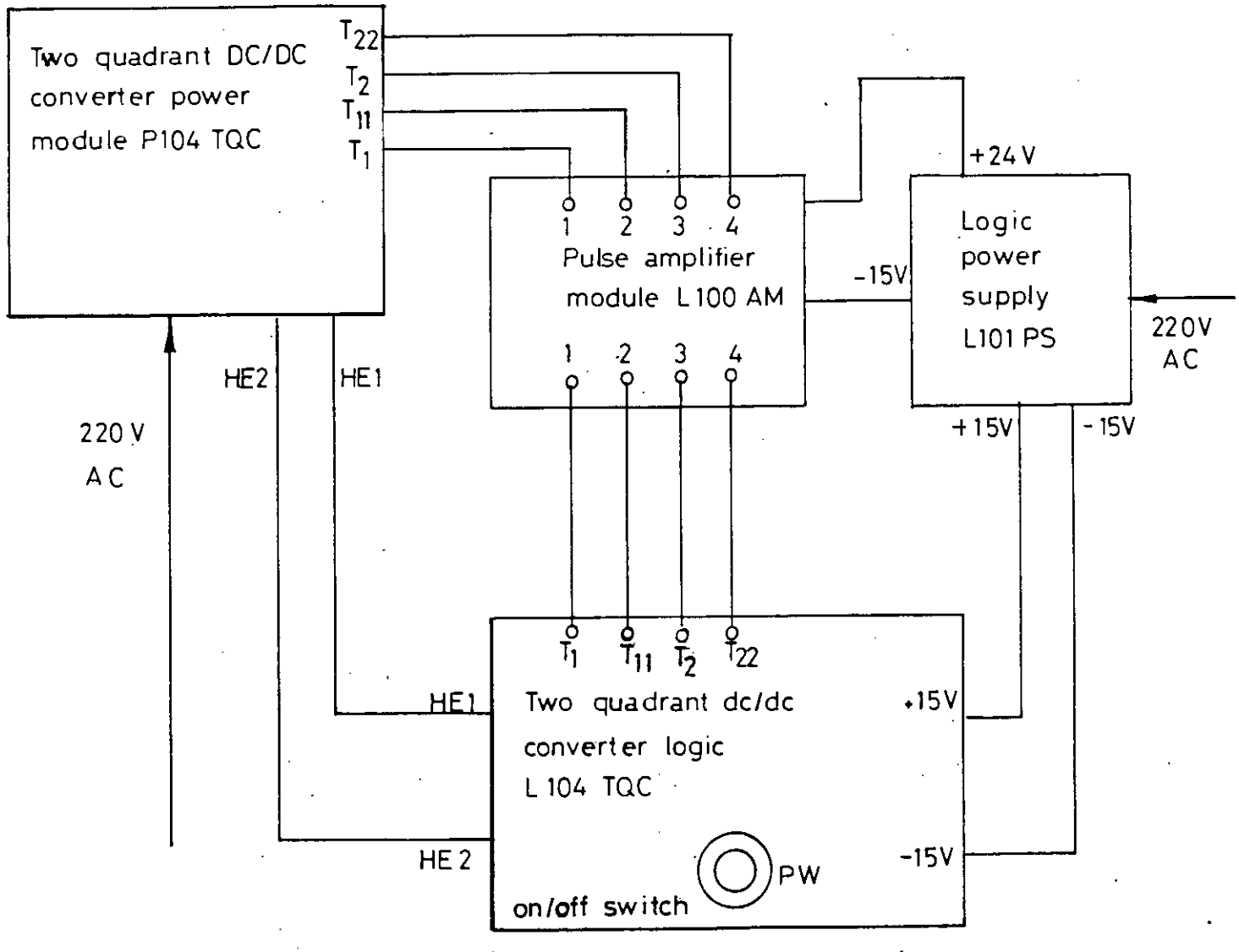

FIGURE-6.2 INTERCONNECTION OF LOGIC MODULES

6.3 TORQUE-SPEED CHARACTERISTICS

For a particular mark period ratio δ, the torque-speed characteristic has been determined by recording the speed and corresponding torque at different load. The motor has been loaded with the help of the eddy current brake. As the loading increases the speed of the motor decreases. Figure 6.3 presents the experimentally determined steady state torque-speed characteristics of the test machine for different mark period ratio δ. The output voltage of the chopper was adjusted at 100 volts.

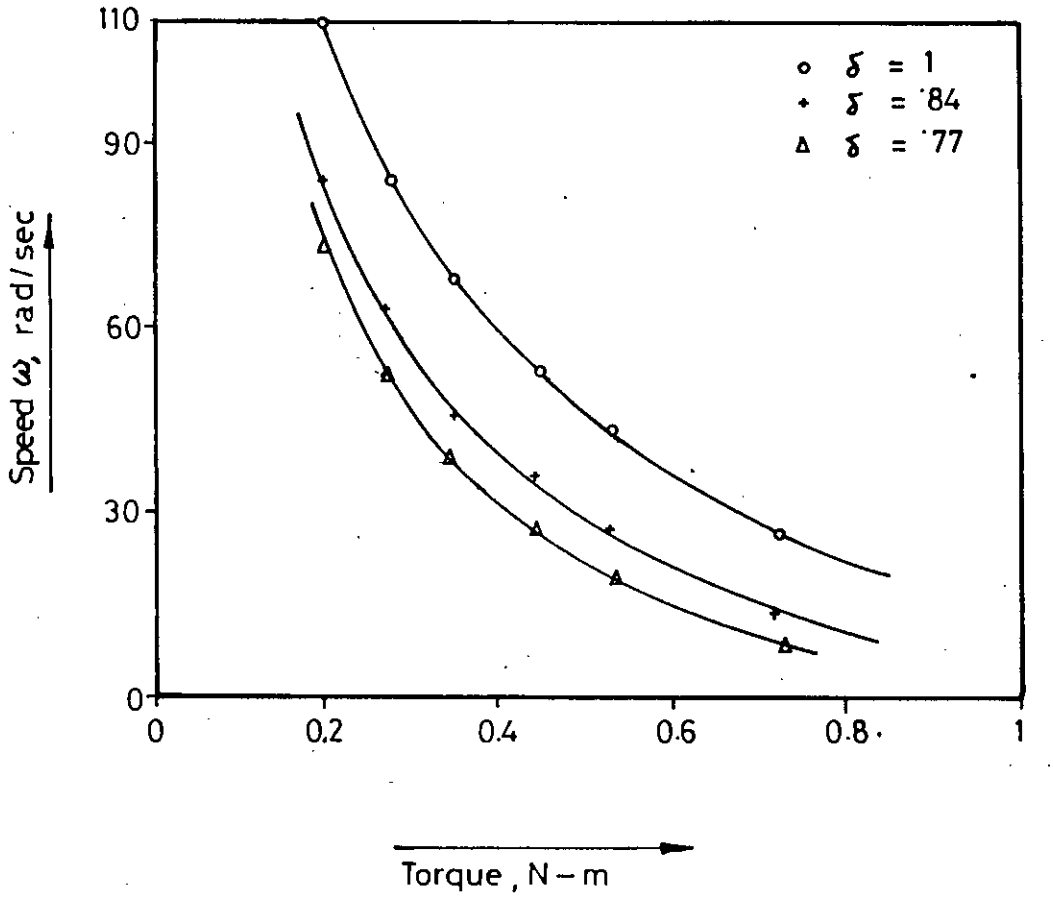

Figure-6.3 Torque-speed characteristics of the test machine (Experimental)

CHAPTER 7

COMPARISON AND ANALYSIS OF THE RESULTS

7.1 INTRODUCTION

The comparison of the analytical results with the experimental one is very much essential to make sure that the mathematical model, based on which the analytical results are obtained is fairly accurate. This chapter provides the facility of such comparison. Here the results obtained, by applying the mathematical models formulated in chapter 4 to a compound wound motor, operated as a series one have been compared with the experimental results of chapter 6. The chapter ends with an analysis of the results.

7.2 COMPARISON OF THE CURVES

The steady state torque-speed characteristics of the test machine as obtained from the empirical model is compared with the experimental one in figure 7.1. It shows that the curve which takes the eddy current effect into account resembles the actual characteristics more closely than the curve that does not consider the effect of eddy current. Similarly figure 7.2 compares the analytical curves obtained from the numerical model with the actual characteristics.

As a measure of correctness of the analytical curves the root mean square error of the curves may be quoted. For the empirical model, with mark period ratio, δ =0.84, the curve which does not consider the eddy current effect has a value of root mean square error of 1.64 rad/sec., while it is 1.12 rad/sec. for the curve which takes into account the effect of eddy currents. On the otherhand the curves obtained from numerical model have a considerably larger value of root mean square error. With δ=0.84, it is 3.20 rad/sec. for the curve which considers the effect of eddy current and 5.04 rad/sec. for the

curve that neglects eddy current effect. The root mean square error as a percentage of the maximum speed that can be achieved with the compound motor operating it as a series one is listed in table 7.1 for δ = 0.84.

Table 7.1

Curves		Root mean square error, rad/sec.	% of r.m.s. error, w.r.t. maximum available motor speed
Empirical model	With eddy current	1.12	1.07%
	Without eddy current	1.64	1.56%
Numerical model	With eddy current	3.20	3.05%
	Without eddy current	5.04	4.81%

The above analysis on the basis of root mean square error criteria, reveals that the inclusion of eddy current effect gives better result. Again it shows that the curves obtained by empirical model resembles the actual curves more closely than those obtained by numerical model. This discrepancy may be due to the following reasons:

1. Consideration of only one eddy current path.
2. Inaccuracy in values of some of the machine parameters due to lack of some machine data and determination of these values from approximate calculations.

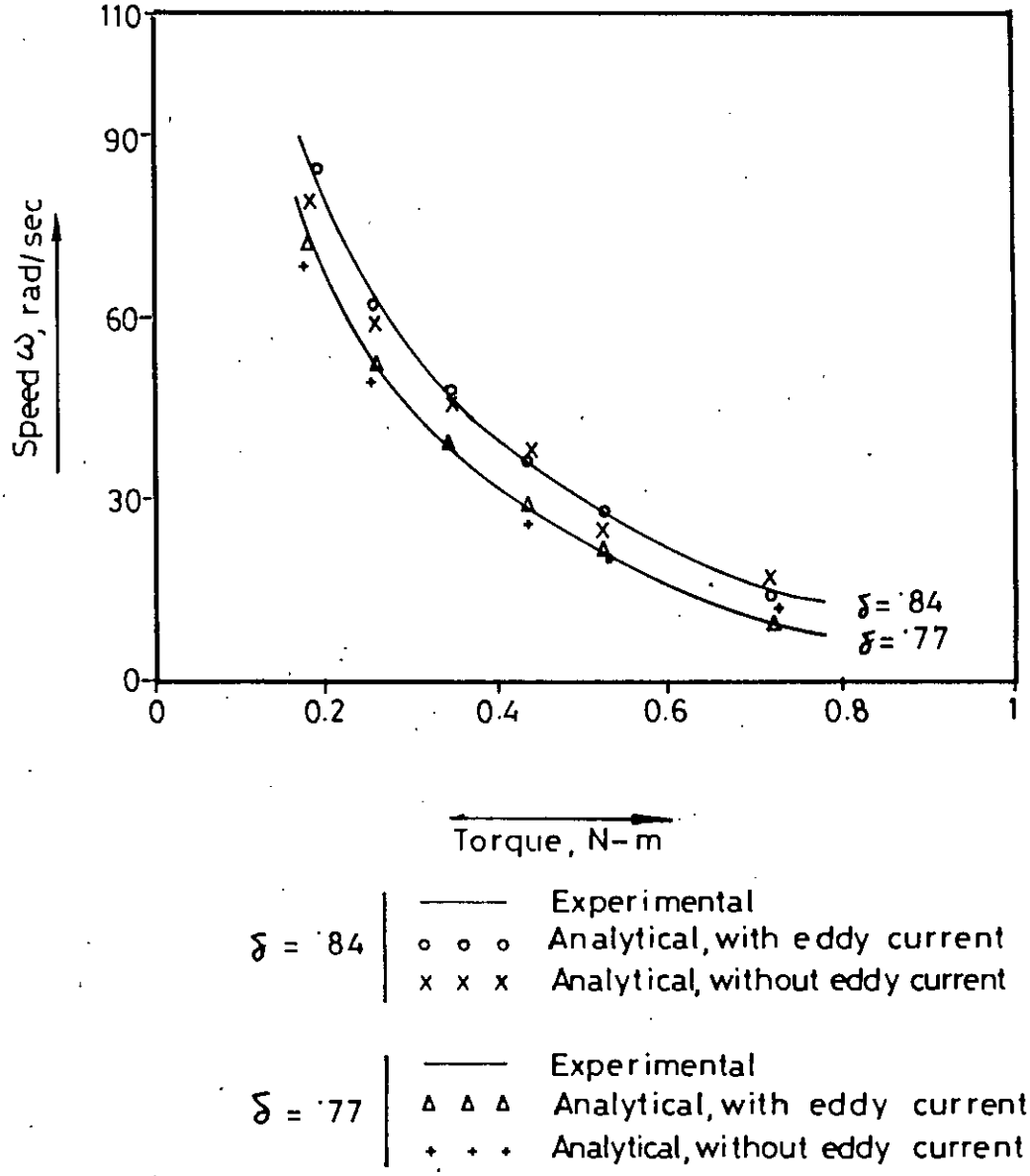

Figure-7.1 Comparison of the experimental curves with those obtained from empirical model

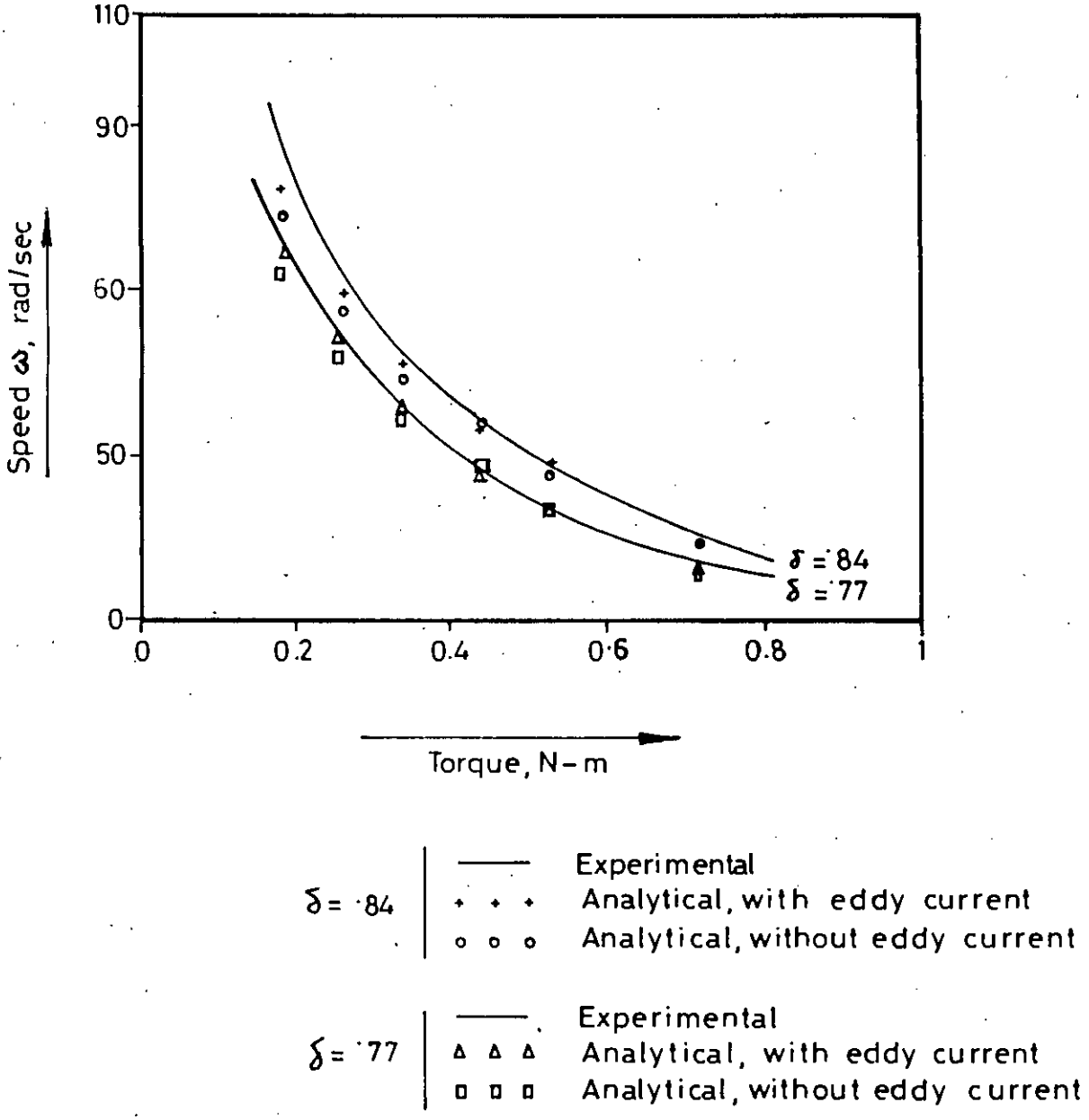

Figure-7.2 Comparison of the experimental curves with those obtained from numerical model.

It is quite obvious that the effect of eddy current is much more severe in transient condition than in normal steady state operation. A transient study should consider at least three (sometimes five) eddy current paths in the equivalent circuit of dc machine field, to represent the effect of eddy current. In case of chopper-fed dc series motor the variation of mmfs and fluxes are such that a single eddy current branch simulates the effect of eddy current more or less satisfactorily. For this reason in the present work only one eddy current path has been considered in the numerical model. Consideration of higher number of eddy current paths will definitely give better agreement of the theoretical curves with the experimental one. But in the first model that is in the empirical model the effect of eddy current has been included in a different way. In this model the effect of eddy current on the armature induced voltage has been recorded experimentally and this effect has been simulated by a generalised empirical relationship as given by equation (4.10). Therefore this model represents the effect of eddy current better than the numerical model with only one eddy current branch.

On the otherhand, value of some of the machine parameters needed for the numerical model solution have been determined on some assumptions, which may not be strictly correct. For example the inductance of the series field coil due to air-gap flux has been taken as ninety percent of the self inductance while the leakage inductance of the series field coil and armature coil have been considered as ten percent of the self inductances of the coils respectively. Again the test machine is a compound wound one whose total number of turns of the field coils per pole pair is known. But in the numerical model the value of N_s, that is, number of turns per pole pair of the series field coil is used. This value is determined on the assumption that the total number of turns is divided between the series and shunt field coils in the ratio of square root of their self inductances. This assumption definitely

gives an approximate value of N_s, which may cause the analytical curve to deviate from the actual one to some extent.

Another thing to be mentioned here that the test machine is supposed to be operated with both of its series and shunt field excitation. But in this work it is used as series motor. As a result some limitations are imposed on the motor. The rated motor voltage and speed are 220 volt and 1500 rpm. But as series motor the machine can not be operated at a speed greater than 1000 rpm without exceeding its rated current. The operating supply voltage has been adjusted at 100 volt only, to keep the machine within its ratings . For these reasons the comparison of the analytical curves with the experimental one is limited to a specified range of operation.

7.3 OBSERVATIONS AND ANALYSIS OF THE RESULTS

On the basis of the results obtained in chapter 5 and 6 and also from the comparison of the theoretical curves with the experimental one the following important points can be noted:

The steady state torque-speed characteristics obtained from the empirical model, when eddy current effect is considered, resembles the practical measurements more closely than that obtained without considering the effect of eddy current. This is also true for the numerical model. The above statement is justified in article 7.2, on the basis of root mean square error criteria. Further examination of the curves gives the informations listed in table 7.2 for mark period ratio, δ=0.84.

Table 7.2

Curves		*Maximum error in speed, rad/sec.	*% of error at maximum error	*Maximum % of error
Empirical model	With eddy current	1.23	1.5%	2.7%
	Without eddy current	3.33	3.9%	4.16%
Numerical model	With eddy current	5.77	6.88%	7.68%
	Without eddy Current	9.77	11.66%	11.66%

In table 7.2

*(a) Maximum error in speed = The maximum deviation of the theoretical curves from the experimental one in rad/sec.

*(b) % of error at maximum error = The error in (a) as a percentage of the actual speed.

*(c) Maximum % of error = The maximum value of percentage of error which may or may not be occurred at the instant of maximum error.

Hence it can be concluded that the eddy currents have a considerable effect on the steady state torque-speed characteristics of a chopper-fed dc series motor and it must be included in the analysis.

Comparison of figure 5.11 with 5.12 shows that the variation of air-gap flux with time, while the eddy current effect is included in the model becomes smooth. But the armature current variation becomes larger. These observations can be explained as follows :

In a chopper-fed dc series motor the air-gap flux depends on three quantities

1. The field current.
2. The armature reaction.
3. The eddy current.

The field current directly affects the air-gap flux. So, increased field current, which is also the armature current for dc series motor, tries to increase the air-gap flux. But the armature reaction that demagnetises the air-gap flux becomes greater at higher armature current. And the eddy current always tries to retard the change in air-gap flux. The effect of these three quantities can be explained clearly by dividing the period of the chopping cycle into two regions. In the region of low armature current ($i_a < I_{av}$) the effect of armature reaction on the air-gap flux may be neglected in comparison to the eddy current effect. In this region the eddy current plays the most important role and opposes any tendency of the air-gap flux to change. But in the high armature current region ($i_a > I_{av}$), as the magnitude of armature reaction is quite large, it plays the vital role on the air-gap flux. As a result of all these phenomena the variation of air-gap flux becomes smooth when the effect of eddy current is included in the model. But as the speed of the machine during a chopping period is assumed constant, a reduction of air-gap flux would result in a reduced back emf voltage. This will definitely increase the armature current. So smoothing of the variation of air-gap flux with time must be followed by larger values in the armature current.

The shape of the armature current within a chopping period as shown in figure 5.11 and 5.12 is such that it may be represented approximately by the exponential curves. Under such representation the system may be linearized in terms of armature current. Then the numerical solution of the second model will no longer be needed and an analytical solution may be formulated.

The maximum value of steady state eddy current as found in figure 5.12 is almost thirty percent of the maximum armature current. This eddy current has two significant effects on the performance of the motor. The first one, which is rather obvious and already mentioned is that it affects the steady state torque-speed characteristics of the motor. Secondly the eddy current has a heating effect and the rate at which energy is dissipated in the eddy current path is given by $I_{ed}^2 R_{ed}$. Figure 7.3 shows the variation of eddy current loss with time in a chopping period for $\delta=0.84$ and $\omega=80$ rad/sec. The eddy current ampere turns as a function of time is also shown in the same figure. The maximum power loss in eddy current path is 0.159 watt, which is 3.12% of the average armature copper loss. Again the maximum armature copper loss is 5.61 watt. So, the eddy current loss is 2.83% of the maximum armature copper loss. This small amount of eddy current loss may be neglected so far efficiency of motor is concerned. But this eddy current loss is about 7% to 8% of the average power loss in the series field coil. So, the pole structure is locally heated by eddy current flowing through the pole cores, yoke, joints and fittings. This heating effect is not negligible so far design of the pole structure for proper cooling facility is concerned. Hence it may be concluded that though the eddy current loss has negligible effect on the efficiency of a chopper-fed dc series motor, it has a significant effect on the design of the pole structure.

In the second model, the speed of the motor has been assumed constant throughout the whole chopping period. The theoretical results obtained with this assumption is in quite close agreement with the practical measurements. This justifies the assumption of constant speed. However analysis can be made without considering the speed to be constant throughout the chopping period. In this condition a differential equation of motion of armature must be included in the model, that represents the relationship among the torque, speed, moment of inertia etc. of the system.

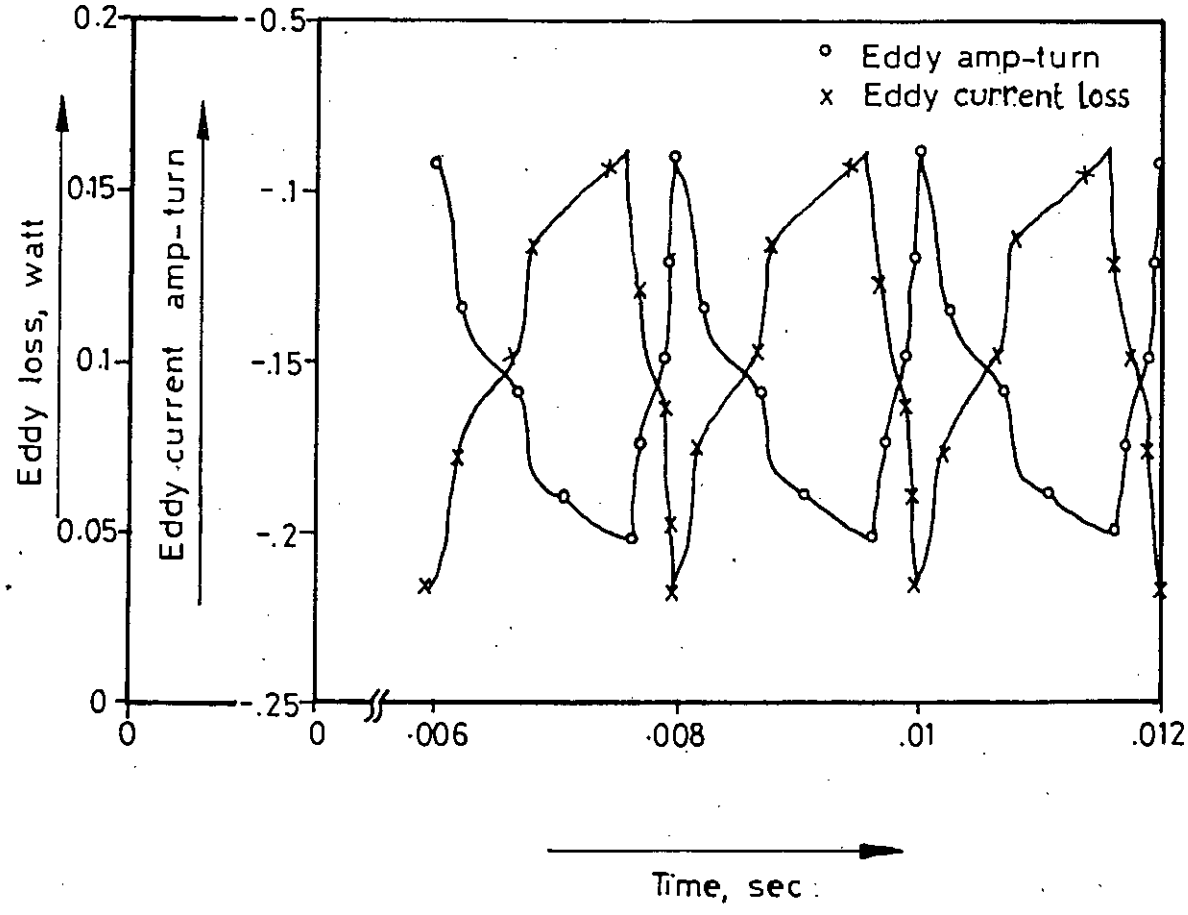

Figure-7.3 Variation of eddy current amp-turn and eddy current loss with time for $\omega = 80$ rad/sec., $\delta = .84$

7.4 COMPARATIVE STUDY OF THE METHODS

The first model is based on some empirical formula, which are to be determined from some experimental results. Therefore to apply this model to a system the system must be tested first in order to determine the value of some constants, such as Frolich's constants, the back emf coefficient and so on. So, the motor whose performance is to be determined must be at hand. On the other hand in the second model the motor is simulated by a system of nonlinear differential equations, which describe the operation of the motor in different modes of a chopper cycle. These system of differential equations can be formulated and solved without testing the motor. In this model only value of some of the motor parameters are required, which can be obtained easily from the design data of the motor. Hence the second model can also be applied to a system which is not at hand. But it is to be mentioned here that this model requires the numerical solution of the differential equations describing the motor performance. As a result this model takes a considerable computation time.

CHAPTER 8

CONCLUSIONS

8.1 CONCLUSIONS

Steady state analysis of chopper-fed dc series motor has been carried out in this thesis. The theoretical results have been compared with the actual values as determined experimentally. The results have also been analysed critically in the previous chapter. The following important conclusions are drawn from this thesis:

1. The approaches suggested in this work for modelling dc series motor fed by chopper is general in the sense that it takes into account the effects of saturation of magnetic circuit, eddy current and armature reaction. There is a satisfactory agreement between predicted and experimental performance.
2. The eddy current has a considerable effect on the steady state torque-speed characteristics of a chopper-fed dc series motor and therefore it must be included in the analysis.
3. The effect of eddy current loss on the efficiency of a chopper-fed dc series motor is negligible.
4. The heating effect of eddy current plays important part on the design of the pole structure of a chopper-fed dc series motor.
5. The first model which is based on some empirical formula permits the derivation of simple analytical methods for the analysis of dc series motor fed by a chopper with pulse-width control. This approach permits considerable reduction of computation time and gives good accuracy.
6. The variation of speed of the motor during chopping cycle is negligible.

8.2 RECOMMENDATIONS FOR FURTHER STUDY

The mathematical models used in this work do not contain all the factors which cause nonlinear relation between the armature induced voltage and the armature current, such as the dc machine commutation, increase in resistance due to skin effect and so on. The study and analysis is also restricted for steady state performance of chopper-fed dc series motor only . . The following points can be taken under consideration for future work on this context:

1. The effect of chopper commutation period can be included in the model.
2. Analysis can be made without considering the speed to be constant through out the chopping period.
3. To take into account the effect of eddy current more than one eddy current path may be considered.
4. The inclusion of dc motor commutation in the model and study of different types of dc motor fed from chopper.
5. Analysis can be made for determining transient response of chopper-fed dc series motor.
6. The model can be modified for the analysis of separately excited dc motor fed from chopper.

APPENDIX A

DERIVATION OF THE PERFORMANCE EQUATIONS OF THE EMPIRICAL MODEL

The quantities in equation (4.10) can be redefined and approximated for the analysis of chopper-fed dc series motor as follows

For rising current,

$$\frac{\triangle i}{(k_2+i)I_{fo}} = \frac{-(I_{a2}-i_a)}{I_{a2}(k_2+i_a)}$$

and

$$\left(\frac{i}{I_{fo}}\right)^n = \left[\frac{(i_a-I_{a1})}{I_{a2}}\right]^n$$

For falling current during free wheeling,

$$\frac{\triangle i}{(k_2+i)I_{fo}} = \frac{i_a-I_{a1}}{I_{a2}(k_2+i_a)}$$

and

$$\left(\frac{i}{I_{fo}}\right)^n = \left[\frac{(i_a-I_{a1})}{I_{a2}}\right]^n$$

Now replacing i_a by I_{av} for taking the average effect

$$\frac{-(I_{a2}-i_a)}{I_{a2}(k_2+i_a)} \simeq \frac{-(I_{a2}-I_{av})}{I_{a2}(k_2+I_{av})}$$

$$= \frac{-(i_p/I_{a2})}{(k_2+I_{av})}$$

$$= \frac{-\alpha}{(k_2+I_{av})} \qquad \text{(A.1a)}$$

where $\alpha = (i_p/I_{a2})$ and i_p = peak value of current ripple,

and

$$\left(\frac{i}{I_{fo}}\right)^n = \left[\frac{(i_a-I_{a1})}{I_{a2}}\right]^n$$

$$\simeq \left[\frac{I_{av}-I_{a1}}{I_{a2}}\right]^n$$

$$= \left(\frac{i_p}{I_{a2}}\right)^n$$

$$= \alpha^n$$

so,

$$\frac{(i/I_{fo})^n}{(k_2+i)^2} = \frac{(i_p/I_{a2})^n}{(k_2+I_{av})^2} = \frac{\alpha^n}{(k_2+I_{av})^2} \qquad \text{(A.1b)}$$

in the above equations may be suitably chosen and taken as a constant.

CASE I : Chopper with Square Wave Output Waveform

(a) Duty Interval ($0 \leqslant t \leqslant \delta T$)

The differential equation describing this mode is

$$L(I_{av})\frac{di_a}{dt} + R.i_a + K.\omega.i_a + \Delta V_e = V \qquad \text{(A.2)}$$

where ΔV_e = Voltage due to eddy currents.

R = Total armature circuit resistance.

K = Back emf coefficient as defined by equation (4.8) and assumption (iv) of section 4.2.4, is a function of I_{av}.

(b) Free Wheeling Interval ($\delta T \leqslant t \leqslant T$)

The differential equation describing this mode is

$$L(I_{av})\frac{di_a}{dt} + R.i_a + K.\omega.i_a + \Delta V_e = 0 \qquad \text{(A.3)}$$

Substitution from equations (A.1a) and (A.1b) into equation (4.10) gives

$$\Delta V_e = \lambda\left(\frac{\omega}{\omega_o}\right)\left[i_a.\frac{-\alpha.\mathrm{sgn}(di_a/dt)}{(k_2+I_{av})} - \frac{k_2.\sigma.\alpha^n}{(k_2+I_{av})^2}.\frac{di_a}{dt}\right] \qquad \text{(A.4)}$$

Substitution of ΔV_e from equation (A.4) into equation (A.2) and (A.3) gives

$$L_{eq}.\frac{di_a}{dt} + i_a.R'_{eq} = V \qquad \text{(A.5)}$$

with $i_a(0)=I_{a1}$; for $0 \leqslant t \leqslant \delta T$

where,

$$L_{eq} = L(I_{av}) - \frac{\lambda.(\omega/\omega_o).k_2.\sigma.\alpha^n}{(k_2+I_{av})^2}$$

$$R_{eq}' = [R+K.\omega - \lambda(\frac{\omega}{\omega_o}).\frac{\alpha}{(k_2+I_{av})}],$$

and

$$L_{eq}.\frac{di_a}{dt} + i_a.R_{eq}' = 0 \qquad (A.6)$$

with $i_a(\delta T)=I_{a2}$; for $\delta T \leqslant t \leqslant T$

Equations (A.5) and (A.6) are linear equations for a specified operating condition under steady state. The average steady state machine speed can be determined from equations (A.5) and (A.6) as

$$\omega_{av} = \omega = \frac{V\delta - RI_{av}}{I_{av}[K - \frac{\lambda}{\omega_o}.\frac{\alpha}{(k_2+I_{av})}]} \qquad (A.7)$$

The electromagnetic torque T_e is given by

$$T_e = \frac{E_{av}.I_{av}}{\omega} \qquad (A.8)$$

CASE II : Chopper with Non-square Output Voltage Waveform due to Load Dependent Commutation

The voltage and current waveforms of a load current commutated chopper are shown in figure 4.4. There are three distinct mode of operations as shown below :

(a) Duty Interval ($0 \leqslant t \leqslant \delta T$)

The equations describing this mode of operation are

$$L_{eq}.\frac{di_a}{dt} + i_a.R_{eq} + K'.\omega_{av} = V \qquad (A.9)$$

with $i_a(0)=I_{a1}$ and $K' = KI_{av}$

where L_{eq} is as defined in case I and

$$R_{eq} = R - \frac{\lambda.(\omega/\omega_o).\alpha}{(k_2+I_{av})}$$

(b) Commutation Interval ($\delta T \leqslant t \leqslant (\delta + \delta_c)T$)

Assuming constant current during commutation interval gives, $I_c = I_{a2}$. Further,

$$\delta_c T = \frac{2CV}{I_{a2}} \qquad (A.10)$$

(c) Free Wheeling Interval ($(\delta + \delta_c)T \leqslant t \leqslant T$)

In this mode, the armature current free wheels through the free wheeling diode and both the main and auxiliary thyristors are off. The equations describing this mode are given by

$$L_{eq} \cdot \frac{di_a}{dt} + i_a \cdot R_{eq} + K' \cdot \omega_{av} = 0 \qquad (A.11)$$

with $i_a((\delta + \delta_c)T) = I_c = I_{a2}$ and $i_a(t=T) = I_{a1}$

The solutions for armature current obtained from equations (A.9) and (A.11) are

$$i_a = \frac{V - K'\omega_{av}}{R_{eq}}(1 - e^{-t/\tau_a}) + I_{a1}e^{-t/\tau_a}) \qquad (A.12)$$

for $0 \leqslant t \leqslant \delta T$; and

$$i_a = \frac{-K'\omega_{av}}{R_{eq}}(1 - e^{-t'/\tau_a}) + I_{a2}e^{-t'/\tau_a}) \qquad (A.13)$$

for $0 \leqslant t' \leqslant (1 - \delta - \delta_c)T$

where,

$$T_a = \frac{L_{eq}}{R_{eq}}$$

From equations (A.12) and (A.13) with $i_a(\delta T) = I_{a2}$ and $i_a((1 - \delta - \delta_c)T) = I_{a1}$ one gets,

$$I_{a1} = \frac{V}{R_{eq}}\left[\frac{1 - e^{\delta T/\tau_a}}{1 - e^{(1-\delta_c)T/\tau_a}}\right] - \frac{K'\omega_{av}}{R_{eq}} \qquad (A.14)$$

and

$$I_{a2} = \frac{V}{R_{eq}}\left[\frac{1 - e^{-\delta T/\tau_a}}{1 - e^{-(1-\delta_c)T/\tau_a}}\right] - \frac{K'\omega_{av}}{R_{eq}} \qquad (A.15)$$

From equations (A.10) and (A.15) the average motor speed is given by

$$\omega_{av} = \omega = \frac{R_{eq}}{K'}\left[\frac{V}{R_{eq}}\left(\frac{1-e^{-\delta T/\tau_a}}{1-e^{-(1-\delta_c)T/\tau_a}} - \frac{2CV}{\delta_c . T}\right)\right]$$

$$= \frac{E_{av}}{K'} \qquad \text{(A.16)}$$

The average armature current is given by

$$I_{av} = \frac{V\delta - (1-\delta_c)K'\omega_{av}}{R_{eq}} + \frac{2CV}{T}$$

$$= \frac{V}{R_{eq}}\left[\delta - (1-\delta_c)\frac{E_{av}}{V}\right] + \frac{2CV}{T} \qquad \text{(A.17)}$$

The average electromagnetic torque is given by equation (A.8).

APPENDIX B

DETERMINATION OF THE EXPRESSION OF AIR-GAP FLUX, ϕ_{ma}

substitution of equation (4.30) in equation (4.29) gives

$$\phi_{ma} = \frac{1}{2F_a}\int_{F_d-F_a}^{F_d+F_a}\phi(F)dF$$

$$= \frac{1}{2F_a}\int_{F_d-F_a}^{F_d+F_a}[a_1\tan^{-1}(b_1F)+d_1F]dF$$

with $F_d+F_a = F_2$ and $F_d-F_a = F_1$ one gets

$$\phi_{ma} = \frac{1}{2F_a}\int_{F_1}^{F_2}(a_1\tan^{-1}b_1F)dF + \frac{1}{2F_a}\int_{F_d-F_a}^{F_d+F_a}(d_1F)dF$$

The second integral can be performed easily as

$$\frac{1}{2F_a}\int_{F_d-F_a}^{F_d+F_a}(d_1F)dF = \frac{d_1}{2F_a}\left[\frac{F^2}{2}\right]_{F_d-F_a}^{F_d+F_a}$$

$$= \frac{d_1}{4F_a}[(F_d+F_a)^2 - (F_d-F_a)^2]$$

$$= d_1F_d$$

In order to evalulate the first integral let

$$y = \tan^{-1}b_1F$$

or $\tan y = b_1F$

or $\frac{1}{b_1}\sec^2y\,dy = dF$

Substitution of these in the first integral gives

$$\frac{1}{2F_a}\int_{F_d-F_a}^{F_d+F_a}(a_1\tan^{-1}b_1F)dF = \frac{a_1}{2F_a}\int_{F_1}^{F_2}\left(\frac{y.\sec^2y}{b_1}\right)dy$$

$$= \frac{a_1}{2F_a}\left[\frac{1}{b_1}(y\tan y\Big|_{F_1}^{F_2} - \int_{F_1}^{F_2}\tan y\,dy)\right]$$

$$= \frac{a_1}{2F_a}\left[\frac{1}{b_1}\{b_1F_2(\tan^{-1}b_1F_2) - b_1F_1(\tan^{-1}b_1F_1)\} - \frac{1}{b_1}(\ln\sec y)\Big|_{F_1}^{F_2}\right]$$

$$= \frac{a_1}{2F_a}\left[(F_2\tan^{-1}b_1F_2 - F_1\tan^{-1}b_1F_1) - \frac{1}{b_1}\ln\sqrt{1+b_1^2F^2}\Big|_{F_1}^{F_2}\right]$$

$$= \frac{a_1}{2F_a}\left[\left(F_2 \tan^{-1} b_1 F_2 - F_1 \tan^{-1} b_1 F_1\right) - \frac{1}{2b_1} \ln \frac{1+b_1^2 F_2^2}{1+b_1^2 F_1^2}\right]$$

Hence the total expression for ϕ_{ma} becomes

$$\phi_{ma} = \frac{a_1}{2F_a}\left[\left(F_2 \tan^{-1}(b_1 F_2) - F_1 \tan^{-1}(b_1 F_1)\right) - \frac{1}{2b_1} \ln \frac{1+b_1^2 F_2^2}{1+b_1^2 F_1^2}\right] + d_1 F_d .$$

APPENDIX C

FORMATION OF THE FIRST ORDER NONLINEAR SIMULTANEOUS DIFFERENTIAL EQUATION

The equation of the armature circuit and that of the eddy current path of a chopper-fed dc series motor is given by

$$(L_{a1}+L_{s1})\frac{di_a}{dt} + \frac{d\psi_{aq}}{dt} + \frac{d\psi_s}{dt} + K.\phi_{ma}.\omega + i_a.R_a + \Delta v_b = v_a \qquad (C.1)$$

and

$$d\psi_{ed}/dt = -i_{ed}.R_{ed} \qquad (C.2)$$

respectively.

where

$$\left.\begin{aligned} \frac{d\psi_{aq}}{dt} &= L_{aq}\frac{di_a}{dt} + M_{ae}\frac{di_d}{dt} \\ \text{and} \\ \frac{d\psi_s}{dt} &= \frac{N_s}{N_e}\left[M_{ea}\frac{di_a}{dt} + L_e\frac{di_d}{dt}\right] \end{aligned}\right\} \qquad (C.3)$$

i_d is given by

$$F_d = N_s(i_a+i_{ed}) = N_e i_d$$

or
$$i_d = \frac{N_s}{N_e}(i_a+i_{ed}) \qquad (C.4)$$

and

$$\psi_{ed} = L_{ed}.i_{ed} + p.N_s.\phi_{ma}$$

which gives

$$i_{ed} = \frac{\psi_{ed} - p.N_s.\phi_{ma}}{L_{ed}} \qquad (C.5)$$

The expressions of L_{aq}, M_{ae}, M_{ea}, L_e and ϕ_{ma} are given by equations (4.37) and (4.31). Again $d\phi_{ma}/dt$ can be written as

$$\frac{d\phi_{ma}}{dt} = \frac{\partial\phi_{ma}}{\partial i_a}.\frac{di_a}{dt} + \frac{\partial\phi_{ma}}{\partial i_d}.\frac{di_d}{dt}$$

$$= L_1\frac{di_a}{dt} + L_2\frac{di_d}{dt} \qquad (C.6)$$

where the expressions of L_1 and L_2 are given by equation (4.46). Now differentiating equation (C.5) with respect to time one gets

$$\frac{di_{ed}}{dt} = \frac{1}{L_{ed}}\left[\frac{d\psi_{ed}}{dt} - p.N_s.\frac{d\phi_{ma}}{dt}\right]$$

$$= \frac{1}{L_{ed}}\left[-i_{ed}.R_{ed} - p.N_s.\frac{d\phi_{ma}}{dt}\right]; \text{ from equation (C.2). or,}$$

$$L_{ed}\frac{di_{ed}}{dt} = -i_{ed}R_{ed} - pN_s\left[L_1\frac{di_a}{dt} + L_2\frac{di_d}{dt}\right]; \text{ from equation (C.6).}$$

$$= -i_{ed}R_{ed} - pN_s\left[L_1\frac{di_a}{dt} + L_2\left\{\frac{d}{dt}\left(\frac{N_s}{N_e}(i_a+i_{ed})\right)\right\}\right], \text{ from equation (C.4)}$$

or,

$$\left[L_{ed}+p\frac{N_s^2}{N_e}L_2\right]\frac{di_{ed}}{dt} = -i_{ed}R_{ed} - \left[pN_sL_1 + p\frac{N_s^2}{N_e}L_2\right]\frac{di_a}{dt} \qquad (C.7)$$

Again substitution of equations (C.3) and (C.4) in equation (C.1) gives

$$(L_{a1}+L_{s1})\frac{di_a}{dt} + L_{aq}\frac{di_a}{dt} + M_{ae}\frac{di_a}{dt} + M_{es}\frac{d}{dt}\left[\frac{N_s}{N_e}(i_a+i_{ed})\right] + \frac{N_s}{N_e}L_e\frac{d}{dt}\left[\frac{N_s}{N_e}(i_a+i_{ed})\right] +$$

$$K\phi_{ma}\omega + i_aR_a + \triangle v_b = v_a$$

or,

$$\left[L_{a1}+L_{s1}+L_{aq}+2\frac{N_s}{N_e}M_{ae}+\frac{N_s^2}{N_e^2}L_e\right]\frac{di_a}{dt} + \left[\frac{N_s}{N_e}M_{ae}+\frac{N_s^2}{N_e^2}L_e\right]\frac{di_{ed}}{dt} + K\phi_{ma}\omega + i_aR_a + \triangle v_b = v_a$$

.....(C.8)

Substituting the value of di_{ed}/dt from equation (C.7) into equation (C.8) one gets

$$\frac{di_a}{dt} = \frac{\left[\left(L_{ed}+p\frac{N_s^2}{N_e}L_2\right)(v_a - \triangle v_b - i_aR_a - K\phi_{ma}\omega) + \left(\frac{N_s}{N_e}M_{ae}+\frac{N_s^2}{N_e^2}L_e\right)i_{ed}R_{ed}\right]}{\left[\left(L_{ed}+p\frac{N_s^2}{N_e}L_2\right)\left(L_{a1}+L_{s1}+L_{aq}+2\frac{N_s}{N_e}M_{ae}+\frac{N_s^2}{N_e^2}L_e\right) - \left(\frac{N_s}{N_e}M_{ae}+\frac{N_s^2}{N_e^2}L_e\right)\left(pN_sL_1+p\frac{N_s^2}{N_e}L_2\right)\right]}$$

.....(C.9)

Similarly subtitution of di_a/dt from equation (C.7) into equation (C.8) gives

$$\frac{di_{ed}}{dt} = \frac{\left[-\left(pN_s L_1 + p\frac{N_s^2}{N_e}L_2\right)\left(v_a - \Delta v_b - i_a R_a - K\phi_{ma}\omega\right) - \left(L_{a1} + L_{s1} + L_{aq} + 2\frac{N_s}{N_e}M_{se} + \frac{N_s^2}{N_e^2}L_e\right) i_{ed} R_{ed}\right]}{\left[\left(L_{ed} + p\frac{N_s^2}{N_e}L_2\right)\left(L_{a1} + L_{s1} + L_{aq} + 2\frac{N_s}{N_e}M_{se} + \frac{N_s^2}{N_e^2}L_e\right) - \left(\frac{N_s}{N_e}M_{se} + \frac{N_s^2}{N_e^2}L_e\right)\left(pN_s L_1 + p\frac{N_s^2}{N_e}L_2\right)\right]}$$

.....(C.10)

Equations (C.9) and (C.10) represent the required first order nonlinear simultaneous differential equation which is of the form

$$\frac{dx}{dt} = f_1(t,x,y)$$

and

$$\frac{dy}{dt} = f_2(t,x,y)$$

APPENDIX D

DETERMINATION OF THE EXPRESSION OF DYNAMIC INDUCTANCES, L_1 AND L_2

The dynamic inductances L_1 and L_2 are defined as

$$L_1 = \frac{\partial \phi_{ma}}{\partial i_a} \qquad \text{and} \qquad L_2 = \frac{\partial \phi_{ma}}{\partial i_d} \tag{D.1}$$

where ϕ_{ma} is given by equation (4.31) as

$$\phi_{ma} = \frac{a_1}{2F_a}\left[F_2 \tan^{-1}(b_1 F_2) - F_1 \tan^{-1}(b_1 F_1) - \frac{1}{2b_1} \ln \frac{1+b_1^2 F_2^2}{1+b_1^2 F_1^2}\right] + d_1 F_d \tag{D.2}$$

Substituting this value of ϕ_{ma} in (D.1)

$$\begin{aligned}
L_1 &= \frac{\partial \phi_{ma}}{\partial i_a} \\
&= \frac{a_1}{2}\left(-\frac{N_a'}{F_a^2}\right)\left(F_2 \tan^{-1}(b_1 F_2) - F_1 \tan^{-1}(b_1 F_1) - \frac{1}{2b_1} \ln \frac{1+b_1^2 F_2^2}{1+b_1^2 F_1^2}\right) + \\
&\quad \frac{a_1}{2F_a}\left[N_a' \tan^{-1}(b_1 F_2) + F_2 \frac{b_1 N_a'}{1+b_1^2 F_2^2} + N_a' \tan^{-1}(b_1 F_1) - F_1 \frac{b_1 (-N_a')}{1+b_1^2 F_1^2}\right. \\
&\quad \left. - \frac{1}{2b_1} \cdot \frac{(1+b_1^2 F_1^2)}{(1+b_1^2 F_2^2)} \cdot \frac{(1+b_1^2 F_1^2) b_1^2 2F_2 N_a' - (1+b_1^2 F_2^2) b_1^2 2F_1 (-N_a')}{(1+b_1^2 F_1^2)^2}\right] \\
&= -\frac{a_1 N_a'}{2F_a^2}\left[F_d(\tan^{-1} b_1 F_2 - \tan^{-1} b_1 F_1) - \frac{1}{2b_1} \cdot \ln \frac{(1+b_1^2 F_2^2)}{(1+b_1^2 F_1^2)}\right]
\end{aligned}$$

and

$$\begin{aligned}
L_2 &= \frac{\partial \phi_{ma}}{\partial i_d} \\
&= \frac{a_1}{2F_a}\left[N_e \tan^{-1} b_1 F_2 + F_2 \frac{b_1 N_e}{(1+b_1^2 F_2^2)} - N_e \tan^{-1} b_1 F_1 - F_1 \frac{b_1 N_e}{(1+b_1^2 F_1^2)}\right. \\
&\quad \left. - \frac{1}{2b_1} \cdot \frac{(1+b_1^2 F_1^2)}{(1+b_1^2 F_2^2)} \cdot \frac{(1+b_1^2 F_1^2) b_1^2 2F_2 N_e - (1+b_1^2 F_2^2) b_1^2 2F_1 N_e}{(1+b_1^2 F_1^2)^2}\right] + d_1 N_e \\
&= \frac{a_1}{2F_a}\left[N_e(\tan^{-1} b_1 F_2 - \tan^{-1} b_1 F_1) + b_1 N_e\left(\frac{F_2}{(1+b_1^2 F_2^2)} - \frac{F_1}{(1+b_1^2 F_1^2)}\right)\right. \\
&\quad \left. - \frac{2b_1^2 N_e}{2b_1}\left(\frac{F_2}{(1+b_1^2 F_2^2)} - \frac{F_1}{(1+b_1^2 F_1^2)}\right)\right] + d_1 N_e \\
&= \frac{a_1 N_e}{2F_a}[\tan^{-1} b_1 F_2 - \tan^{-1} b_1 F_1] + d_1 N_e
\end{aligned}$$

APPENDIX E

MACHINE PARTICULARS

NAME PLATE DATA

1/3 H.P.

220 V D.C.

120 W

1500 R.P.M.

ConsuLab 214-50

Armature resistance = Ra = 24.4 Ω.

Series field resistance = R_s = 17.2 Ω.

Inductance of armature coil = L_a = 0.274 H.

Inductance of series field coil = L_s = .0887 H.

Pole arc/Pole pitch = α_i = 8/12

Number of poles = 2

Number of parallel paths = 2

Number of turns of the armature coil = N_a = 24

Number of turns per pole pair of series field coil = N_s = 16

Number of turns per pole pair of some arbitrarily chosen base coil = N_e = 16

Number of armature conductors = Z = 48

Resistance of the eddy current path = R_{ed} = 10.0056 Ω.

Inductance of the eddy current path = .0006925 H.

External resistance inserted in the armature circuit = 68 Ω.

Brush voltage drop = 2 volt.

Leakage inductance of the series field coil = .01L_s H.

Leakage inductance of the armature coil = .01L_a H.

APPENDIX F

EXTERNAL CHARACTERISTICS OF THE TEST MACHINE

Terminal voltage in volt.

Armature current, I_a in amp.

Field current, I_f in amp.

I_f \ I_a	0	.1	.2	.3	.4	.5	.6	.7	.8
.075	23	20	17	14	10	6	-	-	-
.1	32	29.25	26.5	24	21.25	18	13	-	-
.15	52	49.25	46.75	44	41.25	38	34	-	-
.2	70	67.3	64.5	61.75	59.25	56.3	53	49	-
.25	86	83	80	76.75	74	70.5	67.3	63	-
.3	102	98.75	95.5	92.5	89.25	86	82	79	-
.35	120	117	114	110.5	107.5	104	100	94	-
.4	138	134.5	130.75	127	123.75	120	115.5	110	-
.45	156	152.5	149.25	145.75	141.75	138	132.5	126	-
.5	172	168.7	165.25	161.5	157.5	153	148	142	-
.55	186	182	178	173.5	169.25	165	159.5	153	146
.6	198	194	190.5	187	183	178.5	173	165	158
.65	208	204	200.5	195.5	191	186	180.25	173	166
.7	216	211.5	207	202.5	197	192	186.5	180	172

APPENDIX G

TABLE FOR THE BACK EMF COEFFICIENT, K

Back emf coefficient, K in volt-sec/amp-rad.

Armature current, I_a in amp.

Field current, I_f in amp.

I_f \ I_a	.075	.1	.2	.3	.4	.5	.6	.7
.075	1.90	1.42	.69	.45	.31	.23	-	-
.1	2.69	2.01	.99	.66	.49	.38	.29	-
.2	5.92	4.43	2.20	1.46	1.09	.87	.71	.60
.3	8.59	6.44	3.19	2.11	1.57	1.25	1.02	.87
.4	11.63	8.71	4.31	2.85	2.12	1.68	1.38	1.15
.5	14.54	10.89	5.41	3.58	2.66	2.10	1.72	1.44
.6	16.71	12.50	6.21	4.12	3.06	2.42	1.99	1.65
.7	18.19	13.61	6.74	4.45	3.29	2.59	2.13	1.79

APPENDIX H

COMPUTER PROGRAM 1

```
C
C     THIS PROGRAM IS DONE BY MD.MAHMUDUR RAHMAN
C     THESIS SUPERVISOR DR.ENAMUL BASHER
C     ASSOCIATE PROFESSOR,DEPARTMENT OF E.E.E.BUET,DHAKA
C
C     DETERMINATION OF EDDY CURRENT CONSTANT
C     BY HALF INTERVAL SEARCH METHOD
C
C     A AND B ARE INITIAL LEFT-AND RIGHT-HAND LIMITS,RESPECTIVELY
C     EPS REPRESENTS THE TOLERANCE OF F(X), IT IS A SMALL NUMBER
C
      OPEN(UNIT=8,FILE='IN ',STATUS='OLD ')
      OPEN(UNIT=9,FILE='OUT',STATUS='NEW ')
      READ(8,22)A,B,EPS
22    FORMAT(3F10.4)
C
C     EVALUATE F(A) AND F(B)
C
      FA=1.+(7.417838)*(.083333)**A-(6.448813)*(.333333)**A
      FB=1.+(7.417838)*(.083333)**B-(6.448813)*(.333333)**B
      WRITE(9,81)
81    FORMAT(5X,'I',9X,'X(I)',11X,'LLL',12X,'RRR',17X,'F(X)'//)
      I=0
7     I=I+1
C
C     COMPUTE THE VALUE OF F(X) AT THE MID POINT OF THE INTERVAL
C
```

```
      X=(A+B)/2.
      PP=1.+(7.417838)*(.083333)**X
      QQ=(6.448813)*(.333333)**X
      F=PP-QQ
      WRITE(9,99)I,X,PP,QQ,F
99    FORMAT(I6,3F15.8,F20.8)
C
C     TEST TO SEE WHETHER THE VALUE OF F(X) SATISFIES THE SPECIFIED
C     TOLERANCE. IF IT IS STOP THE COMPUTATION
C
      IF(ABS(F).LE.EPS) GO TO 10
C
C     IF THE PRODUCT OF F TIMES FA IS NEGATIVE,THE TRUE ROOT WOULD LIE
C     IN THE INTERVAL BETWEEN A AND THE MID POINT.IF NOT,IT IS IN THE
C     OTHER INTERVAL.IF IT IS ZERO, A IS THE TRUE ROOT.
C
      IF(F*FA)5,8,6
5     B=X
      FB=F
      GO TO 7
6     A=X
      FA=F
      GO TO 7
8     WRITE(9,9)
9     FORMAT( 'A IS TRUE ROOT ')
10    STOP
      END
```

COMPUTER PROGRAM 2

```
C
C     THIS PROGRAM IS DONE BY MD.MAHMUDUR RAHMAN
C     THESIS SUPERVISOR DR.ENAMUL BASHER
C     ASSOCIATE PROFESSOR,DEPARTMENT OF E.E.E BUET,DHAKA
C
C     COMPUTATION OF THE SPEED-TORQUE CHARACTERISTICS OF A CHOPPER FED
C     D.C SERIES MOTOR,WITHOUT CONSIDERING THE EFFECT OF EDDY CURRENT,
C     BY SOLVING A FIRST ORDER NON LINEAR DIFFERENTIAL EQUATION,
C     WITH THE HELP OF FOURTH ORDER RUNGE-KUTTA METHOD.
C
C     DEFINITION OF SOME PARAMETERS
C
C     IA=ARMATURE CURRENT IN AMPERE
C     VA=APPLIED VOLTAGE TO THE ARMATURE CIRCUIT IN VOLT
C     PHIMA=AIR GAP FLUX IN WEBER
C     OMEGA=ANGULAR VELOCITY IN RADIAN/SEC.
C     T=TIME IN SECOND
C     TP=TIME PERIOD OF ONE CHOPPING CYCLE IN SECOND
C     TON=ON TIME IN SECOND
C     DELT=INCREMENT OF TIME IN SECOND
C     K(1),K(2),K(3),K(4)=RUNGE'S COEFFICIENT
C
      REAL *16 K(4),FLUX,LAL,LSL,IA,LA,LS,K1
C
C     DEFINE THE FUNCTION
C
```

```
      FA(X)=((ALPHAI*NA)/(2*A*P))*X
      FD(X)=NS*X
      F1(X)=FD(X)-FA(X)
      F2(X)=FD(X)+FA(X)
      PHIMA(X)=(A1/(2*FA(X)))*(F2(X)*(ATAN(B1*F2(X)))-F1(X)*(ATAN(
     +B1*F1(X)))-(1/(2*B1))*(ALOG((1+(B1**2)*(F2(X)**2))/(1+(B1**2)*(F
     +1(X)**2)))))+D1*FD(X)
      AQ(X)=(P*(NA1**2))*((A1/(B1*(FA(X)**2)))*(1+(((B1**2)*(FD(X)**2
     +)-1)/(2*B1*FA(X)))*(ATAN(B1*F2(X))-ATAN(B1*F1(X)))-(FD(X)/(2
     +*FA(X)))*(ALOG((1+(B1**2)*(F2(X)**2))/(1+(B1**2)*(F1(X)**2)))))+
     +D1/3)
      AE(X)=-((P*NE*NA1*A1)/(2*(FA(X)**2)))*(FD(X)*(ATAN(B1*F2(X))-ATAN
     +(B1*F1(X)))-(1/(2*B1))*(ALOG((1+(B1**2)*(F2(X)**2))/(1+(B1**2)*(
     +F1(X)**2)))))
      E(X)=(P*(NE**2))*((A1/(2*FA(X)))*(ATAN(B1*F2(X))-ATAN(B1*F1
     +(X)))+D1)
      F(X)=(VA-DELVB-X*RA-K1*PHIMA(X)*OMEGA)/((LAL+LSL)+(AQ(X)+(NS/NE)
     +*AE(X)+(NS/NE)*AE(X)+((NS**2)/(NE**2))*E(X)))
      OPEN(UNIT=8,FILE='IN',STATUS='OLD')
      OPEN(UNIT=9,FILE='OUT',STATUS='NEW')
C
C     VALUE OF SOME OF THE PARAMETERS
C
      PARC=8.0
      PPITCH=12.0
      ALPHAI=PARC/PPITCH
      NA=24
      NS=16
      NE=16
```

```
      A=1.0
      P=1.0
      Z=48.0
      A1=0.115
      B1=0.095
      D1=-0.0007
      NA1=(PARC*NA)/(2*A*P*PPITCH)
      DELVB=2.0
      RA=109.6
      PI=3.14159265
      K1=(Z*P)/(2*A*PI)
      LA=0.274
      LS=0.0887
      LAL=0.01*LA
      LSL=0.01*LS
C
C     MAIN PROGRAM
C
      T=0.0
      TO=T
      READ(8,10)TP,TON,DELT,IA,OMEGA,N
10    FORMAT(5F10.8,I3)
      DO 100 M=1,N
      TMAX1=TON+(M-1)*TP
      TMAX2=M*TP
      WRITE(9,81)
81    FORMAT(5X,'TIME',10X,'CURRENT',9X,'FLUX')
60    X=IA
      FLUX=PHIMA(X)
```

```
      WRITE(9,11)T,IA,FLUX
11    FORMAT(F10.4,2F15.4)
      IF(T.LE.TMAX1)THEN
      VA=100.0
      ELSE IF(T.LE.TMAX2)THEN
      VA=0.0
      ELSE
      GO TO 100
      END IF
C
C     DETERMINATION OF RUNGE'S COEFFICIENT
C
      DO 50 J=1,4
      IF(J.GT.2)THEN
      L=2
      ELSE
      L=1
      END IF
      K(J)=F(X)
      T=TO+(DELT/2)*L
      X=IA+DELT*(K(J)/2)*L
50    CONTINUE
      IA=IA+(DELT/6)*(K(1)+2*K(2)+2*K(3)+K(4))
      TO=T
      GO TO 60
100   CONTINUE
      STOP
      END
```

COMPUTER PROGRAM 3

```
C
C     THIS PROGRAM IS DONE BY MD.MAHMUDUR RAHMAN
C     THESIS SUPERVISOR DR.ENAMUL BASHER
C     ASSOCIATE PROFESSOR,DEPARTMENT OF E.E.E BUET,DHAKA
C
C     COMPUTATION OF THE SPEED-TORQUE CHARACTERISTICS OF A CHOPPER FED
C     DC SERIES MOTOR,TAKING THE EFFECT OF EDDY CURRENT IN TO ACCOUNT,
C     BY SOLVING A FIRST ORDER NON LINEAR SIMULTANEOUS DIFFERENTIAL
C     EQUATION, WITH THE HELP OF FOURTH ORDER RUNGE-KUTTA METHOD.
C
C     DEFINITION OF SOME PARAMETERS
C
C     IA=ARMATURE CURRENT IN AMPERE
C     IED=EDDY CURRENT IN AMPERE
C     VA=APPLIED VOLTAGE TO THE ARMATURE CIRCUIT IN VOLT
C     PHIMA=AIR GAP FLUX IN WEBER
C     OMEGA=ANGULAR VELOCITY IN RADIAN/SEC.
C     T=TIME IN SECOND
C     TP=TIME PERIOD OF ONE CHOPPING CYCLE IN SECOND
C     TON=ON TIME IN SECOND
C     DELT=INCREMENT OF TIME IN SECOND
C     K(1),K(2),K(3),K(4),L(1),L(2),L(3),L(4)=RUNGE'S COEFFICIENT
C
      REAL *16 K(4),L(4),FLUX,LAL,LSL,IA,LA,LS,LED,IED,K1
C
C     DEFINE THE FUNCTION
C
```

```
 FA(X)=((ALPHAI*NA)/(2*A*P1))*X
 FD(X,Y)=NS*(X,Y)
 F1(X,Y)=FD(X,Y)-FA(X)
 F2(X,Y)=FD(X,Y)+FA(X)
 PHIMA(X,Y)=(A1/(2*FA(X)))*(F2(X,Y)*(ATAN(B1*F2(X,Y)))-F1(X,Y)*
+(ATAN(B1*F1(X,Y)))-(1/(2*B1))*(ALOG((1+(B1**2)*(F2(X,Y)**2))/
+(1+(B1**2)*(F1(X,Y)**2)))))+D1*FD(X,Y)
 AQ(X,Y)=(P1*(NA1**2))*((A1/(B1*(FA(X)**2)))*(1+(((B1**2)*(FD(X,Y)
+**2)-1)/(2*B1*FA(X)))*(ATAN(B1*F2(X,Y))-ATAN(B1*F1(X,Y)))-(FD
+(X,Y)/(2*FA(X)))*(ALOG((1+(B1**2)*(F2(X,Y)**2))/(1+(B1**2)*(F1
+(X,Y)**2)))))+D1/3)
 AE(X,Y)=-((P1*NE*NA1*A1)/(2*(FA(X)**2)))*(FD(X,Y)*(ATAN(B1*F2(X,Y
+))-ATAN(B1*F1(X,Y)))-(1/(2*B1))*(ALOG((1+(B1**2)*(F2(X,Y)**2))/
+(1+(B1**2)*(F1(X,Y)**2)))))
 E(X,Y)=(P1*(NE**2))*((A1/(2*FA(X)))*(ATAN(B1*F2(X,Y))-ATAN
+(B1*F1(X,Y)))+D1)
 R1(X,Y)=-((A1*NA1)/(2*(FA(X)**2)))*(FD(X,Y)*(ATAN(B1*F2(X,Y))
+-ATAN(B1*F1(X,Y)))-(1/(2*B1))*(ALOG((1+(B1**2)*(F2(X,Y)**2))/
+(1+(B1**2)*(F1(X,Y)**2)))))
 R2(X,Y)=((A1*NE)/(2*FA(X)))*(ATAN(B1*F2(X,Y))-ATAN(B1*F1(X,Y)))
++D1*NE
 H(X,Y)=LED+(P1*(NS**2)*R2(X,Y))/(NE)
 S(X,Y)=VA-DELVB-X*RA-K1*PHIMA(X,Y)*OMEGA
 P(X,Y)=(NS*AE(X,Y))/(NE)+((NS**2)*E(X,Y))/(NE**2)
 Q(X,Y)=LAL+LSL+AQ(X,Y)+(2*NS*AE(X,Y))/(NE)+((NS**2)*E(X,Y))/
+(NE**2)
 R(X,Y)=P1*NS*R1(X,Y)+(P1*(NS**2)*R2(X,Y))/(NE)
 F(X,Y)=(H(X,Y)*S(X,Y)+P(X,Y)*RED*Y)/(H(X,Y)*Q(X,Y)-P(X,Y)*R(X,Y))
 G(X,Y)=(-R(X,Y)*S(X,Y)-Q(X,Y)*RED*Y)/(H(X,Y)*Q(X,Y)-P(X,Y)*R(X,Y))
```

```
      OPEN(UNIT=8,FILE='IN',STATUS='OLD')
      OPEN(UNIT=9,FILE='OUT',STATUS='NEW')
C
C     VALUE OF SOME OF THE PARAMETERS
C
      PARC=8.0
      PPITCH=12.0
      ALPHAI=PARC/PPITCH
      NA=24
      NS=16
      NE=16
      A=1.0
      P1=1.0
      Z=48.0
      A1=0.115
      B1=0.095
      D1=-0.0007
      NA1=(PARC*NA)/(2*A*P1*PPITCH)
      DELVB=2.0
      RA=109.6
      RED=10.0056
      PI=3.14159265
      K1=(Z*P)/(2*A*PI)
      LA=0.274
      LS=0.0887
      LAL=0.01*LA
      LSL=0.01*LS
      LED=0.0006925
```

```
C
C     MAIN PROGRAM
C
      T=0.0
      TO=T
      READ(8,10)TP,TON,DELT,IA,IED,OMEGA,N
10    FORMAT(6F10.8,I3)
      DO 100 M=1,N
      TMAX1=TON+(M-1)*TP
      TMAX2=M*TP
      WRITE(9,81)
81    FORMAT(5X,'TIME',5X,'ARMATURE CURRENT',5X,'FLUX',5X,'EDDY CURRENT')
60    X=IA
      Y=IED
      FLUX=PHIMA(X,Y)
      WRITE(9,11)T,IA,FLUX,IED
11    FORMAT(F10.4,2F15.5,E15.8)
      IF(T.LE.TMAX1)THEN
      VA=100.0
      ELSE IF(T.LE.TMAX2)THEN
      VA=0.0
      ELSE
      GO TO 100
      END IF
C
C     DETERMINATION OF RUNGE'S COEFFICIENT
C
      DO 50 J=1,4
      IF(J.GT.2)THEN
```

```
      I=2
      ELSE
      I=1
      END IF
      K(J)=F(X,Y)
      L(J)=G(X,Y)
      T=TO+(DELT/2)*I
      X=IA+DELT*(K(J)/2)*I
      Y=IED+DELT*(L(J)/2)*I
50    CONTINUE
      IA=IA+(DELT/6)*(K(1)+2*K(2)+2*K(3)+K(4))
      IED=IED+(DELT/6)*(L(1)+2*L(2)+2*L(3)+L(4))
      TO=T
      GO TO 60
100   CONTINUE
      STOP
      END
```

APPENDIX I

Photograph of the experimental set-up

REFERENCES

1. R. K. Sugandhi and K. K. Sugandhi : "Thyristors (Theory and Application)." Wiley Easter Ltd., 1981.
2. A. P. Jacobs and G. W. Walsh : "Application Consideration for SCR DC Drives and Associated Power Systems." IEEE Trans. Ind. Gen. Appl., vol. IGA-4, pp. 369-409, July/Aug. 1968.
3. A. G. Carter : "Fast Response Speed Regulating Systems." IEEE Trans. Ind. Gen. Appl., vol. IGA-1, pp. 270-273, July/Aug. 1965.
4. R. E. Moore : "High Performance Control for Tandem Cold Mill Main Drive Systems." IEEE Trans. Ind. Gen. Appl., vol. IGA-2, pp. 353-357, Sept./Oct. 1966.
5. G. K. Dubey and W. Shepherd : "Analysis of DC Series Motor Controlled by power Pulses." Proc. IEE, vol. 122, No. 12, pp. 1397-1398, Dec. 1975.
6. G. K. Dubey and W. Shepherd : "Comparative Study of Chopper Control Techniques for DC Motor Control." J. IE(India), pt. EL6, vol. 58, pp. 307, June 1978.
7. P. J. Gregg : "Electronic Motor controls for Battery Powered Vehicles." IEEE INDUSTRIAL STATIC POWER CONVERSION, Philadelphia, Pa., Nov. 1-3, 1965, Power Conference Record 34C20.
8. K. Heintze and R. Wagner : " Electronische Gleichstromsteller zur Geschwindigkeitssteuerung von aus Fahrleitungen gespeisten Gleichstrom-Triebfahrzeugen." ETZ-A, vol. 87(1966) H.5, p165-170.
9. Survey : "DC Motor Control by Pulsed Silicon Controlled Rectifiers." THE ENGINEER, Dec. 27, 1963.
10. L. Abraham, K. Heumann and F. Koppelman : "Anfahren, Regeln und Nutzbremsen von Gleichstromfahrzeugen mit steuerbaren Siliziumzellen." FACHBERICHTE VDE, vol. 27, 1962, pK/89-I/100.

11. Survey : "Loss Free Control of Traction Motors." ENGINEER, Sept. 22, 1961, vol. 212, p.480.

12. F. W. Gutzwiller : "Thyristor Semiconductor Components today." IEEE Trans. Ind. Gen. Appl., vol. IGA-1, No. 6, pp. 403-409, Nov./Dec. 1965.

13. D. W. Borst, E. J. Diebold and F. W. Parrish : "Voltage Control by Means of Power Thyristors." IEEE Trans. Ind. Gen. Appl., vol. IGA-2, No. 2, pp. 102-123, March/April, 1966.

14. E. Schnieder : "Control of DC Drives by Microprocessor." Proc. IFAC Symposium, pp. 603-608, Oct. 1977.

15. A. K. Lin and W. Wkoepsel : "Microprocessor Speed Control System." IEEE Trans. Industrial Electronics and Control Instrumentation, vol. IECI-24, No. 3, pp. 218, Aug. 1977.

16. Y. T. Chan and J. B. Plant : "A Microprocessor Based Current Controller for SCR DC Motor Drives." IEEE Trans. Industrial Electronics and Control Instrumentation, vol. IECI-27, No. 3, pp. 169, Aug. 1980.

17. S. N. Singh and D. R. Kohli : "Analysis and Performance of a Chopper Controlled Separately excited DC Motor." IEEE Trans. Ind. Electronic vol. IE-29, No. 1, pp. 1-5, Feb. 1982.

18. P. W. Franklin : "Theory of the DC Motor Controlled by Power Pulses (Part-1, Motor Operation)." IEEE Trans. Power App. Syst. vol. PAS-92, pp. 249, April, 1972.

19. T. Fujimaki, K. Ohniwa and O. Miyashita : "Simulation of Chopper Controlled DC Series Motor." Proc. IFAC Symposium, pp. 609-618, Oct. 1977.

20. P. C. Sen and M. L. Mcdonald : "Thyristorized DC Drives with Regenerative Braking and Speed Reversal." IEEE Trans. Ind. Elect. and Cont. Instru., vol. IECI-25, No. 4. pp. 347, Nov. 1978.

21. G. K. Dubey and W. Shepherd : "Transient Analysis of Chopper-Fed DC Series Motor." IEEE Trans. Ind. Elect. and Cont. Instru., vol. IECI-28, No. 4, pp. 146-159, Nov. 1981.

22. M. H. Rashid : "Dynamic Response of DC Chopper Controlled Series Motor." IEEE Trans. Ind. Elect. and Cont. Instru., vol. IECI-28, No.4, pp. 323-330, Nov. 1981.

23. R. S. Ramshaw and G. Xie : "Mathematical Model and Electric-Circuit Simulation of DC Machines." Proc. IEE. pt. B vol. 130, No. 3, pp. 218-224, May 1983.

24. T. J. Takeuchi : "Theory of SCR Circuits and Application to Motor Control." Tokyo Electrical Engineering College Press, 1968, pp. 273.

25. K. Nitta, H. Okitsu, T. Suzuki and Y. Kinouchi : "A Separately excited DC Motor Driven By Discontinuous Current." Electrical Engineering in Japan(USA), vol. 89, No. 11, 1969, pp. 19-26.

26. R. Parimelalagan and V. Rajgopalan : "Steady State Investigations of a Chopper-fed DC Motor with Separate Excitation." IEEE Trans. Ind. Gen. Appl., vol. IGA-7, pp. 101, 1971.

27. G. K. Dubey and W. Shepherd : "Transient Analysis of DC Separately Excited Motor Fed by Chopper with Current Limit Control." J. IE(India), vol. 58, pt. EL2, pp. 108, Oct. 1977.

28. P. D. Dample and G. K. Dubey : "Analysis of Chopper Fed DC Series Motor." IEEE Trans. Ind. Electron. Contr. Instr., vol. IECI-23, No. 1, pp. 92, 1976.

29. H. Sathpathi, G. K. Dubey and L. P. Singh : "Performance and Analysis of Chopper Fed DC Separately Excited Motor Under Regenerative Braking." Electric. mach. Electromechan., vol. 5, pp. 292, 1980.

30 S. N. Singh and D. R. Kohli : "Mathematical Foundation of a Chopper Controlled Separately Excited DC Motor." J. IE(India), vol. 60, pt. El3, pp. 94, 1979.

31. H. Sathpathi, G. K. Dubey and L. P. Singh : "A General Method of Analysis of Chopper-Fed DC Separately Excited Motor," IEEE Trans. Power App. Syst. vol. PAS-102, No. 4, pp. 990-997, April, 1983.

32. S. N. Bhadra, Nishit. K. De and A. K. Chattopadhyay: "Regenerative Braking Performance Analysis of a Thyristor-Chopper Controlled DC Series Motor." IEEE Trans. Ind. Elec. and Cont. Instru. vol. IECI-128, No. 4, pp. 342-347, Nov. 1981.

33. A. Yablon and J. Appelbaum : "Transient Analysis to DC Series Motor (Linear Versus Nonlinear Models)." IEEE Trans. Ind. Elec. and Cont. Instru. vol. IECI-28, No. 2. pp. 120-125, May, 1981.

34. F. P. de Mello and L. N. Hennett : " Representation of Saturation in Synchronous Machines." IEEE Trans. Power Syst. vol. PWRS-J, No. 4, pp. 8-14, Nov. 1986.

35. H. Sathpathi, G. K. Dubey and L. P. Singh : "Performance and Analysis of Chopper-Fed DC Series Motor with Magnetic Saturation, Armature Reaction and Eddy Current Effect." IEEE Trans. Power App. and Syst. vol. PAS-102, No. 4, pp. 981-988, April, 1983.

36. E. G. Strangas and H. B. Hamilton : "A Model for the Chopper Controlled DC Series Motor." IEEE Trans, Power App. and Syst. vol. PAS-102, No. 5, pp. 1403-1407, May, 1983.

37. E. Basher and A. R. Khan : "Modelling of DC Machine, Working in Rapid Transients." BICEM Paper, pp. 177-180, Aug. 1987.

38. P. Knapp : "Solid State Regulating Units for Motoring and Braking DC Traction Vehicles." Brown Boveri Rev., vol. 57, pp. 252-270, June/July 1970.

39. B. Berman : "All Solid State Method for Implementing a Traction Drive Control," IEEE-IGA conf. Rec., oct. 18-21, 1971.

40. C. V. Jones : "Unified Theory of Electric Machines." Butterworths, London.

41. B. Mellitt and H. Rashid : "Voltage Time Integral Method for Measuring Machine Inductance." Proc. IEE vol. 121, No. 9, Sept. 1974, pp. 1016.

42. N. Keshavamurthy and P. K. Rajgopalan : "Effects of Eddy Currents on the Rise and Decay of Flux in Solid Magnetic Cores." Proc. IEE, vol. 109 pt. C., 1962, pp. 63-75.

43. S. B. Dewan and A. Straughen : "Power Semiconductor Circuits." John Wiley and Sons, 1975.

44. S. B. Dewan, G. R. Slemon and A. Straughen : "Power Semiconductor Drives." John Wiley and Sons, 1984.